



ONLINE CALIBRATION OF SENSOR ARRAYS USING HIGHER ORDER STATISTICS

A THESIS SUBMITTED TO  
THE GRADUATE SCHOOL OF NATURAL AND APPLIED SCIENCES  
OF  
MIDDLE EAST TECHNICAL UNIVERSITY

BY

METİN AKTAŞ

IN PARTIAL FULFILLMENT OF THE REQUIREMENTS  
FOR  
THE DEGREE OF PHILOSOPHY OF DOCTORATE  
IN  
ELECTRICAL AND ELECTRONICS ENGINEERING

JANUARY 2012

Approval of the thesis:

**ONLINE CALIBRATION OF SENSOR ARRAYS USING HIGHER ORDER STATISTICS**

submitted by **METİN AKTAŞ** in partial fulfillment of the requirements for the degree of **Philosophy of Doctorate in Electrical and Electronics Engineering Department, Middle East Technical University** by,

Prof. Dr. Canan ÖZGEN  
Dean, Graduate School of **Natural and Applied Sciences**

\_\_\_\_\_

Prof. Dr. İsmet ERKMEN  
Head of Department, **Electrical and Electronics Engineering**

\_\_\_\_\_

Prof. Dr. T. Engin TUNCER  
Supervisor, **Electrical and Electronics Engineering Department, METU**

\_\_\_\_\_

**Examining Committee Members:**

Sencer KOÇ  
Prof. Dr.

\_\_\_\_\_

T. Engin TUNCER  
Prof. Dr.

\_\_\_\_\_

Çağatay CANDAN  
Assoc. Prof. Dr.

\_\_\_\_\_

Özgür Barış AKAN  
Assoc. Prof. Dr.

\_\_\_\_\_

Yakup ÖZKAZANÇ  
Asst. Prof. Dr.

\_\_\_\_\_

**Date:**

\_\_\_\_\_

**I hereby declare that all information in this document has been obtained and presented in accordance with academic rules and ethical conduct. I also declare that, as required by these rules and conduct, I have fully cited and referenced all material and results that are not original to this work.**

Name, Last Name: METİN AKTAŞ

Signature :

# ABSTRACT

## ONLINE CALIBRATION OF SENSOR ARRAYS USING HIGHER ORDER STATISTICS

AKTAŞ, Metin

Ph.D., Department of Electrical and Electronics Engineering

Supervisor : Prof. Dr. T. Engin TUNCER

January 2012, 118 pages

Higher Order Statistics (HOS) and Second Order Statistics (SOS) approaches have certain advantages and disadvantages in signal processing applications. HOS approach provides more statistical information for non-Gaussian signals. On the other hand, SOS approach is more robust to the estimation errors than the HOS approach, especially when the number of observations is small. In this thesis, HOS and SOS approaches are jointly used in order to take advantage of both methods. In this respect, the joint use of HOS and SOS approaches are introduced for online calibration of sensor arrays with arbitrary geometries. Three different problems in online array calibration are considered and new algorithms for each of these problems are proposed. In the first problem, the positions of the randomly deployed sensors are completely unknown except the two reference sensors and HOS and SOS approaches are used iteratively for the joint Direction of Arrival (DOA) and sensor position estimation. Iterative HOS-SOS algorithm (IHOSS) solves the ambiguity problem in sensor position estimation by observing the source signals at least in two different frequencies and hence it is applicable for wideband signals. The conditions on these frequencies are presented. IHOSS is the first algorithm in the literature which finds the DOA and sensor position estimations in case of randomly deployed sensors with unknown coordinates. In the second problem, narrowband signals are considered and it is assumed that the nominal sensor positions are known. Mod-

ified IHOSS (MIHOSS) algorithm uses the nominal sensor positions to solve the ambiguity problem in sensor position estimation. This algorithm can handle both small and large errors in sensor positions. The upper bound of perturbations for unambiguous sensor position estimation is presented. In the last problem, an online array calibration method is proposed for sensor arrays where the sensors have unknown gain/phase mismatches and mutual coupling coefficients. In this case, sensor positions are assumed to be known. The mutual coupling matrix is unstructured. The two reference sensors are assumed to be perfectly calibrated. IHOSS algorithm is adapted for online calibration and parameter estimation, and hence CIHOSS algorithm is obtained. While CIHOSS originates from IHOSS, it is fundamentally different in many aspects. CIHOSS uses multiple virtual ESPRIT structures and employs an alignment technique to order the elements of rows of the actual array steering matrix. In this thesis, a new cumulant matrix estimation technique is proposed for the HOS approach by converting the multi-source problem into a single source one. The proposed algorithms perform well even in the case of correlated source signals due to the effectiveness of the proposed cumulant matrix estimate. The iterative procedure in all the proposed algorithms is guaranteed to converge. Closed form expressions are derived for the deterministic Cramér-Rao bound (CRB) for DOA and unknown calibration parameters for non-circular complex Gaussian noise with unknown covariance matrix. Simulation results show that the performances of the proposed methods approach to the CRB for both DOA and unknown calibration parameter estimations for high SNR.

Keywords: Direction-of-Arrival Estimation, Sensor Localization, Higher-Order-Statistics, Deterministic Cramér-Rao Bound, Cumulant Matrix

## ÖZ

### YÜKSEK DERECELİ İSTATİSTİK KULLANARAK ALGILAYICI DİZİLERİNİN ÇEVİRİMİÇİ KALİBRASYONU

AKTAŞ, Metin

Doktora, Elektrik ve Elektronik Mühendisliği Bölümü

Tez Yöneticisi : Prof. Dr. T. Engin TUNCER

Ocak 2012, 118 sayfa

Sinyal işleme uygulamalarında Yüksek Dereceli İstatistik (HOS) ve İkinci Dereceli İstatistik (SOS) yaklaşımları belirli avantaj ve dezavantajlara sahiptir. Gaussian olmayan sinyaller için HOS yaklaşımı daha fazla istatistiksel bilgi sağlamaktadır. Diğer açıdan SOS yaklaşımı özellikle gözlem sayısı küçük olduğunda HOS yaklaşımına göre tahmin hatalarına karşı daha dayanıklıdır. Bu tezde her iki yöntemin avantajlarından yararlanabilmek için HOS ve SOS yaklaşımları birlikte kullanılmıştır. Bu açıdan HOS ve SOS yaklaşımlarının birlikte kullanımı gelişigüzel geometrideki algılayıcı dizilimlerinin çevrimiçi kalibrasyonu için önerilmiştir. Çevrimiçi dizilim kalibrasyonunda üç farklı problem ele alınmış ve herbir problem için yeni algoritmalar önerilmiştir. İlk problemde, gelişigüzel dağıtılmış algılayıcıların konumları iki referans sensor haricinde tamamen bilinmemektedir ve geliş yönü (DOA) ve algılayıcı konumlarının birlikte bulunması için HOS ve SOS yaklaşımları yinelemeli olarak kullanılmıştır. Yinelemeli HOS-SOS algoritması (IHOSS) algılayıcı konumları tahminindeki bilinmezlik problemini kaynak sinyallerinin en az iki frekansta gözlemlenmesi ile çözmektedir ve bu nedenle geniş-bantlı sinyaller için uygulanabilir. Frekanslardaki koşullar belirtilmiştir. IHOSS, gelişigüzel dağıtılmış algılayıcıların konumlarının bilinmemesi durumunda DOA ve algılayıcı konum tahmininin bulunmasında kullanılan literatürdeki ilk algoritmadır. İkinci

problemde dar-banrlı sinyaller ele alınmıř ve algılayıcı konumlarının anma deęerlerinin bilindięi kabul edilmiřtir. Deęiřtirilmiř IHOSS (MIHOSS) algoritması algılayıcı konumlarının tahminindeki belirsizlik problemini ozmek iin algılayıcı konumlarının anma deęerlerini kullanmaktadır. Bu algoritma algılayıcı konumlarındaki hem kuuk hem de buyuk hataları ele alabilmektedir. Tam algılayıcı konum tahmini iin sarsımların st sınırı belirtilmiřtir. En son problemde, algılayıcıların kazanç/faz uyumsuzluęu ve karřılıklı baęlařım katsayılarının bilinmedięi durumdaki algılayıcı dizilimleri iin evrimii dizilim kalibrasyonu yntemi nerilmiřtir. Bu durumda algılayıcı konumlarının bilindięi kabul edilmiřtir. Karřılıklı baęlařım matrisi herhangi bir zel yapıya sahip deęildir. İki adet referans algılayıcısının kalibrasyonunun tam olduęu kabul edilmiřtir. IHOSS algoritması evrimii kalibrasyon ve parametre tahmini iin uyarlanmıř ve bylece CIHOSS algoritması elde edilmiřtir. CIHOSS, IHOSS algoritmasından ıkmıř olmasına raęmen birok bakımdan temel farklılıklar gstermektedir. CIHOSS, birok sanal ESPRIT yapısı kullanmakta ve gerek dizilim steering matrisinin satırlarındaki eleman sıralarının hizalanmasını gerekleřtirmektedir. Birden fazla kaynak problemini tek kaynak problemine evirerek HOS ayaklařımı iin yeni bir cumulant matris tahmini teknięi nerilmiřtir. nerilen algoritmalar, yeni cumulant matris tahmininin etkinlięinden dolayı ilintili kaynak sinyallerinde dahi iyi performans seęilemektedirler. nerilen tm algoritmalarındaki yinelemeli yntemin yakınsaması garantilenmiřtir. Bilinmeyen kovaryans matrisine sahip embersel olmayan karmařık Gaussian grlt sinyali durumu iin sinyal geliř yn ve bilinmeyen kalibrasyon parametreleri kestirimi iin kapalı formda belirlenimci Cram´er-Rao bound (CRB) denklemleri elde edilmiřtir. Benzetim sonuları gstermiřtir ki nerilen yntemlerin performansları DOA ve bilinmeyen kalibrasyon parametreleri tahmini iin yksek SNR deęerinde CRB deęerine yaklařmaktadır.

Anahtar Kelimeler: Geliř Yn Kestirimi, Algılayıcı Konumlama, Yksek Dereceli İstatistik, Belirlenimci Cram´er-Rao Bound, Cumulant Matrisi

*To my wife, Gonca AKTAŞ ...*

## ACKNOWLEDGMENTS

I would like to thank my wife Gonca for her personal support and great patience at all times. My parents have given me their unequivocal support throughout the thesis.

This thesis would not have been possible without the help and support of my supervisor Prof. Dr. T. Engin TUNCER. I would like to thank him for his guidance, advice, criticism and insight throughout the research.

I would also like to thank TÜBİTAK Bilim İnsanı Destekleme Daire Başkanlığı for the financial support.

This study was supported in part by ASELSAN Inc., MGEO Division, Image Processing Department, Turkey.

# TABLE OF CONTENTS

ABSTRACT . . . . .	iv
ÖZ . . . . .	vi
ACKNOWLEDGMENTS . . . . .	ix
TABLE OF CONTENTS . . . . .	x
LIST OF TABLES . . . . .	xiii
LIST OF FIGURES . . . . .	xiv
LIST OF ALGORITHMS . . . . .	xvii
CHAPTERS	
1 INTRODUCTION . . . . .	1
1.1 Motivations and Objectives . . . . .	1
1.2 Literature Overview . . . . .	2
1.3 Thesis Overview . . . . .	4
1.4 Contributions . . . . .	6
1.5 Organization of the Thesis . . . . .	7
1.6 Notations in the Thesis . . . . .	8
2 ITERATIVE HOS-SOS (IHOSS) ALGORITHM FOR DIRECTION-OF-ARRIVAL ESTIMATION AND SENSOR LOCALIZATION . . . . .	9
2.1 Problem Statement for IHOSS Algorithm . . . . .	10
2.2 IHOSS Algorithm . . . . .	12
2.2.1 HOS Based Blind DOA Estimation . . . . .	14
2.2.2 Unambiguous Sensor Localization . . . . .	21
2.2.3 SOS-Based MUSIC Algorithm . . . . .	27
2.2.4 The Cost Function and The Algorithmic Steps . . . . .	27
2.3 Cramér-Rao Bound . . . . .	28

2.4	Performance Results . . . . .	32
2.5	Advantages of IHOSS Algorithm . . . . .	36
3	DIRECTION-OF-ARRIVAL ESTIMATION AND SENSOR POSITION CALIBRATION WITH MODIFIED ITERATIVE HOS-SOS (MIHOSS) ALGORITHM . . . . .	43
3.1	Problem Statement for MIHOSS Algorithm . . . . .	44
3.2	MIHOSS Algorithm . . . . .	45
3.2.1	Unambiguous Sensor Localization . . . . .	46
3.2.2	The Cost Function and The Algorithmic Steps . . . . .	48
3.3	Performance Results . . . . .	48
3.4	Advantages of MIHOSS Algorithm . . . . .	51
4	ONLINE CALIBRATION WITH ITERATIVE HOS-SOS ALGORITHM IN THE PRESENCE OF MUTUAL COUPLING AND GAIN/PHASE MISMATCH 55	
4.1	Problem Statement . . . . .	56
4.2	Cumulant Matrix . . . . .	58
4.3	CIHOSS Algorithm . . . . .	60
4.3.1	HOS Approach . . . . .	61
4.3.1.1	DOA Estimation with HOS Approach . . . . .	62
4.3.1.2	Actual Steering Matrix Estimation with HOS Approach . . . . .	63
4.3.1.3	Calibration Parameter Estimation with HOS Approach . . . . .	64
4.3.1.4	HOS Iteration . . . . .	65
4.3.2	CIHOSS Cost Function . . . . .	65
4.3.3	SOS Approach . . . . .	69
4.3.3.1	DOA Estimation with SOS Approach . . . . .	70
4.3.3.2	Gain/Phase Mismatch Parameter Estimation with SOS Approach . . . . .	70
4.3.3.3	Mutual Coupling Parameter Estimation with SOS Approach . . . . .	72
4.3.3.4	SOS Iteration . . . . .	73
4.3.4	Solvability . . . . .	73
4.3.4.1	Solvability of HOS approach . . . . .	73

4.3.4.2	Solvability of CIHOSS . . . . .	75
4.4	Cramér Rao Bound . . . . .	76
4.5	Performance Results . . . . .	80
4.6	Advantages of CIHOSS Algorithm . . . . .	83
5	CONCLUSION . . . . .	92
	REFERENCES . . . . .	95
APPENDICES		
A	Proof of Lemma-1 . . . . .	99
B	Derivation of (2.32) . . . . .	100
C	Proof of Theorem-1 in IHOSS . . . . .	101
D	Cramér-Rao Bound . . . . .	104
E	Proof of Lemma-2 . . . . .	108
F	Derivation of Hessian Matrix and Gradient Vector in (4.50) . . . . .	111
G	Proof of Lemma-3 . . . . .	113
H	Permutation Ambiguity in CIHOSS . . . . .	114
	CURRICULUM VITAE . . . . .	117

## LIST OF TABLES

### TABLES

Table 2.1	Simulation parameters for IHOSS algorithm. . . . .	33
Table 3.1	Simulation parameters for MIHOSS algorithm. . . . .	50
Table 4.1	Simulation parameters for CIHOSS algorithm. . . . .	81

## LIST OF FIGURES

### FIGURES

Figure 2.1 Array model for IHOSS algorithm. . . . .	10
Figure 2.2 Virtual sensor concept. . . . .	14
Figure 2.3 Virtual ESPRIT structure for randomly deployed sensors. . . . .	15
Figure 2.4 Different Virtual ESPRIT structures for different pairs of the actual sensors. . . . .	16
Figure 2.5 Ambiguous sensor positions for (a) two and (b) three sources. . . . .	23
Figure 2.6 Different ambiguous sensor positions for two and three sources. . . . .	23
Figure 2.7 Ambiguous sensor positions for the frequencies that does not satisfy the condition in (2.53). The selected frequencies are (a) $f_1 = 10MHz$ , $f_2 = 20MHz$ , (b) $f_1 = 10MHz$ , $f_2 = 15MHz$ . . . . .	25
Figure 2.8 Ambiguous sensor positions for the frequencies that satisfy the condition in (2.53). The selected frequencies are $f_1 = 10MHz$ , $f_2 = 13MHz$ . . . . .	25
Figure 2.9 Estimated sensor positions for the errors that (a) does not satisfy and (b) satisfy the condition in (2.54). The selected frequencies are (a) $f_1 = 10MHz$ , $f_2 = 13MHz$ . . . . .	26
Figure 2.10 SNR performance for (a) DOA and (b) position estimation. . . . .	38
Figure 2.11 (a) DOA and (b) position estimation for varying number of snapshots at SNR = 20 dB. . . . .	39
Figure 2.12 (a) DOA and (b) position estimation performance for varying distance between source DOAs at SNR = 20 dB. . . . .	40
Figure 2.13 (a) DOA and (b) position estimation performance for varying sensor density at SNR = 20 dB. . . . .	41
Figure 2.14 (a) DOA and (b) position estimation performance for different frequency differences. SNR = 20 dB. . . . .	42

Figure 3.1	Array model for MIHOSS algorithm. The circle with dashed line represents the bound on the perturbations in sensor positions. . . . .	44
Figure 3.2	Ambiguous sensor positions for the errors that (a) satisfy and (b) does not satisfy the condition in (3.12). . . . .	48
Figure 3.3	(a) DOA and (b) position estimation RMSE values for different SNR values and sensor position perturbation of $0.1\lambda$ . . . . .	53
Figure 3.4	(a) DOA and (b) position estimation RMSE values for different sensor position perturbations and SNR = 30 dB. . . . .	54
Figure 4.1	Array model for CIHOSS algorithm. There are mutual coupling effects between sensors. . . . .	56
Figure 4.2	SNR performance for the DOA estimation. . . . .	82
Figure 4.3	SNR performance for the estimation of the (a) gain and (b) phase terms of the gain/phase mismatch parameters. . . . .	85
Figure 4.4	SNR performance for the estimation of the (a) gain and (b) phase terms of the mutual coupling coefficients. . . . .	86
Figure 4.5	Cost function values in iteration for cluster distribution of (a) $L_h = \{1, 2, 2, 1\}$ and (b) $L_h = \{1, 1, 1, 1, 1, 1\}$ at SNR = 15 dB. . . . .	87
Figure 4.6	SNR performance for the DOA estimation for “Large Error” in mutual coupling coefficients. . . . .	88
Figure 4.7	SNR performance for the estimation of the (a) gain and (b) phase terms of the mutual coupling coefficients for “Large Error” in mutual coupling coefficients. . . . .	89
Figure 4.8	SNR performance for the DOA estimation for “Small Error” in mutual coupling coefficients. . . . .	90
Figure 4.9	SNR performance for the estimation of the (a) gain and (b) phase terms of the mutual coupling coefficients for “Small Error” in mutual coupling coefficients. . . . .	91
Figure H.1	The actual array steering matrix. . . . .	114
Figure H.2	The results of the eigenvalue decomposition of the cumulant matrix for sensor pairs (a) (1,j) and (b) (2,j), $1 \leq j \leq 4$ . . . . .	115
Figure H.3	The cost function evaluation for the aligning process when the alignment is not correct. . . . .	116

Figure H.4 The cost function evaluation for the aligning process when the alignment  
is correct. . . . . 116

# LIST OF ALGORITHMS

## ALGORITHMS

2.1	Pseudocode for IHOSS algorithm. . . . .	29
3.1	Pseudocode for MIHOSS algorithm. . . . .	49
4.1	Pseudocode for Iteration Process of HOS Approach. . . . .	66
4.2	Pseudocode for Iteration Process of SOS Approach. . . . .	74

# CHAPTER 1

## INTRODUCTION

### 1.1 Motivations and Objectives

In the last decade, the direction-of-arrival (DOA) estimation of sources with passive sensor arrays has been widely investigated and many methods have been developed. Eigenstructure based methods, such as the multiple signal classification (MUSIC) algorithm [1] and the estimation of signal parameter via rotation invariance techniques (ESPRIT) [2], have potential advantages due to their high-resolution direction finding capabilities [3], [4]. However, they require precise knowledge of the array model to achieve the theoretical performance and their performances are highly sensitive to the modeling errors [29].

In practical applications, there are many factors that change the response of the sensor array which generate imperfections in the array model. In certain applications, perfect knowledge of the sensor locations is impractical as in the case when the antennas placed on the wing tips of a plane or hydrophone arrays towed behind a ship. Identical sensors assumption is also not realistic in many practical applications. The differences in the electronic circuitry between the sensors or in receiving media such as the cables and antennas can result gain and phase mismatches between the same types of sensors. In addition to these, the interaction among the sensors especially for the antenna arrays is an important problem. In practical antenna arrays, mutual coupling represents the interaction between antennas. These imperfections should be mitigated in order to obtain satisfactory DOA estimations.

The DOA estimation in the presence of array imperfections is considered as an array calibration problem and many techniques are proposed in the literature. The proposed techniques can be grouped in two categories, offline and online array calibration. Offline array calibration

is based on collecting data from the reference sources with known DOA angles and/or signals and measuring array response [10], [11]. Then, the array imperfections are estimated by fitting the measured and modeled array responses. However, this approach is time consuming and very expensive to apply in practical systems, since the array imperfections usually change in time. On the other hand, online array calibration does not require any reference source and calibration parameters as well as DOA angles are estimated directly from the received signals. In this thesis we investigated the online array calibration problem, since it is more applicable to the practical systems.

## 1.2 Literature Overview

Many online array calibration algorithms have been proposed in the literature. Online array calibration in the presence of sensor position errors is investigated in [6], [7], [8], [41] and [42]. Previous methods in this context assume that the nominal sensor positions are known and the errors in sensor positions are small [6], [7], [9], [41]. In addition, sources are assumed to be spatially and temporally disjoint [8] or the source DOA angles are known [10], [11]. In small error approximation, the perturbations are assumed to be small and array calibration is performed by using a first order approximation. The first order approximation is not applicable as the perturbations are increased. Large error approximation [42] is proposed to circumvent the limitations of the small error approximation. However the DOA estimation problem is considered for a uniform circular array and for some fixed DOA angles. Therefore, array calibration algorithms for sensor position errors can only be applied with certain limitations on the array structure and the source characteristics. Some of these limitations are eliminated with the VESPA algorithm [12]. In [12], it is shown that the combination of HOS approach and the ESPRIT algorithm allows the computation of the DOA estimates for arbitrary sensor geometries without knowing the sensor positions. Therefore, the requirement for a special array geometry for the ESPRIT algorithm as well as the requirement for the nominal sensor positions for the array calibration algorithms are eliminated. In this approach, the cumulant matrix, which has the same information as the correlation matrix of the ESPRIT structure, is obtained from the cumulants of the array output. In [12], relative positions of the two reference sensors are required to be known. Also it is assumed that the source signals are independent. When this assumption is not satisfied, the cumulant matrix has error terms.

These error terms become significant for finite length signals and decrease the accuracy of the VESPA algorithm, generating the flooring effect for the multiple sources [13]. The approach in [12] is extended to the case of dependent source signals in [14]. In this case, it is assumed that the sensor array is composed of calibrated and uncalibrated sub-arrays where the calibrated sub-array is a uniform linear array. It is known that the method in [12] can only be used to estimate the DOA angles. In other words, sensor positions cannot be found with the approach in [12].

Online array calibration methods compensating the effect of gain/phase mismatch and/or mutual coupling are also widely investigated in the literature. However, most of the proposed techniques are based on some specific mutual coupling matrix structures and are only applicable for the special array geometries. In [35], only the mutual coupling is considered for the online array calibration and it is assumed that the mutual coupling matrix is a complex symmetric Toeplitz matrix. This method is applicable for only Uniform Linear Array (ULA). The special mutual coupling structure for ULA is slightly modified and online array calibration algorithms specialized for L-shaped [38] and Y-shaped [39] arrays are proposed. For Uniform Circular Array (UCA), mutual coupling matrix is assumed to be complex symmetric circular Toeplitz matrix [37], [40] and [29]. In [37] and [40] only the mutual coupling is considered for an array imperfection and a direct solution for estimating both DOA angles and mutual coupling coefficients is proposed by using Second Order Statistics (SOS) and Higher Order Statistics (HOS) approaches, respectively. In [29], in addition to the mutual coupling coefficients, gain/phase mismatches and the errors in sensor positions are also considered and an iterative method based on SOS approach is proposed for joint DOA and calibration parameter estimations. The algorithms proposed in [29] are applicable for only ULA and UCA. In [33], it is shown that DOA angle estimates can be found with a direct solution without being affected from the mutual coupling coefficients by using auxiliary sensors. The proposed algorithm in [33] is applicable for only Uniform Rectangular Array (URA). In [36], the performance of the online array calibration algorithms for ULA and UCA is investigated and it is shown that the assumptions made on the structure of the coupling matrix of the ULA is incorrect in practice.

### 1.3 Thesis Overview

Previous online array calibration methods in the literature have certain limitations. They are applicable to special array geometries and make small error assumptions. In this thesis, we investigate three different problems in online array calibration and propose new algorithms for each of these problems.

In the first problem, joint DOA and sensor position estimations are considered when the sensor positions are not known except the two reference sensors. The algorithm for this purpose, Iterative HOS-SOS (IHOSS), is presented. Gain/phase mismatches and mutual coupling parameters are ignored in this problem. The proposed technique finds the unknown parameters using only the sensor array outputs and the positions of the two reference sensors. There is no other a priori information including the nominal sensor positions in contrast to the array calibration approaches [6], [7], [9]. To our knowledge, this is the only work that gives a solution for this problem. IHOSS method has several advantages. It eliminates the need to know the nominal sensor positions for the joint DOA and sensor position estimation. It can perform well even for the correlated source signals unlike the work in [12]. Therefore, IHOSS algorithm can be used for the joint DOA and sensor position estimations in a more general problem setting. IHOSS algorithm considers the ambiguity problem in sensor position estimation and solves the problem by using multiple frequencies. Hence it is applicable for wideband signals.

In the second problem, the online array calibration in the presence of sensor position errors is investigated for the narrowband signals. In this respect, IHOSS algorithm is modified for the narrowband signals and the new algorithm, Modified IHOSS (MIHOSS), is proposed. Gain/phase mismatches and mutual coupling parameters are again ignored in this problem. Since the narrowband case is considered, MIHOSS needs to know the nominal sensor positions to solve the ambiguity problem in sensor position estimation. It is proved that the ambiguity problem can be solved if the perturbations in sensor positions are bounded. Parameter estimation accuracy is better even for large perturbations in contrast to the alternatives in the literature [6], [7], [9], [41], [42].

Online array calibration in the presence of gain/phase mismatch and mutual coupling is considered in the last problem. A new method, Calibration with IHOSS (CIHOSS), is proposed

to estimate the DOA angles of multiple sources, gain/phase mismatch and mutual coupling parameters jointly. The proposed method does not assume a special structure for mutual coupling matrix and therefore it is applicable for any arbitrary but known sensor geometry. It requires two reference sensors that are perfectly calibrated with known gain/phase mismatches and mutual coupling coefficients. There is no interaction between the reference and the other sensors. The magnitude of the mutual coupling between sensors is inversely proportional with the distance between sensors and may become negligible if the distance exceeds a few wavelengths [29]. The reference sensors are placed far away from the remaining sensors in order to be in accordance with the above assumption. Due to the perfectly calibrated reference sensors assumption, the proposed algorithm can be categorized as partly calibrated subarray [34]. But in [34], the interaction between calibrated subarrays is not considered and the required calibrated sensors is much higher than that of the proposed algorithm in this thesis. As it is stated in [36], the iterative methods suffer from the poor initial estimates for the DOA angles and calibration parameters. In CIHOSS, the initial estimates for DOA angles as well as gain/phase mismatches and mutual coupling coefficients are obtained directly from the sensor outputs. Therefore, CIHOSS does not take a fixed initial estimate.

All the proposed algorithms are applicable to arbitrarily deployed sensor arrays and use the Higher-Order-Statistics (HOS) and Second-Order-Statistics (SOS) approaches in an iterative framework in order to take advantage of both techniques. In HOS approach, the cumulant matrices composed of the fourth-order cumulants are used. HOS approach can obtain more information for the non-Gaussian signals as compared with the SOS approach. On the other hand, SOS approach is more robust to the statistical estimation errors than the HOS approach. In all the proposed algorithms, HOS approach is used as an initial estimator, since DOA angle estimates can be found without being affected by the errors in calibration parameters. Furthermore, the array steering matrix can be estimated directly from the sensor outputs even for the multi-source case in HOS approach. In [30], it is shown that HOS can effectively be used for the joint estimation of DOA angles, gain/phase mismatches and mutual coupling coefficients when the source signals are statistically independent. In this thesis, the source signals are not assumed to be statistically independent and the performance degradation of the HOS approach is compensated by developing a new cumulant matrix estimation technique, which is more robust to the correlation between source signals. In this technique, the error terms in the cumulant matrix due to the correlation between source signals are decreased by converting

the multi-source problem into a single-source case [15], [16] using the array steering matrix estimate. While this conversion is not perfect, it effectively decreases the undesired signal components in the measurements. The performance of the proposed algorithms depends on the accuracy of the array steering matrix estimate. If the array steering matrix is perfectly known, the error terms in the cumulant matrix are completely eliminated. The accuracy of the array steering matrix estimate is improved iteratively. SOS approach is more robust to the estimation errors than the HOS approach especially when the number of observations is small [13]. Therefore, SOS approach is used to improve the initial estimates obtained from the HOS approach. The iterative procedure in all the proposed algorithms is guaranteed to converge. Performance results show the effectiveness of the proposed algorithms. The deterministic Cramér-Rao bound expressions for the DOA and calibration parameter estimations are derived for the described problem settings. It is shown that the proposed algorithms perform well for a variety of scenarios and closely follow the CRB at high SNR.

## 1.4 Contributions

The contributions of the thesis can be summarized as follows:

- A new cumulant matrix estimation technique, which is more robust to the correlation between source signals is presented for HOS approach [5], [28].
- Joint use of HOS and SOS approaches in an iterative manner for the online array calibration of arbitrarily deployed sensor arrays is presented [5], [28], [31].
- A new online array calibration algorithm for the joint DOA and sensor position estimations when the sensor positions are unknown except the two reference sensors (IHOSS) is proposed. IHOSS eliminates the need to know the nominal sensor positions for the wideband signals [5], [28].
- An online array calibration in the presence of perturbations in sensor positions is investigated and a new algorithm, MIHOSS, [31] is presented that is applicable to large sensor errors. It is shown that the upper bound for the perturbations to achieve accurate parameter estimations is much higher than that of the alternatives in the literature.
- The ambiguity problem in sensor position estimation is considered and the conditions

for the unambiguous sensor position estimation are presented for wideband [28] and narrowband signals.

- A new online array calibration algorithm for estimating DOA angles in the presence of gain/phase mismatches and mutual coupling, CIHOSS, is presented [30]. The proposed algorithm does not assume a special structure for mutual coupling matrix and therefore it is applicable for any arbitrary but known sensor geometry. CIHOSS estimates DOA angles, gain/phase mismatch and mutual coupling parameters jointly.
- The deterministic Cramér-Rao bound expressions for the DOA and calibration parameter estimations are derived for the described problem settings. It is shown that the proposed algorithms perform well for a variety of scenarios.

## 1.5 Organization of the Thesis

The remaining of this thesis is organized as follows. In Chapter 2, IHOSS algorithm is presented. The definition of the problem as well as the constraints for IHOSS algorithm are given in Section 2.1. In Section 2.2.1, we introduce the cumulant matrix and blind DOA and array steering matrix estimates with two reference sensors. Ambiguity problem in sensor position estimation is presented and a new method for unambiguous sensor position estimation by using multiple frequencies is given in Section 2.2.2. The conditions on the frequencies for unambiguous estimation are presented in this section. SOS approach and the algorithmic steps of the IHOSS algorithm are presented in Section 2.2.3 and Section 2.2.4, respectively. The expressions for the deterministic CRB for DOA and sensor position estimations are presented in Section 2.3. The performance results of the IHOSS algorithm for various scenario is given in Section 2.4. The advantages of IHOSS algorithm are summarized in Section 2.5.

In Chapter 3, MIHOSS algorithm is presented. The problem and assumptions of the MIHOSS algorithm are defined in Section 3.1. Unambiguous sensor position estimation with nominal sensor positions is presented and also the conditions for the solution of ambiguity are given in Section 3.2.1. The algorithmic steps of the MIHOSS algorithm are summarized in Section 3.2.2 and the performance results are given in Section 3.3. The advantages of MIHOSS algorithm are summarized in Section 3.4.

In Chapter 4, CIHOSS algorithm is presented. The definitions of the problem and the as-

assumptions for CIHOSS algorithm are given in Section 4.1. The cumulant matrix for different sensor pair selections is presented in Section 4.2. HOS and SOS approaches used in CIHOSS algorithm are explained in Section 4.3.1 and Section 4.3.3, respectively. The cost function used for iterative process is explained in Section 4.3.2. In Section 4.3.4, we give the conditions for the solvability of the CIHOSS algorithm. The expressions for the deterministic CRB for DOA, gain/phase mismatch and mutual coupling are given in Section 4.4. The performance results of the CIHOSS algorithm for various scenarios are given in Section 4.5. The advantages of CIHOSS algorithm are summarized in Section 4.6.

In Section 5, conclusion for the thesis is presented. The proofs of the lemmas and theorem are given in the Appendix A - G.

## 1.6 Notations in the Thesis

The notation used in this thesis is as follows. Matrices and vectors are represented by bold uppercase and lowercase characters, respectively.  $(\cdot)^T$ ,  $(\cdot)^H$ ,  $(\cdot)^*$  and  $tr(\cdot)$  stand for the transpose, conjugate transpose, conjugate and trace operator, respectively.  $\otimes$  and  $\odot$  represent the Kronecker product and Hadamard matrix product, respectively.  $(\cdot)^\dagger$  is used to define the Moore-Penrose pseudoinverse.  $\Re(\cdot)$  and  $\Im(\cdot)$  are the real and the imaginary part operators.  $\lceil x \rceil$  is the smallest integer not less than  $x$  and  $[x]_r$  is the rounding operator that rounds  $x$  to the nearest integer.  $vect(\mathbf{X})$  is the column vector containing all entries of the matrix  $\mathbf{X}$  in a column-wise order.  $diag(x_1, x_2, \dots, x_N)$  is the  $N \times N$  diagonal matrix whose diagonal entries are  $x_n$ ,  $1 \leq n \leq N$ .  $arg(x)$  is the argument of complex variable  $x$ .  $\|\mathbf{X}\|$  is the Frobenious norm of the matrix  $\mathbf{X}$ .  $\mathbf{I}_K$  is used to define the  $K \times K$  identity matrix.

## CHAPTER 2

# ITERATIVE HOS-SOS (IHOSS) ALGORITHM FOR DIRECTION-OF-ARRIVAL ESTIMATION AND SENSOR LOCALIZATION

In this chapter, the online array calibration problem for finding the DOA angles as well as the sensor positions when the sensors are randomly deployed with unknown positions is investigated. For the solution of this problem a new technique, IHOSS, is presented. The proposed technique finds the unknown parameters using only the sensor array output and the positions of the two reference sensors. There is no other a priori information including the nominal sensor positions in contrast to the array calibration approaches in [6], [7], [9]. To our knowledge, this is the only work that gives a solution for this problem. IHOSS method has several advantages. It eliminates the need to know the nominal sensor positions for the joint DOA and sensor position estimation. It can perform well even for the correlated source signals unlike the work in [12]. Therefore, IHOSS algorithm can be used for the unknown parameter estimation in a more general problem setting.

IHOSS method uses the HOS and SOS approaches in an iterative framework in order to take the advantage of both techniques. HOS approach is used to compute the DOA and array steering matrix estimates without knowing the sensor positions except the two reference sensors. A new cumulant matrix estimation technique, which is more robust to the correlation between source signals, is presented for the HOS approach. In this technique, the error terms in the cumulant matrix due to the correlation between source signals are decreased by converting the multi-source problem into a single-source case [15], [16] using the array steering matrix estimate. While this conversion is not perfect, it effectively decreases the undesired signal components in the measurements. The performance of the IHOSS depends on the accuracy

of the array steering matrix estimate. If the array steering matrix is perfectly known, the error terms in the cumulant matrix are completely eliminated. In IHOSS, the accuracy of the array steering matrix estimate is improved iteratively with the joint use of the HOS and SOS approaches. SOS approach is more robust to the estimation errors than the HOS approach especially when the number of observations is small [13]. In order to use the SOS approach, the sensor positions should be found. A new method to find the sensor positions unambiguously is proposed by using multiple frequencies [17]. The conditions for unambiguous sensor position estimation are given. IHOSS uses an iterative process which is guaranteed to converge. The performance of the IHOSS algorithm is investigated in detail in order to show the effectiveness of the iterative approach. The deterministic Cramér-Rao bound expressions for the DOA and sensor position estimations are derived for the described problem setting. It is shown that the proposed approach performs well for a variety of scenarios and closely follows the CRB.

### 2.1 Problem Statement for IHOSS Algorithm

It is assumed that the array is composed of randomly deployed  $M$  sensors on a plane and there are  $L$  far-field sources as shown in Fig. 2.1. The transmitting source signals are assumed to

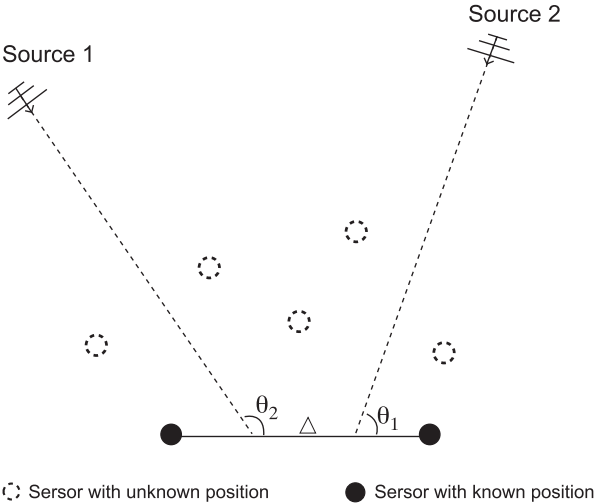


Figure 2.1: Array model for IHOSS algorithm.

be wideband. The received signal at the  $m^{\text{th}}$  sensor can be written as,

$$x_m(t) = \sum_{i=1}^L s_i(t - \tau_{mi}) + v_m(t), \quad m = 1, \dots, M \quad (2.1)$$

where  $s_i(t)$  and  $v_m(t)$  are the source and noise signals, respectively.  $\tau_{mi}$  is the propagation delay from the  $i^{\text{th}}$  source to the  $m^{\text{th}}$  sensor and it can be written as [26],

$$\tau_{mi} = \frac{p_{m,x} \cos(\theta_i) + p_{m,y} \sin(\theta_i)}{\vartheta_s} \quad (2.2)$$

where  $\theta_i$  is the DOA angle of the  $i^{\text{th}}$  source in azimuth.  $\mathbf{p}_m = [p_{m,x}, p_{m,y}]$  is the two dimensional position of the  $m^{\text{th}}$  sensor and  $\vartheta_s$  is the speed of propagation.

It is assumed that multiple wideband signals are observed with overlapping spectra. Narrowband bandpass filters with different center frequencies,  $f_j$ ,  $j = 1, \dots, F$ , are used to extract the narrowband signals. If we assume that the frequency response of the filters is flat over the passband and the signal spectrum varies over the filter passband, the output of the  $m^{\text{th}}$  sensor for the  $j^{\text{th}}$  filter can be written as [25],

$$x_{m,f_j}(t) = \sum_{i=1}^L e^{-j2\pi f_j \tau_{mi}} s_{i,f_j}(t) + v_{m,f_j}(t) \quad (2.3)$$

where  $s_{i,f_j}(t)$  and  $v_{m,f_j}(t)$  are the outputs of the  $j^{\text{th}}$  filter when the inputs are  $s_i(t)$  and  $v_m(t)$ , respectively. By substituting (2.2) into (2.3), the received signal vector for the sensor array at frequency  $f_j$  can be written in a more compact form as,

$$\mathbf{x}_{f_j}(t) = \mathbf{A}_{f_j}(\boldsymbol{\Theta}, \mathbf{P}) \mathbf{s}_{f_j}(t) + \mathbf{v}_{f_j}(t), \quad t = 1, \dots, N \quad (2.4)$$

where  $N$  is the number of snapshots,  $\mathbf{s}_{f_j}(t) = [s_{1,f_j}(t), \dots, s_{L,f_j}(t)]^T$  is the  $L \times 1$  vector of  $L$  source signals for the frequency  $f_j$ .  $\mathbf{v}_{f_j}(t) = [v_{1,f_j}(t), \dots, v_{M,f_j}(t)]^T$  is the  $M \times 1$  vector of noise for the frequency  $f_j$ , which is assumed to be Gaussian.  $\mathbf{A}_{f_j}(\boldsymbol{\Theta}, \mathbf{P})$  is the  $M \times L$  array steering matrix for the frequency  $f_j$ . Source signals are assumed to be non-Gaussian and they can be correlated but not coherent. Noise is assumed to be statistically independent with the source signals. Given the DOA vector,  $\boldsymbol{\Theta} = [\theta_1, \dots, \theta_L]$ , and the sensor positions,  $\mathbf{P} = [\mathbf{p}_1^T, \dots, \mathbf{p}_M^T]^T$ , the array steering matrix for frequency  $f_j$  is written as,

$$\mathbf{A}_{f_j}(\boldsymbol{\Theta}, \mathbf{P}) = \begin{bmatrix} a_{f_j}(\theta_1, \mathbf{p}_1) & \dots & a_{f_j}(\theta_L, \mathbf{p}_1) \\ \vdots & \ddots & \vdots \\ a_{f_j}(\theta_1, \mathbf{p}_M) & \dots & a_{f_j}(\theta_L, \mathbf{p}_M) \end{bmatrix} \quad (2.5)$$

where the array steering matrix element for  $m^{\text{th}}$  sensor and  $i^{\text{th}}$  source at frequency  $f_j$  is written as,

$$a_{f_j}(\theta_i, \mathbf{p}_m) = \exp \left\{ j2\pi f_j \frac{p_{m,x} \cos(\theta_i) + p_{m,y} \sin(\theta_i)}{\vartheta_s} \right\} \quad (2.6)$$

Two sensors are selected as the reference with known positions. In order to avoid the ambiguity problem in DOA estimation, it is also assumed that the distance between the reference sensors is less than or equal to  $\lambda/2$ , where  $\lambda$  is the wavelength corresponding to the largest frequency of interest, i.e.,  $\lambda = \vartheta_s / \max_j(f_j)$ .

The objective in IHOSS is to estimate the DOA angles of  $L$  sources and the positions of the  $M - 2$  sensors simultaneously given the array output and the positions of the two reference sensors.

## 2.2 IHOSS Algorithm

In this section, IHOSS algorithm is introduced for a solution to the problem described in Section 2.1. IHOSS is an iterative algorithm that jointly uses HOS and SOS approaches at each iteration sequentially. The idea behind the IHOSS algorithm is to use the advantages of both HOS and SOS approaches in order to improve the accuracy of the parameter estimation.

IHOSS uses HOS approach to find the DOA and array steering matrix estimates for the arbitrary sensor geometries without knowing the sensor positions except the two reference sensors. In this respect, fourth-order cumulants are used together with the ESPRIT algorithm. It is known that the ESPRIT algorithm can be employed for DOA estimation for the given problem setting as long as the source signals are independent [12]. The performance of [12] degrades significantly due to finite length effects and correlation between source signals [13]. This point is discussed in Section 2.2.1.

In order to overcome the limitations in [12], IHOSS proposes a new cumulant matrix estimation technique. This technique is more robust to the correlation between source signals. It is based on estimating the cumulant matrix as the sum of the cumulant matrices corresponding to the case where each source is acting alone. SOS approach is known to be more robust to the estimation errors than the HOS approach for finite length signals [13]. Therefore SOS approach is used to improve the DOA and array steering matrix estimates obtained from HOS

approach. Sensor positions should be found in order to use the SOS approach. A new sensor position estimation algorithm is proposed for this purpose. The sensor positions are found unambiguously using multiple frequencies [17]. The details of the sensor position estimation algorithm is given in Section 2.2.2. Initially, IHOSS assumes that the array steering matrix is zero. Then the array steering matrix estimation is iteratively improved with the joint use of HOS and SOS approaches. A MUSIC cost function is used to select the best array steering matrix at each iteration. This is done in such a way that the non-negative cost function is improved at each iteration. Therefore IHOSS algorithm is guaranteed to converge. The details of the iterative approach and the cost function are explained in Section 2.2.4.

### 2.2.1 HOS Based Blind DOA Estimation

In IHOSS, HOS approach is used to estimate the DOA angles without knowing the sensor positions except the two reference sensors. To this end, fourth order cumulants are used, since for the non-Gaussian signals, more statistical information can be obtained as compared with SOS approach. In IHOSS, the additional information provided by the fourth-order cumulants is used to generate virtual sensors at certain locations and to obtain the relation between the actual and virtual sensors. Virtual sensor generation concept is illustrated for a single source case in Fig. 2.2. It is assumed that there are three sensors located at different positions to measure the source signal,  $s(t)$ . The measured signals are  $r(t)$ ,  $x(t)$  and  $y(t)$  and there is no sensor to measure the signal  $v(t)$ .

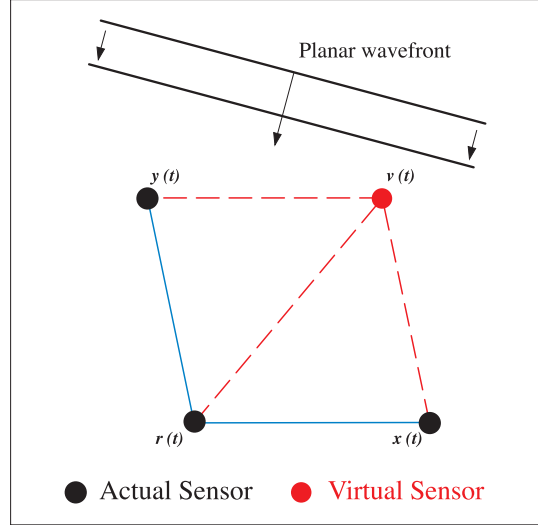


Figure 2.2: Virtual sensor concept.

In this case, the cross-correlation between the measured signal  $r(t)$  and the virtual signal  $v(t)$  can be obtained from the fourth-order cumulants [12], i.e.,

$$E\{v(t)r^*(t)\} = \frac{\sigma_s^2}{\gamma_{4,s}} \text{Cum}(x(t), r^*(t), y(t), r^*(t)) \quad (2.7)$$

where

$$\begin{aligned} \text{Cum}(x(t), r^*(t), y(t), r^*(t)) &= E\{x(t)r^*(t)y(t)r^*(t)\} \\ &\quad - E\{x(t)r^*(t)\}E\{y(t)r^*(t)\} \\ &\quad - E\{x(t)y(t)\}E\{r^*(t)r^*(t)\} \\ &\quad - E\{x(t)r^*(t)\}E\{r^*(t)y(t)\} \end{aligned} \quad (2.8)$$

$$\sigma_s^2 = E \{s(t)s^*(t)\} \quad (2.9)$$

$$\gamma_{4,s} = \text{Cum}(s(t), s^*(t), s(t), s^*(t)) \quad (2.10)$$

In a similar way the cross correlation between two measured signals can also be found from the fourth-order cumulants, i.e.,

$$E \{y(t)r^*(t)\} = \frac{\sigma_s^2}{\gamma_{4,s}} \text{Cum}(y(t), r^*(t), r(t), r^*(t)) \quad (2.11)$$

The details of the “virtual cross-correlation computation” in (2.7) and (2.11) can be found in [12]. Using this concept, it is possible to generate an ESPRIT structure for any arbitrary sensor geometry as shown in Fig. 2.3, which is called as Virtual-ESPRIT (VESPA) in [12].

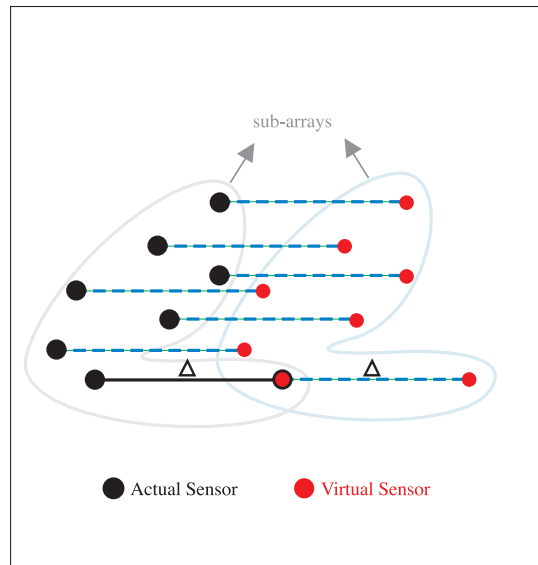


Figure 2.3: Virtual ESPRIT structure for randomly deployed sensors.

In this structure, one of the sub-arrays is composed of the actual sensors and the other sub-array is composed of virtual sensors [18]. The virtual sub-array is aligned with the selected sensor pairs and the distance between the actual and virtual sub-arrays is determined by the distance between selected sensor pairs. By changing the sensor pairs, we can obtain  $M(M - 1)/2$  distinct virtual sub-arrays. Four of the possible distinct virtual sub-arrays are illustrated in Fig. 2.4.

In Virtual-ESPRIT structure, the relation between the actual and virtual sub-arrays is obtained from the cumulant matrix instead of covariance matrix in SOS approach. Cumulant matrix is composed of the fourth-order cumulants corresponding to the selected virtual sensors. When

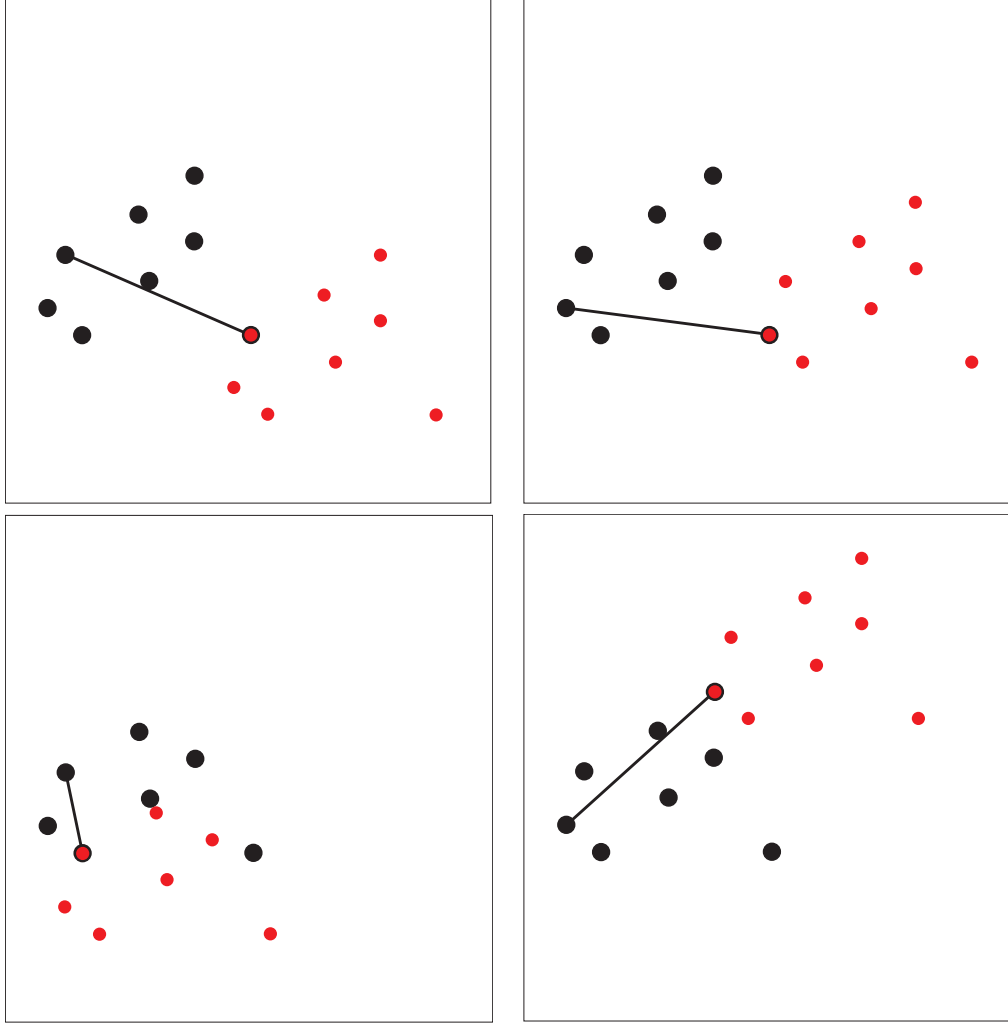


Figure 2.4: Different Virtual ESPRIT structures for different pairs of the actual sensors.

the sensors 1 and 2 are selected as the sensor pair, the cumulant matrix is written as,

$$\mathbf{C} = \begin{bmatrix} c_{11,11} & c_{11,12} & \dots & c_{11,1M} & c_{12,11} & c_{12,12} & \dots & c_{12,1M} \\ c_{11,21} & c_{11,22} & \dots & c_{11,2M} & c_{12,21} & c_{12,22} & \dots & c_{12,2M} \\ \vdots & \vdots & \ddots & \vdots & \vdots & \vdots & \ddots & \vdots \\ c_{11,M1} & c_{11,M2} & \dots & c_{11,MM} & c_{12,M1} & c_{12,M2} & \dots & c_{12,MM} \\ c_{21,11} & c_{21,12} & \dots & c_{21,1M} & c_{22,11} & c_{22,12} & \dots & c_{22,1M} \\ c_{21,21} & c_{21,22} & \dots & c_{21,2M} & c_{22,21} & c_{22,22} & \dots & c_{22,2M} \\ \vdots & \vdots & \ddots & \vdots & \vdots & \vdots & \ddots & \vdots \\ c_{21,M1} & c_{21,M2} & \dots & c_{21,MM} & c_{22,M1} & c_{22,M2} & \dots & c_{22,MM} \end{bmatrix} \quad (2.12)$$

where

$$c_{11,ij} = \text{Cum}(x_1(t), x_1^*(t), x_i(t), x_j^*(t)) \quad (2.13)$$

$$c_{12,ij} = \text{Cum}(x_1(t), x_2^*(t), x_i(t), x_j^*(t)) \quad (2.14)$$

$$c_{21,ij} = \text{Cum}(x_2(t), x_1^*(t), x_i(t), x_j^*(t)) \quad (2.15)$$

$$c_{22,ij} = \text{Cum}(x_2(t), x_2^*(t), x_i(t), x_j^*(t)) \quad (2.16)$$

Using the properties of cumulants in [12], the cumulant matrix in (2.12) can be written in a more compact form [5], i.e.,

$$\mathbf{C} = \begin{bmatrix} (\mathbf{A} \otimes \mathbf{a}_{r_1}^*) \mathbf{C}_s (\mathbf{A} \otimes \mathbf{a}_{r_1}^*)^H & (\mathbf{A} \otimes \mathbf{a}_{r_1}^*) \mathbf{C}_s (\mathbf{A} \otimes \mathbf{a}_{r_2}^*)^H \\ (\mathbf{A} \otimes \mathbf{a}_{r_2}^*) \mathbf{C}_s (\mathbf{A} \otimes \mathbf{a}_{r_1}^*)^H & (\mathbf{A} \otimes \mathbf{a}_{r_2}^*) \mathbf{C}_s (\mathbf{A} \otimes \mathbf{a}_{r_2}^*)^H \end{bmatrix} \quad (2.17)$$

where  $\mathbf{a}_{r_i}$  is the  $i^{\text{th}}$  row of the array steering matrix,  $\mathbf{A}$ , in (2.5) and  $\mathbf{C}_s$  is the  $L^2 \times L^2$  source cumulant matrix in the form of,

$$\mathbf{C}_s(i, j) = \text{Cum}(s_k(t), s_l^*(t), s_m(t), s_n^*(t)) \quad (2.18)$$

$$i = L(m-1) + l, \quad 1 \leq m, l \leq L$$

$$j = L(n-1) + k, \quad 1 \leq n, k \leq L$$

Note that the frequency dependency of the cumulant matrix in (2.17) is dropped for simplicity. The same form of the cumulant matrix is obtained for each frequency,  $f_j$ .

The source cumulant matrix in (2.17),  $\mathbf{C}_s$ , involves an error term,  $\mathbf{C}_s^e$ , due to the dependency of the source signals, i.e.,

$$\mathbf{C}_s = \mathbf{C}_s^d + \mathbf{C}_s^e \quad (2.19)$$

In (2.19),  $\mathbf{C}_s^d$  is the desired source cumulant matrix which represents the part assuming that the source signals are statistically independent, i.e.,

$$\mathbf{C}_s^d = \text{diag}(\gamma_1, 0, \dots, 0, \gamma_2, 0, \dots, 0, \gamma_L) \quad (2.20)$$

and

$$\gamma_i = \text{Cum}(s_i(t), s_i^*(t), s_i(t), s_i^*(t)) \quad (2.21)$$

$$= \mathbf{C}_s^d(L(i-1) + i, L(i-1) + i), \quad 1 \leq i \leq L$$

As shown in (2.21), the non-zero diagonal elements,  $\gamma_i$ , are located with the indices  $L(i-1) + i$  for  $1 \leq i \leq L$ . The relation in (2.20) is based on the fact that if a subset of random variables

are independent of the rest, then the cumulant of these random variables is equal to zero as stated in [12] as [CP5]. When the source signals are independent,  $\mathbf{C}_s^e = \mathbf{0}$ , and  $\mathbf{C}_s$  in (2.17) has the desired form.

When the source signals are not independent, (2.19) can be used in (2.17) to obtain the following cumulant matrix,

$$\mathbf{C} = \mathbf{C}^d + \mathbf{C}^e \quad (2.22)$$

$\mathbf{C}^d$  is the desired cumulant matrix assuming that the source signals are statistically independent and  $\mathbf{C}^e$  represents the error term due to the dependency of the source signals, i.e.,

$$\mathbf{C}^d = \begin{bmatrix} \mathbf{A}\mathbf{R}_s^{HOS}\mathbf{A}^H & \mathbf{A}\mathbf{R}_s^{HOS}\mathbf{D}\mathbf{A}^H \\ \mathbf{A}\mathbf{D}^H\mathbf{R}_s^{HOS}\mathbf{A}^H & \mathbf{A}\mathbf{D}^H\mathbf{R}_s^{HOS}\mathbf{D}\mathbf{A}^H \end{bmatrix} \quad (2.23)$$

$$\mathbf{C}^e = \begin{bmatrix} (\mathbf{A} \otimes \mathbf{a}_{r_1}^*) \mathbf{C}_s^e (\mathbf{A} \otimes \mathbf{a}_{r_1}^*)^H & (\mathbf{A} \otimes \mathbf{a}_{r_1}^*) \mathbf{C}_s^e (\mathbf{A} \otimes \mathbf{a}_{r_2}^*)^H \\ (\mathbf{A} \otimes \mathbf{a}_{r_2}^*) \mathbf{C}_s^e (\mathbf{A} \otimes \mathbf{a}_{r_1}^*)^H & (\mathbf{A} \otimes \mathbf{a}_{r_2}^*) \mathbf{C}_s^e (\mathbf{A} \otimes \mathbf{a}_{r_2}^*)^H \end{bmatrix} \quad (2.24)$$

where  $L \times L$  diagonal matrices  $\mathbf{R}_s^{HOS}$  and  $\mathbf{D}$  are defined as,

$$\mathbf{R}_s^{HOS} = \text{diag}(\gamma_1, \gamma_2, \dots, \gamma_L) \quad (2.25)$$

$$\mathbf{D} = \text{diag}\left(e^{j2\pi f_j \Delta \frac{\cos(\theta_1)}{\theta_s}}, \dots, e^{j2\pi f_j \Delta \frac{\cos(\theta_L)}{\theta_s}}\right) \quad (2.26)$$

The reference sensors are assumed to be located at  $(0, 0)$  and  $(\Delta, 0)$  on the coordinate system for simplicity where  $\Delta \leq \lambda/2$ .

Note that  $\mathbf{C}^d$  in (2.23) has the similar form of a correlation matrix used in the ESPRIT algorithm. Therefore, it can be used to find the DOA and array steering matrix estimates as in [2]. However, the desired cumulant matrix,  $\mathbf{C}^d$ , can only be obtained when the source signals are independent, i.e.,  $\mathbf{C}_s^e = \mathbf{0}$ . In practical situations, where there is limited number of observations, source signals cannot be assumed to be independent. In this case, the cumulant matrix in (2.22) is not in the form of a correlation matrix suitable for the ESPRIT algorithm. In [12], the error term,  $\mathbf{C}^e$ , is assumed to be zero even for the limited number of observations and the DOA estimates are found from the cumulant matrix in (2.22) by using the ESPRIT algorithm. It is known that the nonzero  $\mathbf{C}^e$  matrix significantly degrades the performance of the DOA estimation [13].

In the IHOSS algorithm, a new cumulant matrix estimation technique, which is more robust to the correlation between source signals, is proposed. In this technique, the effect of the error term in (2.22) is decreased by exploiting the fact given in Lemma-1.

**Lemma-1:** Assume that the noise is Gaussian and independent of the source signals. Then, the desired cumulant matrix,  $\mathbf{C}^d$ , in (2.23) can be written as the sum of the cumulant matrices,  $\mathbf{C}^{(i)}$ ,  $1 \leq i \leq L$ , i.e.,

$$\mathbf{C}^d = \sum_{i=1}^L \mathbf{C}^{(i)} \quad (2.27)$$

where  $\mathbf{C}^{(i)}$  corresponds to the cumulant matrix in (2.17) when only the  $i^{\text{th}}$  source signal is received.

Therefore, if the array outputs for each source is available, it is possible to obtain the desired cumulant matrix,  $\mathbf{C}^d$  in (2.23), even when the source signals are not independent. The proof of Lemma-1 is given in Appendix A.

For the practical applications, IHOSS estimates the array outputs for each source by suppressing the components of the other source signals in the measurements [15], [16]. If we assume that  $\hat{\mathbf{A}}$  is the array steering matrix estimate, IHOSS estimates the source signals as,

$$\hat{\mathbf{s}}(t) = \hat{\mathbf{A}}^\dagger \mathbf{x}(t) \quad (2.28)$$

Then, the array output for the  $i^{\text{th}}$  source is found as,

$$\hat{\mathbf{x}}^{(i)}(t) = \mathbf{x}(t) - \sum_{\substack{j=1 \\ j \neq i}}^L \hat{\mathbf{a}}_j \hat{\mathbf{s}}_j(t) \quad (2.29)$$

where  $\hat{\mathbf{a}}_j$  is the  $j^{\text{th}}$  column of the array steering matrix estimate,  $\hat{\mathbf{A}}$ , and  $\hat{\mathbf{s}}_j(t)$  is the estimate of the  $j^{\text{th}}$  source signal found from (2.28). By substituting (2.28) into (2.29), the array output for the  $i^{\text{th}}$  source can be rewritten as,

$$\hat{\mathbf{x}}^{(i)}(t) = \mathbf{Q}_i \mathbf{x}(t) \quad (2.30)$$

where  $M \times M$  matrix,  $\mathbf{Q}_i$  is defined as,

$$\mathbf{Q}_i = \mathbf{I} - \hat{\mathbf{A}} \mathbf{Z}_i \hat{\mathbf{A}}^\dagger \quad (2.31)$$

$\mathbf{Z}_i$  is the  $L \times L$  diagonal matrix whose diagonal elements are one except the  $i^{\text{th}}$  element. The  $i^{\text{th}}$  element is set to zero. The estimate of the desired cumulant matrix,  $\mathbf{C}_{est}^d$ , is found from (2.27) by using (2.30) for the computation of  $\mathbf{C}^{(i)}$ , i.e.,

$$\mathbf{C}_{est}^d = \sum_{i=1}^L \begin{bmatrix} \bar{\mathbf{Q}}_1^{(i)} \mathbf{C}_x \left( \bar{\mathbf{Q}}_1^{(i)} \right)^H & \bar{\mathbf{Q}}_1^{(i)} \mathbf{C}_x \left( \bar{\mathbf{Q}}_2^{(i)} \right)^H \\ \bar{\mathbf{Q}}_2^{(i)} \mathbf{C}_x \left( \bar{\mathbf{Q}}_1^{(i)} \right)^H & \bar{\mathbf{Q}}_1^{(i)} \mathbf{C}_x \left( \bar{\mathbf{Q}}_1^{(i)} \right)^H \end{bmatrix} \quad (2.32)$$

where  $\overline{\mathbf{Q}}_j^{(i)} = \mathbf{Q}_i \otimes \mathbf{q}_j^{(i)*}$  and  $\mathbf{q}_j^{(i)*}$  is the complex conjugate of the  $j^{\text{th}}$  row of the matrix  $\mathbf{Q}_i$ .  $\mathbf{C}_x$  is the  $M^2 \times M^2$  cumulant matrix which contains all the cumulants of the array output, i.e.,

$$\mathbf{C}_x(k, l) = \text{Cum}(x_{l_1}, x_{k_1}^*, x_{k_2}, x_{l_2}^*) \quad (2.33)$$

$$k = (k_2 - 1)M + k_1 \quad , 1 \leq k_1, k_2 \leq M$$

$$l = (l_2 - 1)M + l_1 \quad , 1 \leq l_1, l_2 \leq M$$

$\mathbf{C}_x$  can be written in matrix form as,

$$\mathbf{C}_x = (\mathbf{A} \otimes \mathbf{A}^*) \mathbf{C}_s (\mathbf{A} \otimes \mathbf{A}^*)^H \quad (2.34)$$

The derivation of (2.32) is given in Appendix B.

IHOSS algorithm finds the DOA and array steering matrix estimates from the eigenvalue decomposition of  $\mathbf{C}_{est}^d$ , i.e.,  $\mathbf{C}_{est}^d \mathbf{S} = \mathbf{S} \mathbf{\Lambda}_s$  as in the ESPRIT algorithm [2].  $\mathbf{\Lambda}_s$  is the diagonal matrix composed of the  $L$  largest eigenvalues of the matrix  $\mathbf{C}_{est}^d$  and  $2M \times L$  matrix  $\mathbf{S} = [\mathbf{S}_1^T \quad \mathbf{S}_2^T]^T$  is obtained from the eigenvectors corresponding to these eigenvalues.  $\mathbf{S}_1$  and  $\mathbf{S}_2$  are  $M \times L$  matrices. The DOA and the array steering matrix estimates are found by applying the ESPRIT algorithm [2], i.e.,

$$\hat{\theta}_i = \cos^{-1} \left( -\frac{\angle \Phi(i, i)}{2\pi f_j \Delta} \vartheta_s \right) \quad (2.35)$$

$$\overline{\mathbf{A}} = \mathbf{S}_1 \mathbf{\Psi} \quad (2.36)$$

where  $\angle \Phi(i, i)$  is the phase angle of the  $i^{\text{th}}$  diagonal element of the matrix  $\Phi$ .  $L \times L$  diagonal matrix,  $\Phi$ , and  $L \times L$  matrix,  $\Psi$ , are related as,

$$\mathbf{S}_1^\dagger \mathbf{S}_2 \mathbf{\Psi} = \mathbf{\Phi} \quad (2.37)$$

As it can be seen from (2.37),  $\Phi$  is the diagonal matrix composed of the eigenvalues of the matrix  $\mathbf{S}_1^\dagger \mathbf{S}_2$  and  $\Psi$  is the matrix whose columns are the corresponding eigenvectors.

Note that knowing the distance and the direction between the two reference sensors are sufficient for the DOA estimation as in (2.35). However, it is not the case for the array steering matrix estimation. In the ESPRIT algorithm the array steering matrix estimation is found up to an unknown scale factor as in (2.36). To find the scale factor, in addition to the distance and the direction between the two reference sensors, it is required to know one of the reference sensor position. Since it is assumed that the first reference sensor is located at (0,0), the first

row of the array steering matrix has to consist of all ones. Then, the actual array steering matrix can be estimated from (2.36), i.e.,

$$\hat{\mathbf{A}} = \bar{\mathbf{A}}\mathbf{H}^{-1} \quad (2.38)$$

where  $\mathbf{H} = \text{diag}(\bar{a}_{11}, \bar{a}_{12}, \dots, \bar{a}_{1L})$  and  $\bar{a}_{ij}$  is the  $i^{\text{th}}$  row and  $j^{\text{th}}$  column of matrix  $\bar{\mathbf{A}}$ .

Note that, the proposed cumulant matrix in (2.32) can be seen as the weighted sum of all the possible cumulants that can be found from the given array output as in (2.33). The weight terms,  $\mathbf{Q}_i \otimes \mathbf{q}_j^{(i)*}$ ,  $j \in 1, 2$  are determined from the array steering matrix estimation as in (2.31). The effect of the weight terms can be easily seen by substituting (2.34) into (2.32), which results,

$$\mathbf{C}_{est}^d = \sum_{i=1}^L \begin{bmatrix} \bar{\mathbf{A}}_1^{(i)} \mathbf{C}_s \left( \bar{\mathbf{A}}_1^{(i)} \right)^H & \bar{\mathbf{A}}_1^{(i)} \mathbf{C}_s \left( \bar{\mathbf{A}}_2^{(i)} \right)^H \\ \bar{\mathbf{A}}_2^{(i)} \mathbf{C}_s \left( \bar{\mathbf{A}}_1^{(i)} \right)^H & \bar{\mathbf{A}}_1^{(i)} \mathbf{C}_s \left( \bar{\mathbf{A}}_1^{(i)} \right)^H \end{bmatrix} \quad (2.39)$$

where  $\bar{\mathbf{A}}_j^{(i)} = \mathbf{Q}_i \mathbf{A} \otimes \mathbf{q}_j^{(i)*} \mathbf{A}^*$ ,  $j \in \{1, 2\}$ .

If  $\mathbf{Q}_i$  in (2.31) is obtained by taking the initial estimate for the array steering matrix as  $\hat{\mathbf{A}} = \mathbf{0}$  and substituted in (2.39), we obtain  $\mathbf{C}_{est}^d = L\mathbf{C}$  which is used in [12]. On the other hand, the desired cumulant matrix,  $\mathbf{C}^d$ , in (2.23), is obtained when  $\hat{\mathbf{A}} = \mathbf{A}$ , namely,  $\mathbf{C}_{est}^d = \mathbf{C}^d$ . In this case, the desired cumulant matrix,  $\mathbf{C}^d$ , is obtained even when the source signals are dependent. In this respect, the proposed cumulant matrix estimate is a generalized cumulant matrix estimate which improves the parameter estimates depending on the accuracy of the array steering matrix estimation.

## 2.2.2 Unambiguous Sensor Localization

In this section, the algorithm for unambiguous sensor localization is introduced. It is assumed that, the DOA and array steering matrix estimates are obtained for multiple frequencies [17]. The conditions for the frequencies for unambiguous localization are also given in this section.

Let  $f_j$ ,  $1 \leq j \leq F$ , represent the frequencies, where the array output is observed for the same sources. Then, the elements of the array steering matrix estimate corresponding to  $m^{\text{th}}$  sensor and  $i^{\text{th}}$  source with frequency  $f_j$  can be written in the following form,

$$\hat{a}(\hat{\theta}_i(f_j), \mathbf{p}_m) = \exp \left\{ j2\pi \frac{f_j}{\vartheta_s} \left( \mathbf{p}_m \mathbf{u}(\hat{\theta}_i(f_j)) - \frac{\vartheta_s}{f_j} k_{f_j}^{(i)} \right) \right\} \quad (2.40)$$

where  $k_{f_j}^{(i)}$  is an integer specified for the frequency  $f_j$  and the  $i^{\text{th}}$  source due to  $2\pi$  ambiguity.  $\hat{\theta}_i(f_j)$  is the DOA angle estimate of the  $i^{\text{th}}$  source for frequency  $f_j$ .  $\mathbf{u}(\hat{\theta}_i(f_j))$  is the unit direction vector estimate, i.e.,  $\mathbf{u}(\hat{\theta}_i(f_j)) = [\cos(\hat{\theta}_i(f_j)) \quad \sin(\hat{\theta}_i(f_j))]^T$ . When all the incoming signals for frequency  $f_j$  are considered, the following relation can be specified from (2.40),

$$\mathbf{p}_m \mathbf{U}(\hat{\mathbf{\Theta}}(f_j)) = \frac{\vartheta_s}{2\pi f_j} \hat{\mathbf{\Xi}}_m(f_j) + \frac{\vartheta_s}{f_j} \mathbf{k}_{f_j}, \quad 1 \leq j \leq F \quad (2.41)$$

where

$$\mathbf{U}(\hat{\mathbf{\Theta}}(f_j)) = \begin{bmatrix} \mathbf{u}(\hat{\theta}_1(f_j)) & \mathbf{u}(\hat{\theta}_2(f_j)) & \dots & \mathbf{u}(\hat{\theta}_L(f_j)) \end{bmatrix} \quad (2.42)$$

$$\hat{\mathbf{\Xi}}_m(f_j) = \begin{bmatrix} \hat{\xi}_m^{(1)}(f_j) & \hat{\xi}_m^{(2)}(f_j) & \dots & \hat{\xi}_m^{(L)}(f_j) \end{bmatrix} \quad (2.43)$$

$$\mathbf{k}_{f_j} = \begin{bmatrix} k_{f_j}^{(1)} & k_{f_j}^{(2)} & \dots & k_{f_j}^{(L)} \end{bmatrix} \quad (2.44)$$

$\hat{\xi}_m^{(i)}(f_j)$  is the phase term of the array steering matrix element in (2.40), i.e.,

$$\hat{\xi}_m^{(i)}(f_j) = \angle \hat{a}(\hat{\theta}_i(f_j), \mathbf{p}_m) \quad (2.45)$$

Then, the position of the  $m^{\text{th}}$  sensor is found from (2.41) as

$$\hat{\mathbf{p}}_m(\mathbf{k}_{f_j}) = \left( \frac{\vartheta_s}{2\pi f_j} \hat{\mathbf{\Xi}}_m(f_j) + \frac{\vartheta_s}{f_j} \mathbf{k}_{f_j} \right) \mathbf{U}^\dagger(\hat{\mathbf{\Theta}}(f_j)) \quad (2.46)$$

Note that the position estimate in (2.46) takes different values for different  $\mathbf{k}_{f_j}$  values. Therefore, the  $m^{\text{th}}$  sensor position estimate in (2.46) is ambiguous and  $\mathbf{k}_{f_j}$  is defined as the ambiguity term for the frequency  $f_j$ . The possible values of  $\mathbf{k}_{f_j}$  is determined by considering the error in least squares solution,  $\epsilon$ , i.e.,

$$\mathbf{k}_{f_j} = \left\{ \mathbf{k} \in Z \left\| \left\| \hat{\mathbf{p}}_m(\mathbf{k}) \mathbf{U}(\hat{\mathbf{\Theta}}(f_j)) - \frac{\vartheta_s}{2\pi f_j} \hat{\mathbf{\Xi}}_m(f_j) - \frac{\vartheta_s}{f_j} \mathbf{k} \right\|^2 \leq \epsilon \right\} \quad (2.47)$$

Substituting (2.46) into (2.47) simplifies the relation as,

$$\mathbf{k}_{f_j} = \left\{ \mathbf{k} \in Z \left\| \left( \frac{\vartheta_s}{2\pi f_j} \hat{\mathbf{\Xi}}_m(f_j) + \frac{\vartheta_s}{f_j} \mathbf{k} \right) (\mathbf{I}_{L \times L} - \mathbf{U}^\dagger(\hat{\mathbf{\Theta}}(f_j)) \mathbf{U}(\hat{\mathbf{\Theta}}(f_j))) \left( \frac{\vartheta_s}{2\pi f_j} \hat{\mathbf{\Xi}}_m(f_j) + \frac{\vartheta_s}{f_j} \mathbf{k} \right)^H \right\| \leq \epsilon \right\} \quad (2.48)$$

where  $\mathbf{I}_{L \times L}$  is the  $L \times L$  identity matrix. Note that when there are two sources,  $L = 2$ , all integers satisfy the condition in (2.48) due to the fact that  $\mathbf{U}^\dagger(\hat{\mathbf{\Theta}}) \mathbf{U}(\hat{\mathbf{\Theta}}) = \mathbf{I}_{2 \times 2}$  as shown in Fig. 2.5-a. Ambiguous sensor positions are illustrated in Fig. 2.5-b for three sources. In this case, as stated in (2.48) only certain integer values generate ambiguous sensor positions.

Therefore, different ambiguous sensor positions are obtained for different number of sources as shown in Fig. 2.6.

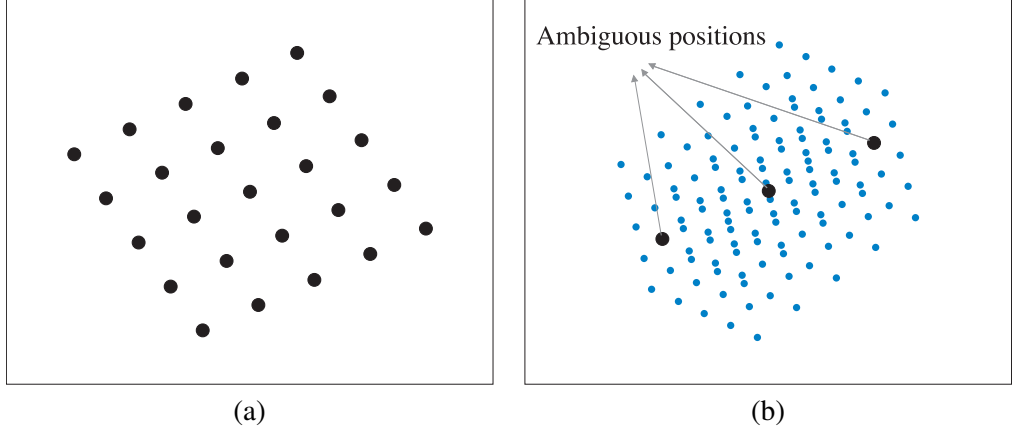


Figure 2.5: Ambiguous sensor positions for (a) two and (b) three sources.

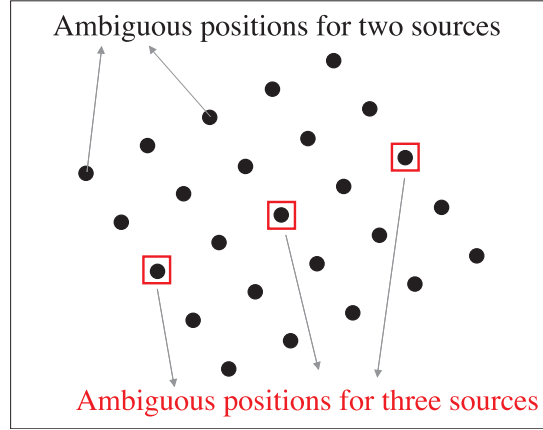


Figure 2.6: Different ambiguous sensor positions for two and three sources.

The ambiguity problem can only be solved by finding unique  $\{\mathbf{k}_{f_j}\}_{j=1}^F$  values for which the right hand side of (2.41) is the same for different frequencies. When there are errors in estimated parameters,  $\hat{\xi}_m^{(i)}(f_j)$ , unambiguous sensor positions can be found as long as the errors are bounded by a limiting value. This fact is discussed in Theorem-1 given below.

The desired  $\{\mathbf{k}_{f_j}\}_{j=1}^F$  values are found by solving the following minimization problem, i.e.,

$$\{\bar{\mathbf{k}}_{f_j}\}_{j=1}^F = \arg \min_{\{\mathbf{k}_{f_j}\}_{j=1}^F} \sum_{i=1}^L \sum_{j=2}^F \left( \frac{\vartheta_s}{2\pi f_1} \hat{\xi}_m^{(i)}(f_1) + \frac{\vartheta_s}{f_1} k_{f_1}^{(i)} - \frac{\vartheta_s}{2\pi f_j} \hat{\xi}_m^{(i)}(f_j) - \frac{\vartheta_s}{f_j} k_{f_j}^{(i)} \right)^2 \quad (2.49)$$

Since the minimum value of the sum of positive quantities is obtained by minimizing each quantity separately, (2.49) can be rewritten as,

$$\{\bar{k}_{f_j}^{(i)}\}_{j=1}^F = \arg \min_{\{k_{f_j}^{(i)}\}_{j=1}^F} \sum_{j=2}^F \left( \frac{\vartheta_s}{2\pi f_1} \hat{\xi}_m^{(i)}(f_1) + \frac{\vartheta_s}{f_1} k_{f_1}^{(i)} - \frac{\vartheta_s}{2\pi f_j} \hat{\xi}_m^{(i)}(f_j) - \frac{\vartheta_s}{f_j} k_{f_j}^{(i)} \right)^2, \quad 1 \leq i \leq L \quad (2.50)$$

Then, the unambiguous position of the  $m^{\text{th}}$  sensor is found by substituting (2.50) into (2.41), i.e.,

$$\hat{\mathbf{p}}_m = \begin{bmatrix} \frac{\vartheta_s}{2\pi f_1} \hat{\boldsymbol{\xi}}_m(f_1) + \frac{\vartheta_s}{f_1} \bar{\mathbf{k}}_{f_1} & \dots & \frac{\vartheta_s}{2\pi f_F} \hat{\boldsymbol{\xi}}_m(f_F) + \frac{\vartheta_s}{f_F} \bar{\mathbf{k}}_{f_F} \\ \mathbf{U}(\hat{\boldsymbol{\Theta}}(f_1)) & \dots & \mathbf{U}(\hat{\boldsymbol{\Theta}}(f_F)) \end{bmatrix}^\dagger \quad (2.51)$$

It is important to note that, the frequencies,  $f_j$ , should satisfy certain conditions in order to obtain unambiguous sensor position estimates. The constraints on the frequencies are given in Theorem-1.

**Theorem-1:** Let the coordinate of the most distant sensor with respect to the reference sensor positioned at  $(0, 0)$  is given as  $\mathbf{h} = (h_x, h_y)$  and  $f_1$  be the minimum frequency, i.e.,  $f_1 < f_j, \quad \forall j \in \{2, \dots, F\}$ . Also let the ratio of the frequencies,  $f_j/f_1$ , be bounded by,

$$\left( \frac{2h_{\max} + 1}{2h_{\max} + 2} \right) \left[ \frac{f_j}{f_1} \right]_r < \frac{f_j}{f_1} < \left( \frac{2h_{\max} + 2}{2h_{\max} + 1} \right) \left[ \frac{f_j}{f_1} \right]_r \quad (2.52)$$

where  $h_{\max} = \left\lceil \frac{1}{\vartheta_s} \max_j (f_j) \sqrt{h_x^2 + h_y^2} \right\rceil$ . Then, the ambiguity in sensor positions is resolved if the following constraints on the frequencies and the estimation errors are satisfied, i.e.,

$$\left| g_j - g_1 \frac{f_j}{f_1} \right| \geq \left| \frac{f_j}{f_1} - \left[ \frac{f_j}{f_1} \right]_r \right|, \quad \forall i \in \{1, \dots, L\} \quad (2.53)$$

$$\exists j \in \{2, \dots, F\}$$

$$\frac{\vartheta_s}{\pi^2} \sum_{j=2}^F \left( \frac{\Delta \xi_m^{(i)}(f_1)}{f_1} - \frac{\Delta \xi_m^{(i)}(f_j)}{f_j} \right)^2 < \sum_{j=2}^F \left( \frac{\vartheta_s}{f_j} \left| \frac{f_j}{f_1} - \left[ \frac{f_j}{f_1} \right]_r \right| \right)^2 \quad (2.54)$$

where  $1 \leq i \leq L$  and  $g_j, \quad 1 \leq j \leq F$ , is the integer bounded by

$$-2 \left\lceil \frac{f_j}{\vartheta_s} \sqrt{h_x^2 + h_y^2} \right\rceil - 1 \leq g_j \leq 2 \left\lceil \frac{f_j}{\vartheta_s} \sqrt{h_x^2 + h_y^2} \right\rceil + 1 \quad (2.55)$$

and  $\Delta \xi_m^{(i)}(f_j)$  is the estimation error for the phase term of the array steering matrix element for  $m^{\text{th}}$  sensor and  $i^{\text{th}}$  source at frequency  $f_j$ , i.e.,

$$\Delta \xi_m^{(i)}(f_j) = \hat{\xi}_m^{(i)}(f_j) - \xi_m^{(i)}(f_j) \quad (2.56)$$

As stated in Theorem-1, there are two constraints that should be satisfied for the solution of ambiguity problem in sensor position estimation as given in (2.53) and (2.54). The constraint in (2.53) guarantees that the sensor position estimates for each frequency coincide at a single point. When this constraint is not satisfied, there are many possible solutions for the sensor

positions for the given array steering matrix and the DOA angle estimates as shown in Fig. 2.7 for two frequencies. Fig. 2.7-a illustrates the sensor position estimates for the frequencies  $f_1 = 10MHz$  and  $f_2 = 20MHz$ . Since these frequencies do not satisfy the constraint in (2.53), all the sensor position estimates for  $f_1$  coincide with the sensor position estimates for  $f_2$  and we can not find a single solution for the sensor position estimation. When the second frequency is changed to  $f_2 = 15MHz$ , even though the number of coinciding points is decreased, there are still multiple possible sensor positions. When the frequencies are selected such that the constraint in (2.53) is satisfied, i.e.,  $f_1 = 10MHz$  and  $f_2 = 13MHz$ , the sensor position estimates for each frequency coincide only at single point as shown in Fig. 2.8. In this case, the sensor position estimate is found unambiguously.

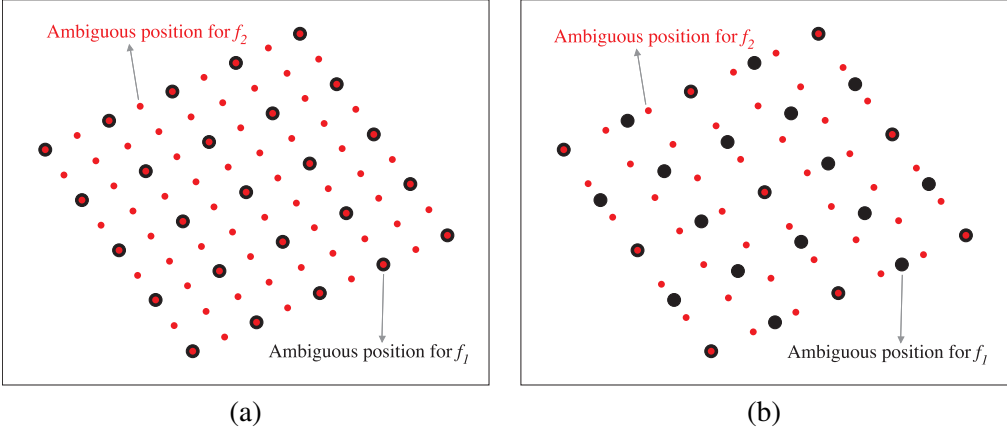


Figure 2.7: Ambiguous sensor positions for the frequencies that does not satisfy the condition in (2.53). The selected frequencies are (a)  $f_1 = 10MHz$ ,  $f_2 = 20MHz$ , (b)  $f_1 = 10MHz$ ,  $f_2 = 15MHz$

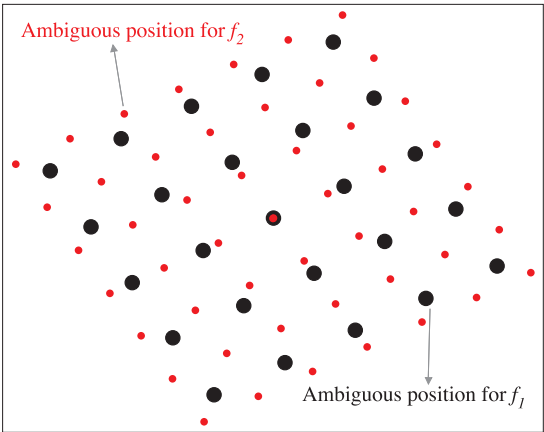


Figure 2.8: Ambiguous sensor positions for the frequencies that satisfy the condition in (2.53). The selected frequencies are  $f_1 = 10MHz$ ,  $f_2 = 13MHz$

Note that, due to the estimation errors in phase terms,  $\hat{\xi}_m^{(i)}(f_j)$ , the sensor position estimates for each frequency may not coincide. In this case, we select the sensor position estimate such that the sensor position estimates for each frequency are closest. Although the constraint in (2.53) guarantees that the two sensor position estimates are closest at single point, the minimum error in sensor position estimation is not guaranteed. To estimate the sensor position estimation with minimum error, in addition to the constraint in (2.53) the estimation errors in phase terms of array steering matrix should be bounded as given in (2.54). When the estimation errors are bounded to satisfy the constraint in (2.54) for the frequencies that satisfy the constraint in (2.53), it is guaranteed that the sensor position estimates for each frequency are closest at the point that is closest to the actual sensor position as shown in Fig. 2.9-a. When the estimation errors are increased such that the constraint in (2.54) is not satisfied, sensor position estimates for each frequency may be closest at the point far away from the actual sensor position as shown in Fig. 2.9-b. In this case, even though there is a single solution for the sensor positions estimation, the estimation errors in sensor positions are large.

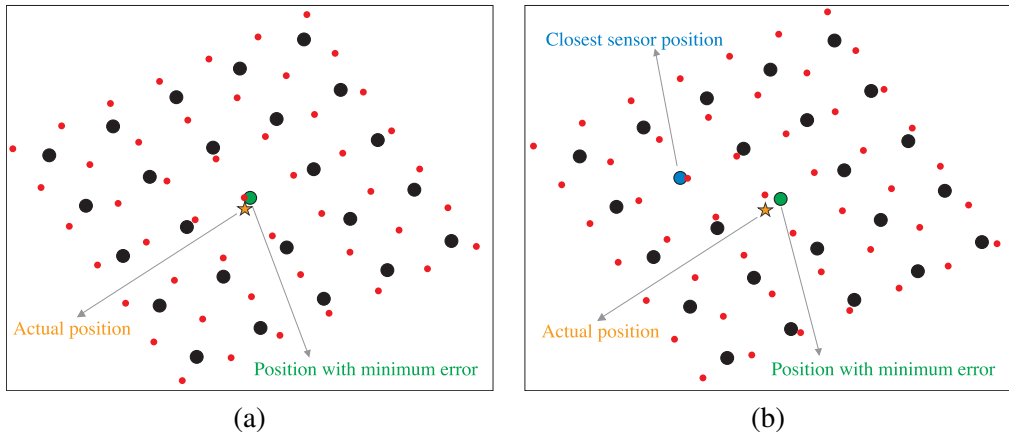


Figure 2.9: Estimated sensor positions for the errors that (a) does not satisfy and (b) satisfy the condition in (2.54). The selected frequencies are (a)  $f_1 = 10MHz$ ,  $f_2 = 13MHz$ .

The proof of Theorem-1 is presented in Appendix C. While two frequencies constrained as in Theorem-1 are sufficient for unambiguous sensor position estimation, more than two frequencies can improve the performance especially at low SNR.

### 2.2.3 SOS-Based MUSIC Algorithm

Sensor position matrix estimate,  $\hat{\mathbf{P}}$ , is constructed using (3.11) and used in the MUSIC algorithm to generate the MUSIC pseudospectrum [1], i.e.,

$$\Gamma(\theta) = \frac{1}{\mathbf{a}^H(\theta, \hat{\mathbf{P}}) \mathbf{G} \mathbf{G}^H \mathbf{a}(\theta, \hat{\mathbf{P}})} \quad (2.57)$$

$\mathbf{G}$  is the  $M \times (M - L)$  matrix whose columns are composed of the eigenvectors corresponding to  $M - L$  smallest eigenvalues of the correlation matrix obtained in the SOS approach. Note that for the proposed IHOSS algorithm, MUSIC pseudospectrum is constructed for each frequency separately as it is explained in Section 2.2.4. The DOA and the array steering matrix estimates for the SOS approach are obtained by finding the  $L$  largest peaks of the MUSIC pseudospectrum, i.e.,

$$\{\hat{\theta}_i\}_{i=1}^L = \arg \max_{\theta} \Gamma(\theta) \quad (2.58)$$

$$\hat{\mathbf{A}} = [\mathbf{a}(\hat{\theta}_1, \hat{\mathbf{P}}), \mathbf{a}(\hat{\theta}_2, \hat{\mathbf{P}}), \dots, \mathbf{a}(\hat{\theta}_L, \hat{\mathbf{P}})] \quad (2.59)$$

### 2.2.4 The Cost Function and The Algorithmic Steps

The iterative process used in IHOSS algorithm is composed of three steps. The first step is to find the proposed cumulant matrix estimate,  $\mathbf{C}_{est}^d$ , in (2.32) using the array output and the array steering matrix estimate obtained from the previous iteration for each frequency. Then, using the HOS approach, the DOA and array steering matrix estimates are found for each frequency from (2.35) and (2.38), respectively. Note that the initial array steering matrix estimate is selected as zero, i.e.,  $\hat{\mathbf{A}} = \mathbf{0}$  for each frequency. The second step is to find the sensor position estimates using the DOA and the array steering matrix estimates obtained from the first step as given in (2.51). In the last step, SOS approach is used through the MUSIC algorithm to find the DOA and array steering matrix estimates from (2.58) and (2.59), respectively. Then, the cost function is used to select the best array steering vector estimates for each source and frequency. The cost function is defined as the value of the MUSIC pseudospectrum for the estimated array steering vector for each source, i.e.,

$$\Gamma(\hat{\mathbf{a}}_i(f_j)) = \frac{1}{(\hat{\mathbf{a}}_i(f_j))^H \mathbf{G}_{f_j} \mathbf{G}_{f_j}^H \hat{\mathbf{a}}_i(f_j)} \quad (2.60)$$

where  $\hat{\mathbf{a}}_i(f_j)$  is the array steering vector estimate for the  $i^{th}$  source at the frequency  $f_j$ .  $\mathbf{G}_{f_j}$  is the  $M \times (M - L)$  matrix whose columns are composed of the eigenvectors corresponding

to  $M - L$  smallest eigenvalues of the correlation matrix obtained for frequency  $f_j$  in the SOS approach [1]. In order to guarantee the convergence at each iteration, only the array steering vectors that increase the cost function value over the previous iteration are selected. If the cost function is not increased, the previous estimates are kept for the current iteration. The iterations are terminated when there is no increment in the cost function for any source and any frequency. After the iterations are completed, the final DOA angle estimate is selected as the DOA angle estimate at the frequency where the cost function is maximum. The final sensor position estimates are found by using the DOA and the array steering matrix estimates at each frequency as in (2.51). This process can be described better as it is shown in Algorithm 2.1 where the algorithmic steps of the IHOSS algorithm are presented. As it is shown in Table 2.1, IHOSS algorithm takes only the sensor outputs as input. In this respect, there is no need to know or estimate an initial value for the DOA or sensor positions except the two reference sensors to start the iterations.

The convergence of the proposed IHOSS algorithm is essentially similar to the one in [27]. The cost function in (2.60) is non-negative and by checking the value of the cost function at each iteration we are guaranteed to obtain non-decreasing function for the cost values, i.e.,  $\Gamma(\hat{\mathbf{a}}_i^{(n)}(f_j)) \geq \Gamma(\hat{\mathbf{a}}_i^{(n-1)}(f_j)) \geq 0$ . Therefore, the proposed IHOSS algorithm is guaranteed to converge to a certain value,  $\bar{\Gamma}$ , at the end of the iterations. However, the convergence to this value does not mean that the global optimum is reached as it is the general disadvantage of all iterative algorithms [27].

### 2.3 Cramér-Rao Bound

CRB expressions for DOA estimation in case of known sensor positions and different noise models are derived in [9], [20], [22], [23], [24]. In [9], the uncertainty on sensor positions is considered and the CRB for sensor position estimation is presented. It is assumed that the nominal sensor positions are known and the small displacement from the nominal locations is modeled as Gaussian. In this work, there is no a priori information about the sensor positions except the two reference sensors. Therefore, none of the previous CRB expressions in literature can be used for the DOA and sensor position estimations in this work, and a new CRB expression is derived for the problem setting in this work.

---

**Algorithm 2.1:** Pseudocode for IHOSS algorithm.

---

- 1 *The sensor array output and the positions of the two reference sensors are given. Set the iteration counter to zero, i.e.,  $n = 0$ . Initialize the array steering vector for each source and frequency as zero,  $\hat{\mathbf{a}}_i^{(0)}(f_j) = \mathbf{0}$ ;*
  - 2 *Set the iteration termination condition to true, i.e.,  $Termination = true$ . Estimate the proposed cumulant matrix,  $\mathbf{C}_{est}^d$  from the array output and  $\hat{\mathbf{a}}_i^{(n)}(f_j)$  as in (2.32). Then, from the estimated cumulant matrix find DOA estimates,  $\hat{\theta}_i^{HOS}(f_j)$  using (2.35) and array steering matrix  $\hat{\mathbf{A}}^{HOS}(f_j)$ , using (2.38), for  $1 \leq i \leq L$  and  $1 \leq j \leq F$ ;*
  - 3 *Find the sensor position estimates,  $\hat{\mathbf{P}}$ , as in (2.51) using (2.42) and (2.50) with  $\hat{\theta}_i^{HOS}(f_j)$  and  $\hat{\mathbf{A}}^{HOS}(f_j)$ , for  $1 \leq i \leq L$  and  $1 \leq j \leq F$ ;*
  - 4 **for  $j = 1$  to  $F$  do**
  - 5     *Find  $\hat{\theta}_i^{(SOS)}(f_j)$  using  $\hat{\mathbf{P}}$  as in (2.58). Then, find  $\hat{\mathbf{a}}_i^{(SOS)}(f_j)$  using  $\hat{\mathbf{P}}$  and  $\hat{\theta}_i^{(SOS)}(f_j)$  as in (2.59);*
  - 6     **if  $\Gamma(\hat{\mathbf{a}}_i^{(SOS)}(f_j)) \geq \Gamma(\hat{\mathbf{a}}_i^{(n-1)}(f_j))$  then**
  - 7         *Update the DOA and the array steering vectors for the  $i^{th}$  source and  $j^{th}$  frequency, i.e.,  $\hat{\mathbf{a}}_i^{(n)}(f_j) = \hat{\mathbf{a}}_i^{(SOS)}(f_j)$ ,  $\hat{\theta}_i^{(n)}(f_j) = \hat{\theta}_i^{(SOS)}(f_j)$ ;*
  - 8         *Update the cost function, i.e.,  $\Gamma(\hat{\mathbf{a}}_i^{(n)}(f_j)) = \Gamma(\hat{\mathbf{a}}_i^{(SOS)}(f_j))$ ;*
  - 9         *Set the iteration termination condition to false, i.e.,  $Termination = false$ ;*
  - 10     **else**
  - 11         *Do not update the DOA and the array steering vectors for the  $i^{th}$  source and  $j^{th}$  frequency, i.e.,  $\hat{\mathbf{a}}_i^{(n)}(f_j) = \hat{\mathbf{a}}_i^{(n-1)}(f_j)$ ,  $\hat{\theta}_i^{(n)}(f_j) = \hat{\theta}_i^{(n-1)}(f_j)$ ;*
  - 12     **end**
  - 13 **end**
  - 14 **if  $Termination = false$  then**
  - 15     *Increment the iteration counter, i.e.,  $n = n + 1$ ;*
  - 16     *Go to Step 2;*
  - 17 **else**
  - 18     *Find the final estimate of DOA as  $\hat{\theta}_i^{final} = \hat{\theta}_i^{(n)}(f_{j^*})$ , where  $j^* = \arg \max_j \Gamma(\hat{\mathbf{a}}_i^{(n)}(f_j))$ ;*
  - 19     *Find the final estimate of sensor positions using  $\hat{\theta}_i^{(n)}(f_{j^*})$  and  $\hat{\mathbf{a}}_i^{(n)}(f_j)$ ,*  
       *$1 \leq i \leq L, \quad 1 \leq j \leq F$ ;*
  - 20 **end**
-

The signal waveforms are considered to be deterministic unknown process and the noise is assumed to be temporally uncorrelated complex Gaussian process. It is also assumed that noise is uncorrelated for different frequencies. In this work, CRB expressions are derived by considering a non-circular complex Gaussian distribution for the noise with unknown covariance matrix. The modification for circular case is also given. Noise may be spatially correlated. Then, the CRB for DOA,  $CRB_\theta$ , and sensor position estimation,  $CRB_p$ , are given by,

$$CRB_\theta = \frac{1}{L} \text{tr}(\mathbf{K}_\theta^{-1}) \quad (2.61)$$

$$CRB_p = \frac{1}{2M_u} \text{tr}(\mathbf{K}_2^{-1} + \mathbf{K}_2^{-1} \mathbf{K}_1^T \mathbf{K}_\theta^{-1} \mathbf{K}_1 \mathbf{K}_2^{-1}) \quad (2.62)$$

where  $\mathbf{K}_\theta = \mathbf{K}_3 - \mathbf{K}_1 \mathbf{K}_2^{-1} \mathbf{K}_1^T$ ,  $M_u$  is the number of unknown sensor positions, and the matrices  $\mathbf{K}_1$ ,  $\mathbf{K}_2$ , and  $\mathbf{K}_3$  are defined as,

$$\mathbf{K}_1 = \sum_{t=1}^N \sum_{j=1}^F \mathbf{FIM}_\Theta^T(t, f_j) \mathbf{\Pi}^\perp(t, f_j) \mathbf{FIM}_P(t, f_j) \quad (2.63)$$

$$\mathbf{K}_2 = \sum_{t=1}^N \sum_{j=1}^F \mathbf{FIM}_P^T(t, f_j) \mathbf{\Pi}^\perp(t, f_j) \mathbf{FIM}_P(t, f_j) \quad (2.64)$$

$$\mathbf{K}_3 = \sum_{t=1}^N \sum_{j=1}^F \mathbf{FIM}_\Theta^T(t, f_j) \mathbf{\Pi}^\perp(t, f_j) \mathbf{FIM}_\Theta(t, f_j) \quad (2.65)$$

The matrix,  $\mathbf{\Pi}^\perp(t, f_j)$ , is defined as in (2.68).  $2M \times 2M$  matrix  $\mathbf{R}(t, f_j)$  is the real covariance matrix of the noise for time  $t$  and frequency  $f_j$  defined as,

$$\mathbf{R}(t, f_j) = E \left\{ \begin{bmatrix} \Re(\mathbf{v}(t, f_j)) \\ \Im(\mathbf{v}(t, f_j)) \end{bmatrix} \begin{bmatrix} \Re(\mathbf{v}(t, f_j)) \\ \Im(\mathbf{v}(t, f_j)) \end{bmatrix}^T \right\} \quad (2.66)$$

The matrix  $\mathbf{A}^{(c)}(f_j)$  is defined for real and complex source signals as,

$$\mathbf{A}^{(c)}(f_j) = \begin{cases} \begin{bmatrix} \Re(\mathbf{A}(f_j)) & -\Im(\mathbf{A}(f_j)) \\ \Im(\mathbf{A}(f_j)) & \Re(\mathbf{A}(f_j)) \end{bmatrix}, & \text{complex} \\ \begin{bmatrix} \Re(\mathbf{A}(f_j)) \\ \Im(\mathbf{A}(f_j)) \end{bmatrix}, & \text{real} \end{cases} \quad (2.67)$$

The matrices  $\mathbf{FIM}_\Theta(t, f_j)$  and  $\mathbf{FIM}_P(t, f_j)$  are defined in (2.69) and (2.70), respectively.  $\mathbf{I}_{2 \times 2}$

$$\begin{aligned} \mathbf{\Pi}^\perp(t, f_j) &= \mathbf{R}^{-1}(t, f_j) \times \\ &\quad \left( \mathbf{I} - \mathbf{A}^{(c)}(f_j) \left( \mathbf{A}^{(c)T}(f_j) \mathbf{R}^{-1}(t, f_j) \mathbf{A}^{(c)}(f_j) \right)^{-1} \mathbf{A}^{(c)T}(f_j) \mathbf{R}^{-1}(t, f_j) \right) \end{aligned} \quad (2.68)$$

$$\begin{aligned} \mathbf{FIM}_\Theta(t, f_j) &= \left[ \left[ \begin{bmatrix} -1 \\ 1 \end{bmatrix} \otimes \mathbf{\Pi}_1^L(f_j) \right] \mathbf{D}_{\mathbf{s}^{(r)}}(t) \right] \odot \begin{bmatrix} \mathfrak{I}(\mathbf{A}(f_j)) \\ \mathfrak{R}(\mathbf{A}(f_j)) \end{bmatrix} - \left[ \left[ \begin{bmatrix} 1 \\ 1 \end{bmatrix} \otimes \mathbf{\Pi}_1^L(f_j) \right] \mathbf{D}_{\mathbf{s}^{(i)}}(t) \right] \\ &\quad \odot \begin{bmatrix} \mathfrak{R}(\mathbf{A}(f_j)) \\ \mathfrak{I}(\mathbf{A}(f_j)) \end{bmatrix} \end{aligned} \quad (2.69)$$

$$\begin{aligned} \mathbf{FIM}_\mathbf{P}(t, f_j) &= \left( \begin{bmatrix} \mathfrak{I}(\mathbf{A}(f_j)) & \mathfrak{R}(\mathbf{A}(f_j)) \\ \mathfrak{R}(\mathbf{A}(f_j)) & -\mathfrak{I}(\mathbf{A}(f_j)) \end{bmatrix} \begin{bmatrix} \mathbf{D}_{\mathbf{s}^{(r)}}(t) \\ \mathbf{D}_{\mathbf{s}^{(i)}}(t) \end{bmatrix} \begin{bmatrix} \mathbf{T}_c(f_j) & \mathbf{T}_s(f_j) \end{bmatrix} (\mathbf{I}_{2 \times 2} \otimes \mathbf{1}_{1 \times M_u}) \right) \\ &\quad \odot \left( \begin{bmatrix} -1 & -1 \\ 1 & 1 \end{bmatrix} \otimes \mathbf{\Sigma} \right) \end{aligned} \quad (2.70)$$

is the  $2 \times 2$  identity matrix and  $\mathbf{1}_{1 \times M_u}$  is the  $1 \times M_u$  vector composed of all ones and,

$$\mathbf{D}_{\mathbf{s}^{(r)}}(t) = \mathfrak{R}(\text{diag}(s_1(t), s_2(t), \dots, s_L(t))) \quad (2.71)$$

$$\mathbf{D}_{\mathbf{s}^{(i)}}(t) = \mathfrak{I}(\text{diag}(s_1(t), s_2(t), \dots, s_L(t))) \quad (2.72)$$

$$\mathbf{\Pi}_1^L(f_j) = \frac{2\pi f_j}{\vartheta_s} \mathbf{P} \begin{bmatrix} -\sin(\theta_1) & -\sin(\theta_2) & \dots & -\sin(\theta_L) \\ \cos(\theta_1) & \cos(\theta_2) & \dots & \cos(\theta_L) \end{bmatrix} \quad (2.73)$$

$$\mathbf{T}_s(f_j) = \frac{2\pi f_j}{\vartheta_s} \begin{bmatrix} \sin(\theta_1) & \sin(\theta_2) & \dots & \sin(\theta_L) \end{bmatrix}^T \quad (2.74)$$

$$\mathbf{T}_c(f_j) = \frac{2\pi f_j}{\vartheta_s} \begin{bmatrix} \cos(\theta_1) & \cos(\theta_2) & \dots & \cos(\theta_L) \end{bmatrix}^T \quad (2.75)$$

$\mathbf{\Sigma}$  is the  $M \times M_u$  matrix whose columns contain only one nonzero element which is set to one. The location of the nonzero element at each column is determined by the sensor index with unknown positions. If it is assumed that the positions of the first two sensors are known and the other sensor positions are unknown, the matrix  $\mathbf{\Sigma}$  is composed of,  $\mathbf{\Sigma} = \begin{bmatrix} \mathbf{0}_{2 \times M_u}^T & \mathbf{I}_{M-2 \times M_u}^T \end{bmatrix}^T$ . The subscripts are used to define the sizes of the zero matrix,  $\mathbf{0}$ , and identity matrix,  $\mathbf{I}$ .

Note that the Cramér-Rao bound expressions in (2.61) and (2.62) are given for non-circular complex Gaussian noise case. When the noise is circular, expressions given above are valid with the change in noise covariance matrix in (2.66). For circular noise case, the real covari-

ance matrix to be used in CRB expressions is found as [19],

$$\mathbf{R}(t, f_j) = \frac{1}{2} \begin{bmatrix} \Re(\mathbf{\Gamma}(t, f_j)) & -\Im(\mathbf{\Gamma}(t, f_j)) \\ \Im(\mathbf{\Gamma}(t, f_j)) & \Re(\mathbf{\Gamma}(t, f_j)) \end{bmatrix} \quad (2.76)$$

where  $M \times M$  matrix  $\mathbf{\Gamma}(t, f_j)$  is defined as,

$$\mathbf{\Gamma}(t, f_j) = E \{ \mathbf{v}(t, f_j) \mathbf{v}^H(t, f_j) \} \quad (2.77)$$

Derivations of the CRB expressions in (2.63) - (2.65) are given in Appendix D.

## 2.4 Performance Results

The performance of the IHOSS algorithm is evaluated for different cases for both DOA and position estimation. VESPA [12] is considered only for DOA estimation comparison since it cannot estimate the sensor positions. The CRB expressions in (2.61) and (2.62) are used to show the effectiveness of the IHOSS algorithm.

It is assumed that there are two far-field sources and  $M = 10$ . The received wideband source signals are passed through three narrowband bandpass filters with center frequencies which satisfy the conditions in Theorem-1, i.e.,  $f_1 = 9.85$  MHz,  $f_2 = 9.925$  MHz and  $f_3 = 10.0$  MHz. Each sensor position except the two reference sensors is randomly selected from a uniform distribution in the deployment area of 50x50 meters. The reference sensors are placed at (0, 0) and (15, 0) in meters where the wavelength corresponding to the highest frequency is  $\lambda = 30$  meters. For the parameter estimation,  $N = 1000$  snapshots are collected for each frequency. The performance results are the average of 100 trials. At each trial, source signals, noise, the sensor positions except the reference sensors and the DOA angles of source signals are changed randomly. The difference between the DOA angles of the source signals is set to 40 degrees. The source signals have a uniform distribution and the noise is additive white Gaussian and uncorrelated with the source signals. In the simulations, source signals are generated from a uniform distribution. Note that the fourth-order cumulants used in HOS approach is zero for Gaussian signals. On the other hand, for the finite length signals, the Gaussian assumption is not always satisfied especially for the small number of samples and IHOSS algorithm can also be used for the source signals generated from Gaussian distribution. The simulation parameters are summarized in Table 2.1.

Table 2.1: Simulation parameters for IHOSS algorithm.

Number of sensors	$M = 10$
Number of sources	$L = 2$
Number of snapshots	$N = 1000$
Frequencies	[9.85, 9.925, 10.0] MHz
Deployment area	[50 × 50] meters
Distance between reference sensors	$\Delta = 15$ meters
Separation of source DOAs	$40^\circ$
Number of trials	100

For the simulation, a maximum number of iterations,  $n_{max}$ , is defined for the iterative approach. When a predefined maximum number of iterations is reached, iterative approach is terminated even if the termination condition given in Table 2.1 is not satisfied. The performance results of the IHOSS algorithm are illustrated for three different maximum number of iterations, namely,  $n_{max} = 4$ ,  $n_{max} = 15$ , and  $n_{max} = 30$  in order to show the convergence of the IHOSS algorithm. In the simulations the effect of the additive noise on the performance is controlled by the Signal-to-Noise Ratio (SNR) value. SNR is defined as the ratio of the signal power and the noise power at the sensor outputs, i.e.,

$$SNR = 10 \log_{10} \frac{\|\mathbf{a}_{ri,f_j} \mathbf{S}_{f_j}\|^2}{\|\mathbf{v}_{ri,f_j}\|^2}, \quad \begin{array}{l} 1 \leq i \leq M \\ 1 \leq j \leq F \end{array} \quad (2.78)$$

where  $\mathbf{a}_{ri,f_j}$  is the  $i^{th}$  row of array steering matrix  $\mathbf{A}_{f_j}(\Theta, \mathbf{P})$  in (2.5),  $L \times N$  matrix  $\mathbf{S}_{f_j}$  and  $1 \times N$  vector  $\mathbf{v}_{ri,f_j}$  are the received source signals and noise for  $1 \leq t \leq N$  as in (2.4), i.e.,

$$\mathbf{S}_{f_j} = \begin{bmatrix} \mathbf{s}_{f_j}(1) & \mathbf{s}_{f_j}(2) & \dots & \mathbf{s}_{f_j}(N) \end{bmatrix} \quad (2.79)$$

$$\mathbf{v}_{ri,f_j} = \begin{bmatrix} v_{i,f_j}(1) & v_{i,f_j}(2) & \dots & v_{i,f_j}(N) \end{bmatrix} \quad (2.80)$$

The parameter estimation errors in performance results are defined as the averaged root mean squared error (RMSE), i.e.,

$$RMSE = \sqrt{\frac{1}{N_{pr} N_{tr}} \sum_{pr=1}^{N_{pr}} \sum_{tr=1}^{N_{tr}} (\beta_{est} - \beta_{corr})^2} \quad (2.81)$$

where  $N_{pr}$  and  $N_{tr}$  are the number of estimated parameters and the number of trials, respectively.  $\beta_{est}$  and  $\beta_{corr}$  are the estimated and correct value of the parameter  $\beta$ , respectively. In the following performance results,  $\beta$  can be DOA angles or the  $x$  and  $y$  components of the sensor positions.

The performance results for the DOA and sensor position estimations at different SNR values and maximum number of iterations are illustrated in Fig. 2.10. In Fig. 2.10(a), it is seen that VESPA has a flooring effect. This is due to the errors in the cumulant matrix for finite length data and multiple sources. IHOSS performs well and closely follows the CRB as the number of iterations is increased. This is due to the fact that IHOSS converts the multiple source problem into a single source case and effectively uses HOS and SOS techniques with a robust cumulant matrix (2.32). The position estimation accuracy in Fig. 2.10(b) is especially good at high SNR, where the position ambiguity is solved accurately. The performance degradation at low SNR is related with the condition in Theorem-1. In this case, the errors in array steering matrix estimates are higher than the threshold given in Theorem-1. It is also seen that the required number of iterations for the best result in DOA and sensor position estimation is SNR dependent. As the SNR increases, IHOSS requires more iteration in order to follow the CRB closely. As it is seen in Fig. 2.10, the performance results for  $n_{max} = 15$  and  $n_{max} = 30$ , are almost the same. Therefore, a small number of iterations is sufficient to get a satisfactory performance.

In Fig. 2.11, the performance of the algorithm is shown when the number of snapshots is changed. SNR is set to 20 dB. Fig. 2.11(a) shows that the IHOSS algorithm performs significantly better than VESPA and approaches to the CRB even when  $N$  is small. In Fig. 2.11(b), it is seen that IHOSS finds the sensor positions effectively and closely follows the CRB after  $N = 250$  snapshots. When  $N$  is small, the accuracy of the array steering matrix estimation is not sufficient to satisfy the condition in Theorem-1 and a significant performance degradation in sensor position estimation is observed as illustrated in Fig. 2.11(b).

The effect of the difference between the DOA angles of the sources on the performance of DOA and sensor position estimations is illustrated in Fig. 2.12. In this example, two sources are located randomly in a 100 degrees sector between 40 and 140 degrees. The difference between the DOA angles of the two sources is changed from 1 to 50 degrees. SNR is set to 20 dB. As it is seen in Fig. 2.12(a), IHOSS follows the CRB after the DOA separation of approximately 10 degrees and performs significantly better than VESPA whose performance is also reported in [13]. The DOA RMSE of IHOSS increases as the source separation is increased for four iterations (IHOSS, ItNum = 4). CRB also increases with the source separation even though the increase is small. Note that this is due to the fact that the source DOA's

are close to the endfire of the baseline determined by the two reference sensors as the source separation increases. IHOSS makes larger errors for small number of iterations. This problem is solved by increasing the maximum number of iterations. As it is seen in Fig. 2.12(a), a few iterations are enough to obtain a good accuracy. The sensor position estimation performance is illustrated in Fig. 2.12(b). It is seen that IHOSS solves the position ambiguity effectively when two sources are separated by more than 18 degrees. For the closely spaced sources, the condition on estimation errors in Theorem-1 is not satisfied and the ambiguity problem is not solved accurately.

Fig. 2.13 shows the performance results of the DOA and sensor position estimations when the sensor density is changed. The sensor density is defined as  $M/d_a^2$ , where  $d_a^2$  is the area in square wavelength, i.e.,  $d_a^2 = d_x d_y \left( \frac{1}{\vartheta_s} \min_j(f_j) \right)^2$ .  $d_x$  and  $d_y$  are the lengths of the sensor deployment area in the x and y axes, respectively. The number of sensors is set as  $M = 10$ . Two reference sensors are located at (0,0) and (15,0) coordinates in meters and the remaining  $M - 2$  sensors are randomly deployed. The positions of the randomly deployed  $M - 2$  sensors are scaled to change the sensor density without changing the sensor geometry. Two far-field sources are located randomly in the range of 40-140 degrees with a DOA separation of 40 degrees. SNR is set to 20 dB. The sensor positions except the reference sensors and source DOAs are changed at each trial. As it is seen in Fig. 2.13(a), IHOSS closely follows the CRB for the DOA estimation. It is also seen that DOA RMSE increases by increasing the sensor density. In this case, sensors are close to each other. When the sensors are very close to each other, a small perturbation on sensor positions results large DOA deviations. The sensor position estimation performance is shown in Fig. 2.13(b). Since sensor density is varied by changing the deployment area, the sensor position estimation error is shown by scaling with the size of the deployment area. It is seen that IHOSS closely follows the CRB when the sensor density is greater than 1. For small sensor densities, the position estimation performance is decreased due to the large errors in array steering matrix estimates as explained in Theorem-1.

Since IHOSS uses multiple frequencies to resolve the ambiguity problem in sensor position estimation, the effect of the frequency selection on DOA and sensor position estimations is also investigated. For this example, it is assumed that there are two different frequencies that the array output is observed for the same sources. SNR is set to 20 dB. The first frequency

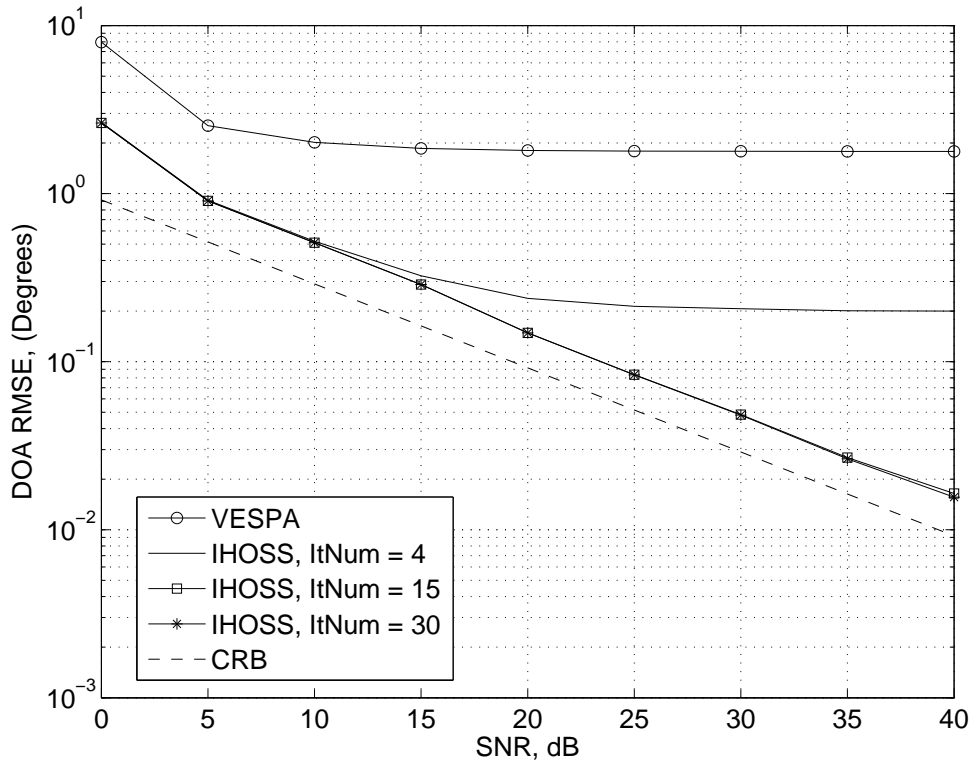
is fixed at 9.75 MHz and the second frequency is varied from 9.75 MHz to 10 MHz, in such a way that the conditions in Theorem-1 are satisfied. The performance results are shown in Fig. 2.14. As it is seen in Fig. 2.14(a), the frequency difference does not significantly affect the DOA estimation performance of the IHOSS. On the other hand, the sensor position performance is sensitive to the difference between the frequencies as seen in Fig. 2.14(b). The ambiguity problem in position estimation is solved effectively when the frequency difference is greater than 100 kHz. Note that as mentioned in section 2.2.2, the required frequency difference for the best position estimation performance can be decreased by using more than two frequencies. When three frequencies are used, it is possible to decrease the overall frequency difference to less than 50 kHz. As it is seen from Fig. 2.14, the CRB for both DOA and sensor position estimation does not change with changing frequency difference. This observation is reasonable, since in the CRB expressions, the contribution of each frequency component is taken independent of the others. Therefore, the frequency difference does not affect the CRB values as shown in Fig. 2.14-a. Also the CRB for the position estimation is a flat curve as shown in Fig. 2.14-b, since the CRB formulation does not consider ambiguity in sensor positions.

## 2.5 Advantages of IHOSS Algorithm

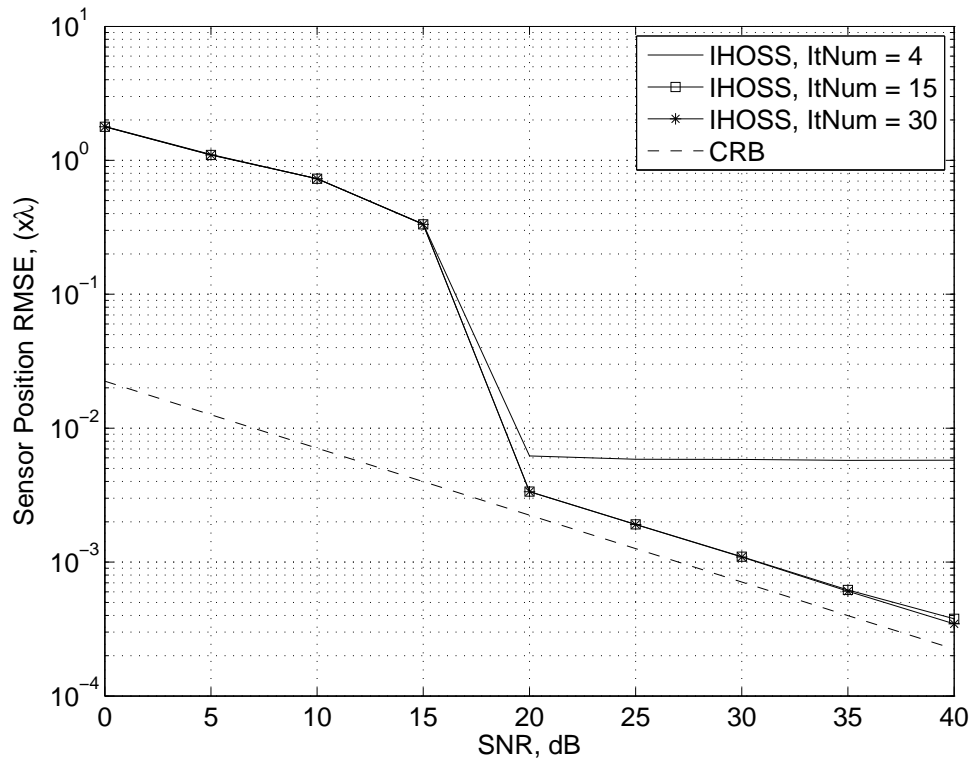
The advantages of the IHOSS algorithm can be summarized as follows:

- IHOSS algorithm jointly estimates the DOA angles and sensor positions when the sensor positions are unknown except the two reference sensors. In this respect, IHOSS is the first algorithm in the literature which finds the DOA and sensor position estimations in case of randomly deployed sensors with unknown coordinates.
- The ambiguity problem in sensor position estimation is solved by observing the source signals at least in two different frequencies.
- Sensor positions are estimated accurately.
  - 4 cm accuracy in sensor position estimation is achieved at SNR = 30 dB for  $\lambda = 30$  m.
- DOA angles are estimated accurately even for large error in sensor positions.

- 0.025 degrees accuracy in DOA estimation is achieved at SNR = 30 dB.
- IHOSS algorithm is applicable to any sensor geometry.

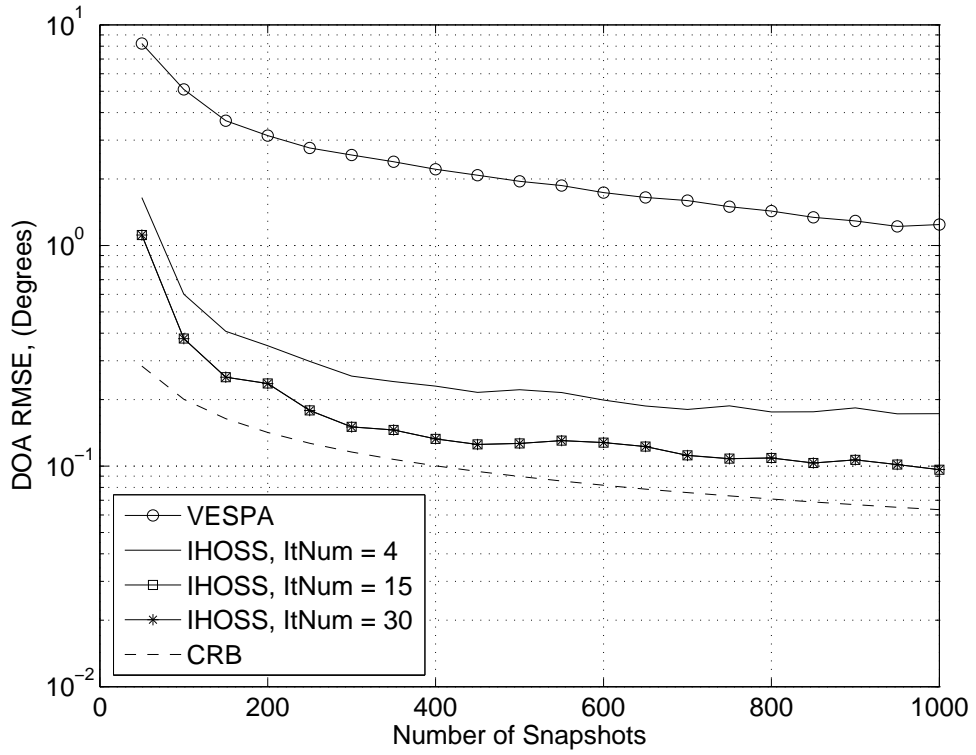


(a)

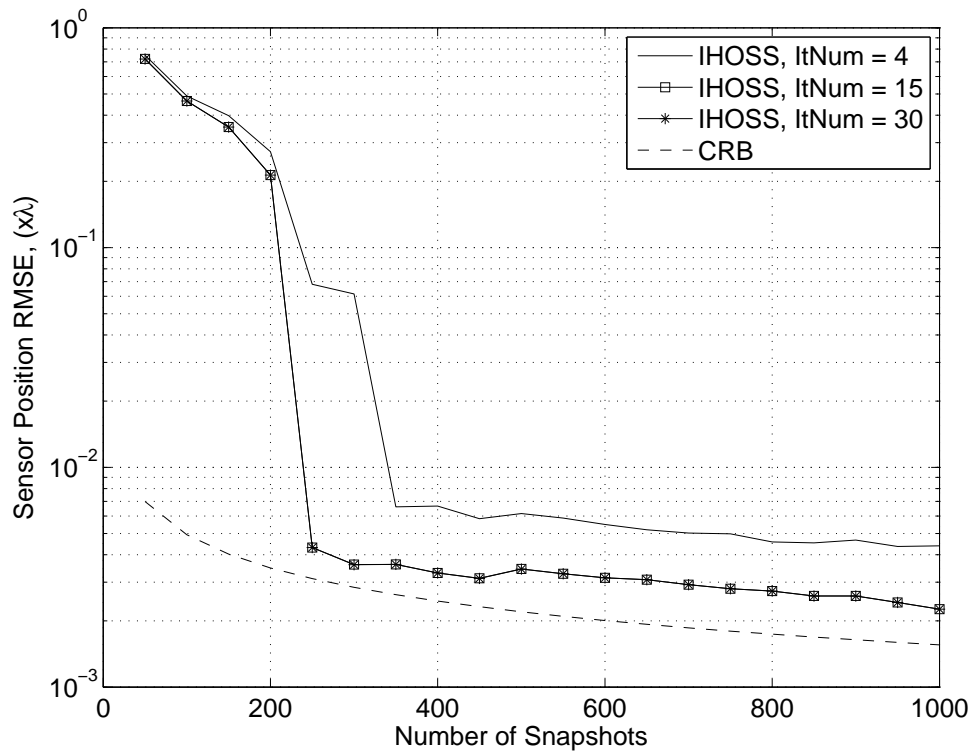


(b)

Figure 2.10: SNR performance for (a) DOA and (b) position estimation.

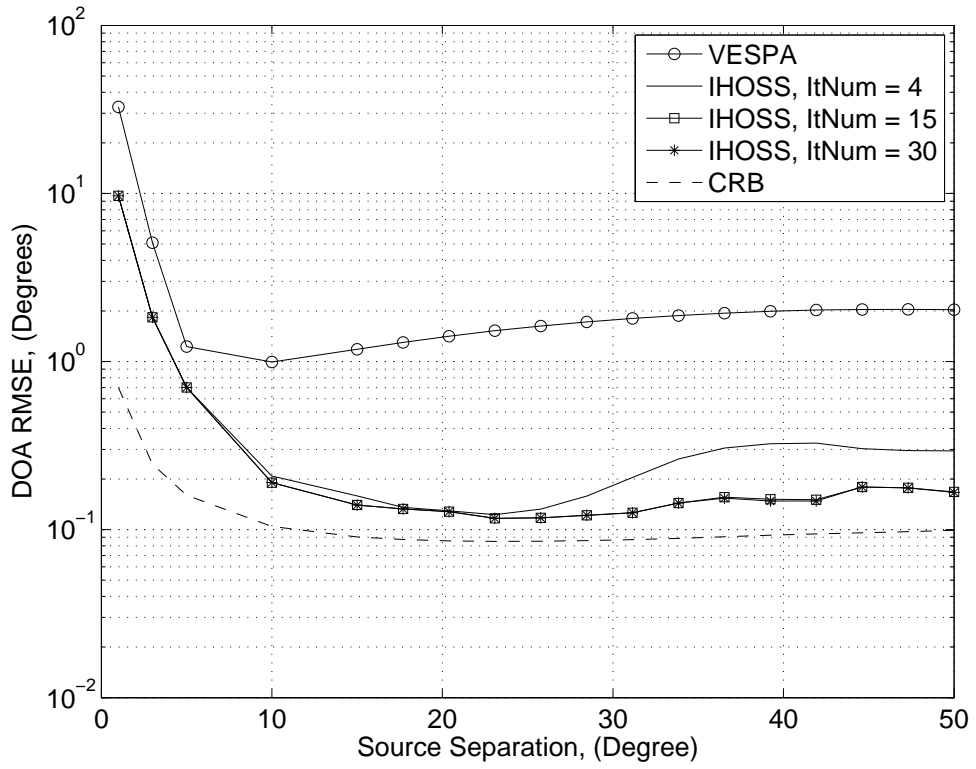


(a)

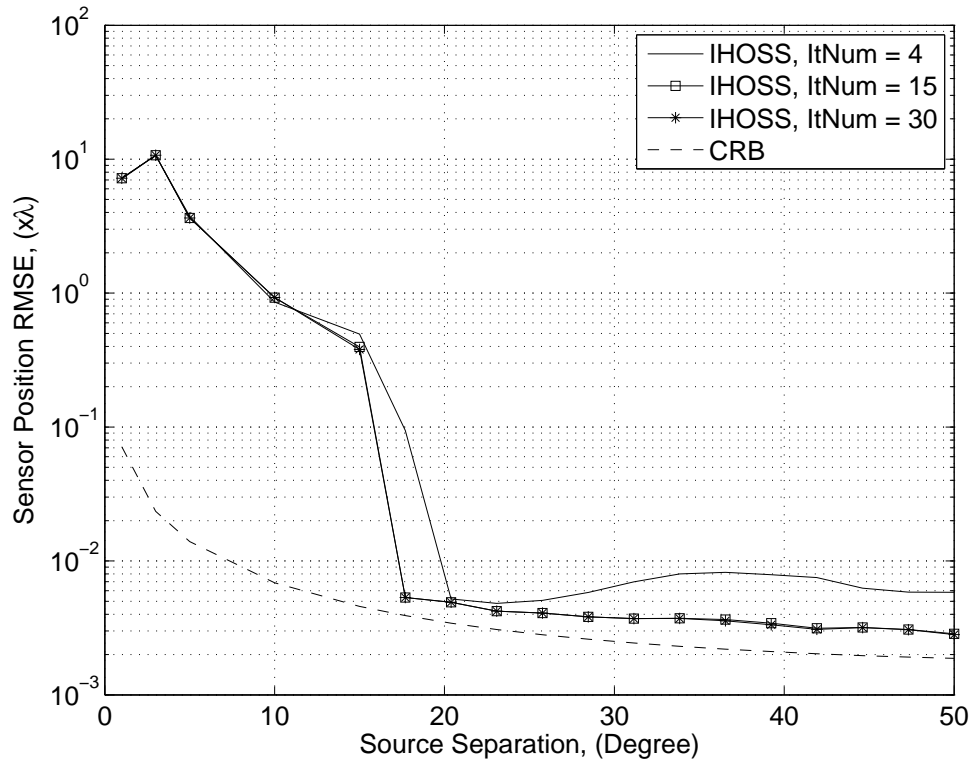


(b)

Figure 2.11: (a) DOA and (b) position estimation for varying number of snapshots at SNR = 20 dB.

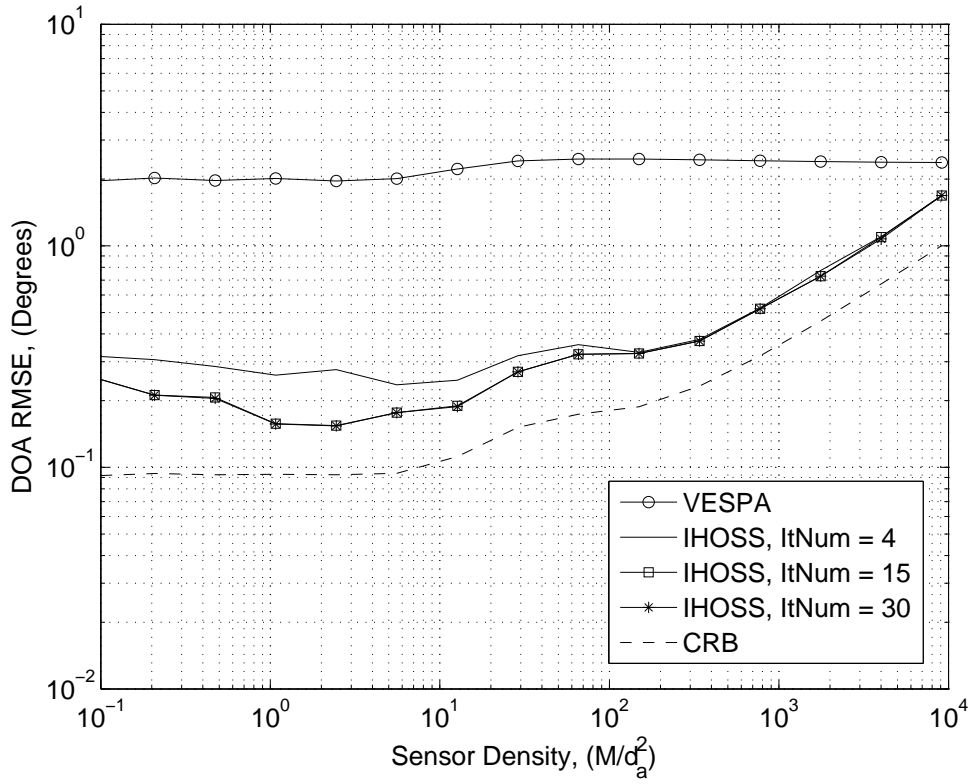


(a)

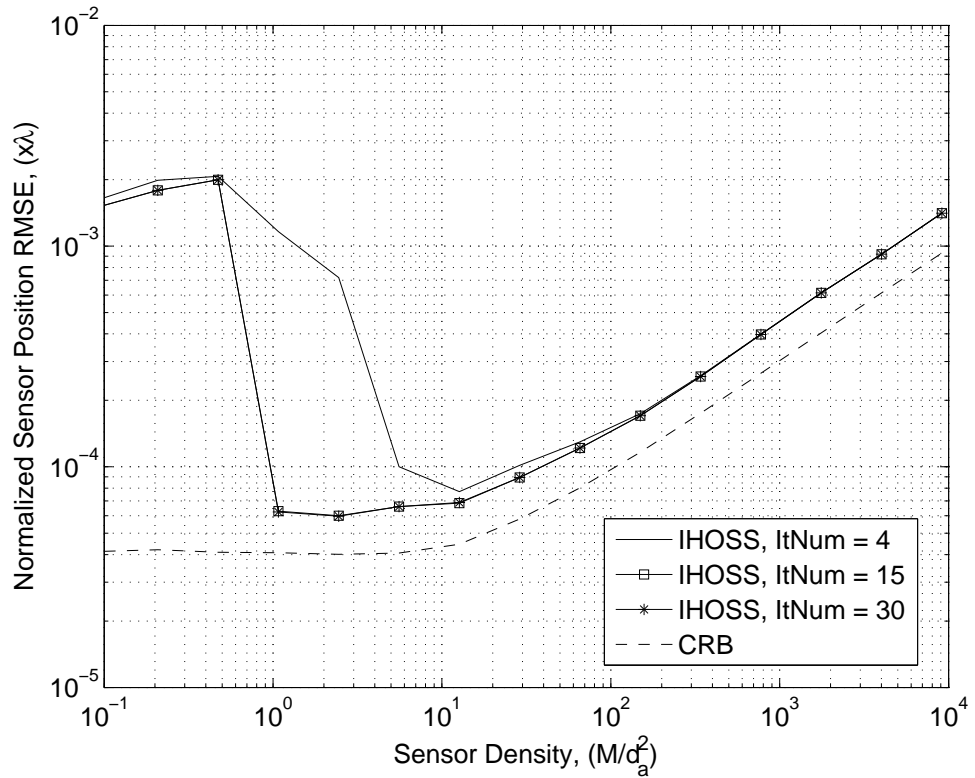


(b)

Figure 2.12: (a) DOA and (b) position estimation performance for varying distance between source DOAs at SNR = 20 dB.

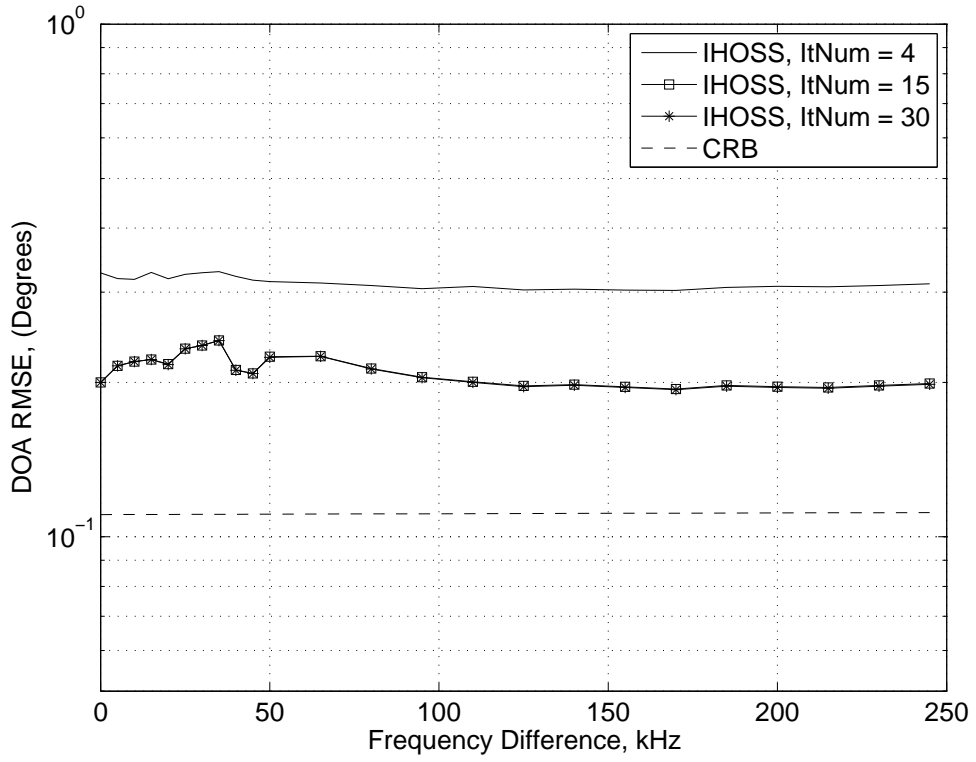


(a)

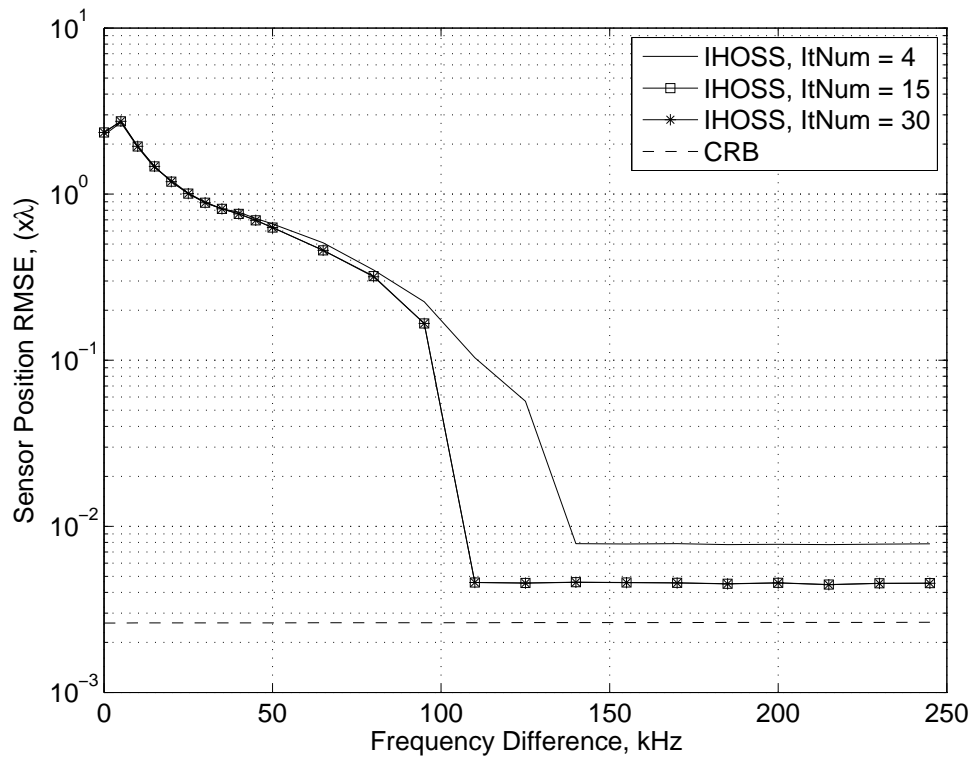


(b)

Figure 2.13: (a) DOA and (b) position estimation performance for varying sensor density at SNR = 20 dB.



(a)



(b)

Figure 2.14: (a) DOA and (b) position estimation performance for different frequency differences. SNR = 20 dB.

## CHAPTER 3

### **DIRECTION-OF-ARRIVAL ESTIMATION AND SENSOR POSITION CALIBRATION WITH MODIFIED ITERATIVE HOS-SOS (MIHOSS) ALGORITHM**

In Chapter 2, IHOSS algorithm [5], [28] is presented, which jointly uses HOS and SOS approaches iteratively for the estimation of both source DOAs and sensor positions. In IHOSS algorithm, except the two reference sensors there is no a priori information about the sensor positions. The positions of the two reference sensors are assumed to be known. IHOSS algorithm considers the ambiguity problem in sensor position estimation and solves the problem by using the source signals observed at multiple frequencies. Hence it is applicable for wideband signals.

In this chapter, the DOA estimation problem in the presence of sensor position errors is investigated for the narrowband signals. Since the ambiguity in sensor position estimations can be solved by observing the source signals at least in two different frequencies, IHOSS algorithm can not be used directly for the narrowband signals. We have modified the sensor position estimation method in IHOSS to solve the ambiguity problem for narrowband signals and the new algorithm is called MIHOSS (Modified Iterative HOS-SOS). HOS and SOS approaches for the DOA estimations are the same as in IHOSS algorithm. MIHOSS requires to know the nominal sensor positions to solve the ambiguity problem. It is proved that the ambiguity problem can be solved if the perturbations in sensor positions are bounded. The upper bound for the perturbations is also presented.

In the literature, array calibration problem for the sensor position errors is investigated in two settings, namely, small error [41] and large error approximations [42]. In small error approxi-

mation, the perturbations are assumed to be small and array calibration is performed by using a first order approximation. The first order approximation is not applicable as the perturbations are increased. Large error approximation [42] is proposed to circumvent the limitations of the small error approximation. However the DOA estimation problem is considered for a uniform circular array and for some fixed source DOAs.

In MIHOSS, HOS approach can estimate the DOA angles and array steering matrix without knowing the sensor positions except the two reference sensors. Therefore, MIHOSS does not require small error assumptions and can handle the calibration problem for large position errors. Furthermore, MIHOSS algorithm can be applied for any arbitrary sensor geometry.

### 3.1 Problem Statement for MIHOSS Algorithm

It is assumed that the array is composed of randomly deployed  $M$  sensors and there are  $L$  far-field sources. Two sensors are selected as the reference sensors. The sensor positions are randomly perturbed from their nominal positions except the two reference sensors. The array model for MIHOSS algorithm is illustrated in Fig. 3.1 The positions of the reference sensors

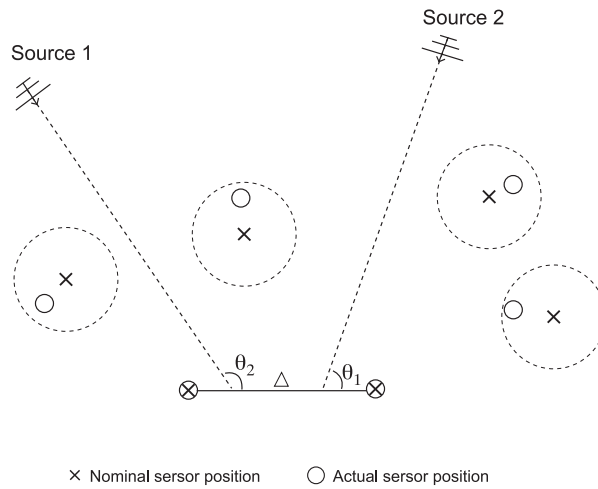


Figure 3.1: Array model for MIHOSS algorithm. The circle with dashed line represents the bound on the perturbations in sensor positions.

are assumed to be known and the distance between them is less than or equal to  $\lambda/2$ , where  $\lambda$  is the wavelength of the incoming source signals. Under these assumptions, the received

signal vector for the sensor array can be written as,

$$\mathbf{x}(t) = \mathbf{A}(\boldsymbol{\Theta}, \mathbf{P}^0 + \tilde{\mathbf{P}})\mathbf{s}(t) + \mathbf{v}(t), \quad t = 1, 2, \dots, N \quad (3.1)$$

where,  $N$  is the number of snapshots,  $\mathbf{s}(t) = [s_1(t), \dots, s_L(t)]^T$  is the  $L \times 1$  vector of  $L$  sources,  $\mathbf{v}(t)$  is the  $M \times 1$  vector of Gaussian noise. Source signals are assumed to be non-Gaussian and they can be correlated but not coherent. Noise is assumed to be statistically independent with the source signals.  $\boldsymbol{\Theta} = [\theta_1, \dots, \theta_L]$  is the source DOA vector,  $\mathbf{P}^0 = [\mathbf{p}_1^{0T}, \dots, \mathbf{p}_M^{0T}]^T$  and  $\tilde{\mathbf{P}} = [\tilde{\mathbf{p}}_1^T, \dots, \tilde{\mathbf{p}}_M^T]^T$  are the nominal sensor positions and the perturbations in positions, respectively.  $\mathbf{A}(\boldsymbol{\Theta}, \mathbf{P})$  is the  $M \times L$  array steering matrix, composed of,

$$[\mathbf{A}(\boldsymbol{\Theta}, \mathbf{P}^0 + \tilde{\mathbf{P}})]_{mi} = \exp \left\{ j \frac{2\pi}{\lambda} \left[ (p_{m,x}^0 + \tilde{p}_{m,x}) \cos \theta_i + (p_{m,y}^0 + \tilde{p}_{m,y}) \sin \theta_i \right] \right\} \quad (3.2)$$

where,  $\theta_i$  is the direction-of-arrival of  $i^{th}$  source in azimuth,  $\mathbf{p}_m^0 = [p_{m,x}^0, p_{m,y}^0]$  and  $\tilde{\mathbf{p}}_m = [\tilde{p}_{m,x}, \tilde{p}_{m,y}]$  are the 2D nominal position of the  $m^{th}$  sensor and the 2D perturbation of the  $m^{th}$  sensor position, respectively. Since the positions of the two reference sensors are known, their perturbations are zero, i.e.,  $\tilde{\mathbf{p}}_m = \mathbf{0}$ ,  $m = 1, 2$ .  $(\cdot)^T$  is the transpose operator.

The goal in MIHOSS is to estimate both DOAs of  $L$  sources and the perturbation parameters of  $M - 2$  sensors.

### 3.2 MIHOSS Algorithm

In this section, MIHOSS algorithm is introduced for a solution to the problem described in Section 3.1. MIHOSS algorithm is based on the IHOSS algorithm [28], described in Section 2.2, which uses the HOS and SOS approaches jointly. The basic differences between the IHOSS and MIHOSS are the solution of the ambiguity in sensor positions and the parameter updating process in the iteration mechanism. IHOSS algorithm requires observations at multiple frequencies for solving the ambiguity problem in sensor position estimations. Also the DOA and array steering matrix estimates obtained for each frequency are jointly used to obtain the best parameter updates at each iteration. On the other hand, MIHOSS observes the source signals in one frequency and updates the parameters at each iteration by using the DOA and array steering matrix estimates obtained from single frequency. In MIHOSS, the ambiguity problem in sensor position estimations is solved by using the nominal sensor positions.

The details of the sensor position estimation and the parameter update mechanism are given in the following subsections.

### 3.2.1 Unambiguous Sensor Localization

Once the DOA and array steering matrix estimations are found using HOS approach as in (2.35) and (2.38), sensor locations can be estimated using (3.2). Due to  $2\pi$  ambiguity, the elements of the array steering matrix in (3.2), corresponding to  $m^{th}$  sensor and  $i^{th}$  source can be rewritten in the following form,

$$a_{m,i} = e^{j\frac{2\pi}{\lambda}[(\mathbf{p}_m^0 + \tilde{\mathbf{p}}_m)\mathbf{u}(\theta_i) - \lambda k_{m,i}]} \quad (3.3)$$

where  $\mathbf{u}(\theta_i) = [\cos(\theta_i), \sin(\theta_i)]^T$  is the unit direction vector of the  $i^{th}$  incoming source and  $k_{m,i}$  is an integer specified for the  $m^{th}$  sensor and the  $i^{th}$  source. When all the incoming sources are considered, the following relation can be written,

$$(\mathbf{p}_m^0 + \tilde{\mathbf{p}}_m)\mathbf{U}(\hat{\Theta}) = \frac{\lambda}{2\pi}\hat{\mathbf{\Xi}}_m + \lambda\mathbf{k}_m, \quad 1 \leq m \leq M \quad (3.4)$$

where

$$\hat{\mathbf{\Xi}}_m = \begin{bmatrix} \angle(\hat{a}_{m,1}) & \angle(\hat{a}_{m,2}) & \dots & \angle(\hat{a}_{m,L}) \end{bmatrix} \quad (3.5)$$

$$\mathbf{k}_m = \begin{bmatrix} k_{m,1} & k_{m,2} & \dots & k_{m,L} \end{bmatrix} \quad (3.6)$$

$$\mathbf{U}(\hat{\Theta}) = \begin{bmatrix} \mathbf{u}(\hat{\theta}_1) & \dots & \mathbf{u}(\hat{\theta}_L) \end{bmatrix} \quad (3.7)$$

$\hat{x}$  stands for the estimation of  $x$  and  $\angle(\hat{a}_{m,i})$  is the phase term of the array steering matrix element estimate in (3.3).

The position perturbation of the  $m^{th}$  sensor can easily be found from (3.4) in the least squares sense as,

$$\hat{\mathbf{p}}_m(\mathbf{k}_m) = \left( \frac{\lambda}{2\pi}\hat{\mathbf{\Xi}}_m + \lambda\mathbf{k}_m \right) \mathbf{U}^\dagger(\hat{\Theta}) - \mathbf{p}_m^0, \quad 1 \leq m \leq M \quad (3.8)$$

where

$$\mathbf{U}^\dagger(\hat{\Theta}) = \mathbf{U}^T(\hat{\Theta}) \left( \mathbf{U}^T(\hat{\Theta})\mathbf{U}(\hat{\Theta}) \right)^{-1} \quad (3.9)$$

Note that the position perturbation estimate in (3.8) takes different values for different  $\mathbf{k}_m$  values. Therefore,  $\hat{\mathbf{p}}_m(\mathbf{k}_m)$  values are considered as the ambiguous position perturbation estimates of the  $m^{th}$  sensor. The possible values of  $\mathbf{k}_m$  are determined in a similar way as in

(2.48), i.e.,

$$\mathbf{k}_m = \left\{ \mathbf{k} \in Z \left| \left( \frac{\lambda}{2\pi} \hat{\mathbf{e}}_m + \lambda \mathbf{k} \right) (\mathbf{I}_{L \times L} - \mathbf{U}^\dagger(\hat{\mathbf{\Theta}}) \mathbf{U}(\hat{\mathbf{\Theta}})) \left( \frac{\lambda}{2\pi} \hat{\mathbf{e}}_m + \lambda \mathbf{k} \right)^H \leq \epsilon \right. \right\} \quad (3.10)$$

If the position perturbation is limited, the ambiguity problem can be solved by selecting the sensor position perturbation estimate with minimum norm, i.e.,

$$\hat{\mathbf{p}}_m = \arg \min_{\mathbf{k}_m} \|\hat{\mathbf{p}}_m(\mathbf{k}_m)\| \quad (3.11)$$

Then, the sensor position matrix estimate,  $\hat{\mathbf{P}} = \mathbf{P}^0 + \hat{\mathbf{P}}$ , is constructed using (3.11) for  $3 \leq m \leq M$  with the nominal sensor positions. The upper bound of perturbations for unambiguous sensor position estimations is given in Lemma-2.

**Lemma-2:** Let  $e_m$  be the error in position estimation of the  $m^{\text{th}}$  sensor, i.e.,  $\|\hat{\mathbf{p}}_m - \tilde{\mathbf{p}}_m\| = e_m$ . Then, the ambiguity problem in sensor position estimation is solved if the perturbations in sensor positions are bounded, i.e.,

$$\|\tilde{\mathbf{p}}_m\| < \frac{\lambda}{2} \min_{\mathbf{k}_m \neq \hat{\mathbf{k}}_m^0} \left\| (\mathbf{k}_m - \hat{\mathbf{k}}_m^0) \mathbf{U}^\dagger(\hat{\mathbf{\Theta}}) \right\| - e_m, \quad 1 \leq m \leq M \quad (3.12)$$

When the condition in (3.12) is satisfied, it is guaranteed that the sensor position estimate that is closest to the nominal sensor position is also closest to the actual sensor position. Note that, ‘‘closest to the nominal sensor position’’ corresponds to the minimum position perturbation estimation as in (3.11). This case is illustrated in Fig. 3.2-a. When the upper bound of perturbations in sensor positions are increased such that the condition in (3.12) is no more valid, the sensor position estimate with minimum perturbation estimation (3.11), may be far away from the actual position of the sensor as shown in Fig. 3.2-b.

Note that  $e_m$  in (3.12) relates with the least squares error of the position estimation algorithm that can be estimated from the CRB expressions and decreases with increasing SNR. The term that is tried to be minimized in (3.12) depends on the distribution of DOA angles and numerical results show that its value is approximately  $\lambda/2$ . Therefore, for the high SNR case, MIHOSS algorithm can estimate the sensor positions unambiguously up to the perturbation of  $\lambda/2$ , which is also high for the large error case in literature [42].

The proof of Lemma-2 is given in Appendix E.

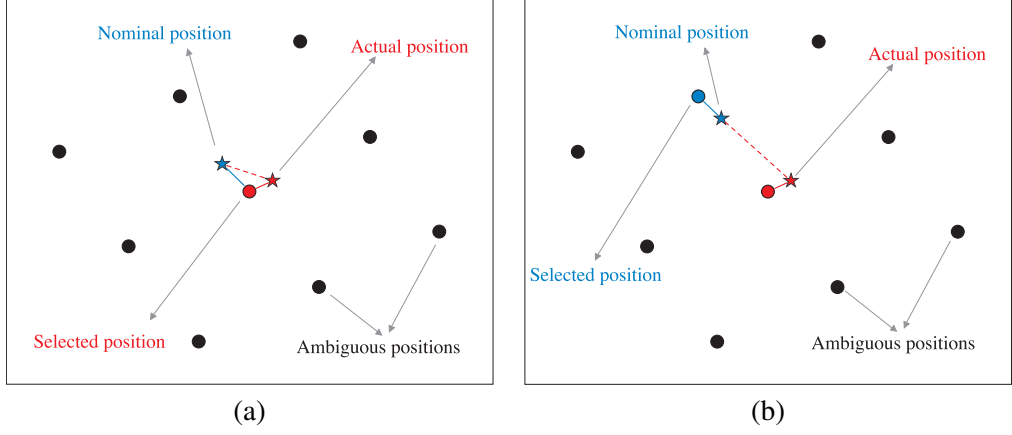


Figure 3.2: Ambiguous sensor positions for the errors that (a) satisfy and (b) does not satisfy the condition in (3.12).

### 3.2.2 The Cost Function and The Algorithmic Steps

MIHOSS algorithm iteratively updates the DOA and array steering matrix estimates using the HOS and SOS approaches sequentially as summarized in Algorithm 3.1. The cost function used at each iteration to select the best array steering vector estimates for each source is defined by the MUSIC pseudospectrum, i.e.,

$$\Gamma(\hat{\mathbf{a}}_i) = \left( \hat{\mathbf{a}}_i^H \mathbf{G} \mathbf{G}^H \hat{\mathbf{a}}_i \right)^{-1} \quad (3.13)$$

where  $\hat{\mathbf{a}}_i$  is the array steering vector estimate for the  $i^{\text{th}}$  source and  $\mathbf{G}$  is the  $M \times (M-L)$  matrix whose columns are composed of the eigenvectors corresponding to  $M-L$  smallest eigenvalues of the correlation matrix obtained in the SOS approach. Note that the cost function,  $\Gamma(\hat{\mathbf{a}}_i)$  is non-negative. At each iteration,  $n$ , we have  $\Gamma(\hat{\mathbf{a}}_i^{(n)}) \geq \Gamma(\hat{\mathbf{a}}_i^{(n-1)}) \geq 0$ . Therefore, the proposed MIHOSS algorithm is guaranteed to converge to a certain value,  $\bar{\Gamma}$ , at the end of the iterations. However, the convergence to this value does not mean that the global optimum is reached as it is the general disadvantage of all iterative algorithms [27].

### 3.3 Performance Results

MIHOSS algorithm is compared with the MUSIC [1] and small error approximation [41], illustrated as SmallError in the figures, for DOA and sensor position estimations. CRB [28] is also evaluated for both DOA and sensor position estimation. While MIHOSS and Small-Error algorithms are iterative methods, MUSIC algorithm is non iterative one. As stated in

---

**Algorithm 3.1:** Pseudocode for MIHOSS algorithm.

---

```

1  $n = 0$ . Initialize the array steering vector for each source,  $\hat{\mathbf{a}}_i^{(0)}$ , as zero vector. Initialize
   the cost function for each source to zero,  $\Gamma_i^{(0)} = 0$  for  $1 \leq i \leq L$ ;
2 Termination = true. Estimate the proposed cumulant matrix from the array output and
    $\hat{\mathbf{a}}_i^{(n)}$  as in (2.39). Then, find the DOA estimates,  $\hat{\theta}_i^{HOS}$  using (2.35) and the array
   steering matrix  $\hat{\mathbf{A}}^{HOS}$ , using (2.38), for  $1 \leq i \leq L$ ;
3 Find the sensor position estimates,  $\hat{\mathbf{P}} = \mathbf{P}^0 + \hat{\mathbf{P}}$ , as in (3.11) using (3.7) and (3.5) with
    $\hat{\theta}_i^{HOS}$  and  $\hat{\mathbf{A}}^{HOS}$ , for  $1 \leq i \leq L$ ;
4 Find  $\hat{\theta}_i^{(SOS)}$  using  $\hat{\mathbf{P}}$  as in (2.58). Then, find  $\hat{\mathbf{a}}_i^{(SOS)}$  using  $\hat{\mathbf{P}}$  and  $\hat{\theta}_i^{(SOS)}$  as in (2.59);
5 for  $i = 1$  to  $L$  do
6   if  $\Gamma(\hat{\mathbf{a}}_i^{(SOS)}) \geq \Gamma_i^{(n)}$  then
7      $\hat{\mathbf{a}}_i^{(n+1)} = \hat{\mathbf{a}}_i^{(SOS)}$ ,  $\hat{\theta}_i^{(n+1)} = \hat{\theta}_i^{(SOS)}$ ,  $\Gamma_i^{(n+1)} = \Gamma(\hat{\mathbf{a}}_i^{(SOS)})$ , Termination = false;
8   else
9      $\hat{\mathbf{a}}_i^{(n+1)} = \hat{\mathbf{a}}_i^{(n)}$ ,  $\hat{\theta}_i^{(n+1)} = \hat{\theta}_i^{(n)}$ ;
10  end
11 end
12 if Termination = false then
13    $n = n + 1$ , Go to Step 2;
14 else
15   Find the final estimate of sensor positions using  $\hat{\theta}_i^{(n)}$  and  $\hat{\mathbf{a}}_i^{(n)}$ ,  $1 \leq i \leq L$ ;
16 end

```

---

Algorithm 3.1, MIHOSS starts with the SOS MUSIC algorithm and iterates HOS and SOS approaches to update both DOA and sensor position estimations. Also SmallError [41] algorithm starts with MUSIC algorithm and iteratively updates both DOA and sensor position estimations using SOS approach. Therefore, comparing MUSIC algorithm with MIHOSS and SmallError algorithms shows the effectiveness of the iteration processes. Note that for a fair comparison, the sensor position estimation algorithm described in Section 3.2.1 is also applied for the MUSIC algorithm.

It is assumed that there are two far-field sources and  $M = 10$  sensors. Each sensor position except the two reference sensors is randomly selected from a uniform distribution in the deployment area of  $2\lambda \times 2\lambda$ . The reference sensors are placed at  $(0, 0)$  and  $(\lambda/2, 0)$ . The

positions of the sensors other than the reference sensors are arbitrarily perturbed. The perturbation values are randomly selected with a uniform distribution. For the parameter estimation,  $N = 1000$  snapshots are collected. The performance results are the average of 100 trials. At each trial, source signals, noise, the sensor positions except the reference sensors, the perturbations and the DOA angles of source signals are changed randomly. The difference between the DOA angles of the source signals is set to 40 degrees. The source signals have a uniform distribution and the noise is additive white Gaussian and uncorrelated with the source signals. The simulation parameters are summarized in Table 3.1.

Table 3.1: Simulation parameters for MIHOSS algorithm.

Number of sensors	$M = 10$
Number of sources	$L = 2$
Number of snapshots	$N = 1000$
Wavelength	$\lambda = 30$ meters
Deployment area	$[2\lambda \times 2\lambda]$
Distance between reference sensors	$\Delta = \lambda/2$
Separation of source DOAs	$40^\circ$
Number of trials	100

The performance results for the DOA and sensor position estimations at different SNR values are illustrated in Fig. 3.3. The sensor position perturbation is limited to  $0.1\lambda$ . It is seen that both MUSIC and small error approach algorithm (SmallError) have a flooring effect for both DOA and sensor position estimations. As it is seen in Fig. 3.3, SmallError algorithm slightly improves the MUSIC performance. It is also seen that after approximately SNR = 7 dB MIHOSS algorithm significantly outperforms and closely follows CRB for both DOA and sensor position estimations.

In Fig. 3.4, the performance of the algorithms is presented for different position perturbations. SNR is set to 30 dB. As it is seen in Fig. 3.4, the parameter estimation performance of MIHOSS algorithm is not affected from the value of perturbations and closely follows CRB. It is also observed in Fig. 3.4-(b) that, MIHOSS algorithm effectively solves the ambiguity problem up to a perturbation value of  $0.42\lambda$ . The condition presented in Lemma-2 is not satisfied for further increase in perturbations and sensor positions can not be found unambiguously. Note that DOA estimation is accurate and is not affected by the sensor position ambiguity as shown in Fig. 3.4-(a). This is due to the fact that array steering matrix estimate

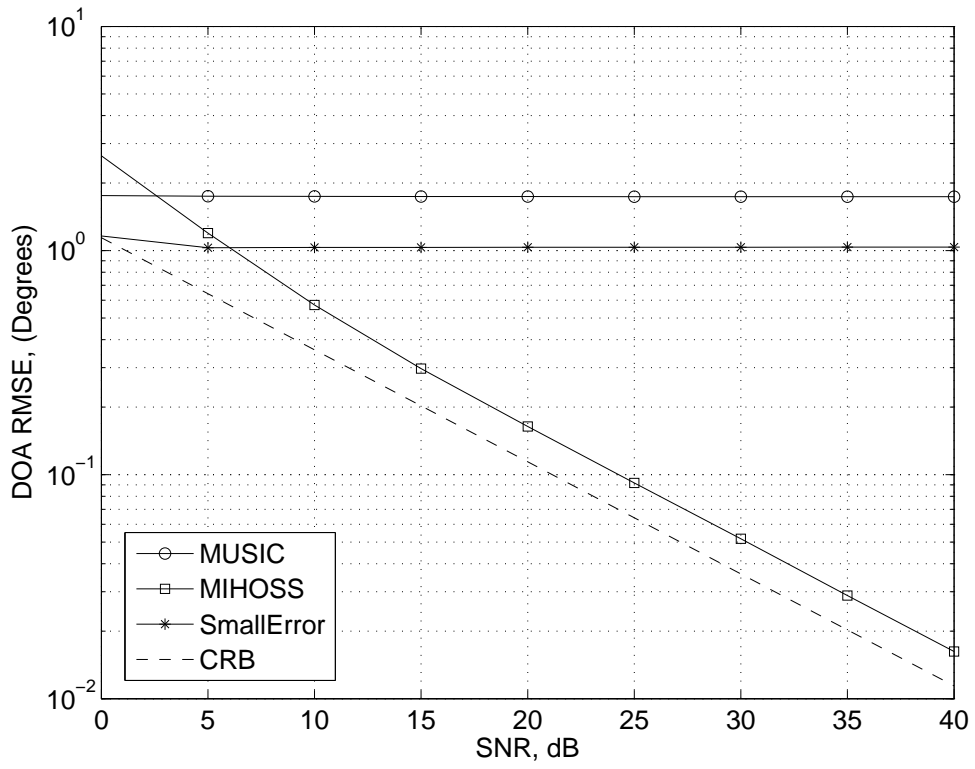
is accurate while the positions are ambiguous. The performance of both MUSIC and Small-Error algorithm degrade significantly for the large perturbation values. SmallError algorithm slightly outperforms MIHOSS algorithm only for very small perturbations (less than  $0.01\lambda$ ). For the perturbations less than  $0.0016\lambda$  MUSIC outperforms both MIHOSS and SmallError algorithms as well as CRB. The reason for this fact is that iterative processes in MIHOSS and SmallError algorithms decrease the estimation performances for the extremely small perturbations. As shown in (3.8), pseudoinverse operator is used for sensor position estimation, which is not an exact solution. Iteratively updating sensor positions may result worse position estimation than the nominal sensor positions when the perturbation is extremely small. The similar explanation is also valid for the SmallError algorithm. While CRB does not specify any algorithm for sensor position estimation, it uses perturbations as unknown parameters and tries to find the minimum variance for both DOA and sensor position estimations jointly. Hence, CRB assumes that there are always errors in sensor positions even if there is not. On the other hand MUSIC algorithm finds the DOA and sensor position estimations in a single step. It does not assume that there are errors in sensor positions and does not update the estimations iteratively.

### 3.4 Advantages of MIHOSS Algorithm

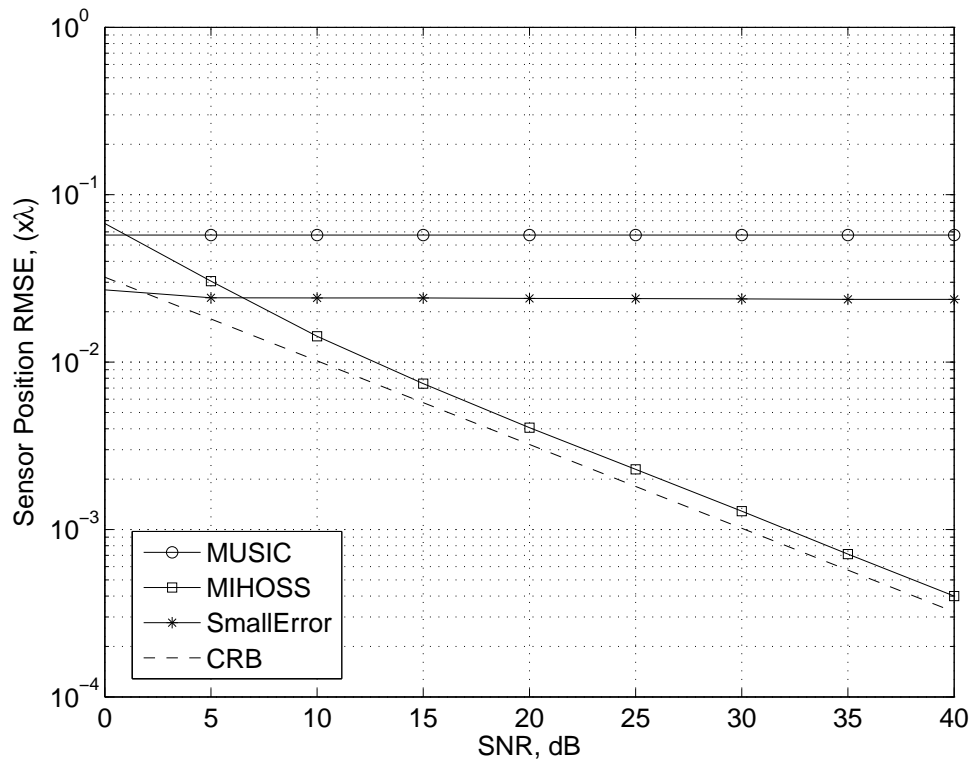
The advantages of the MIHOSS algorithm can be summarized as follows:

- MIHOSS algorithm jointly finds the DOA and sensor position estimates when there are perturbations in sensor positions except the two reference sensors.
- The ambiguity problem in sensor position estimation is solved by selecting the sensor position closest to the nominal sensor position.
- Sensor positions are estimated accurately for larger perturbations compared to the previous works in literature [42].
  - 12 m uncertainty in sensor positions can be reduced to 4 cm at  $\text{SNR} = 30$  dB.
- DOA angles are estimated accurately even for large error in sensor positions.
  - 0.025 degrees accuracy in DOA estimation is achieved at  $\text{SNR} = 30$  dB.

- MIHOSS algorithm is applicable to any sensor geometry.

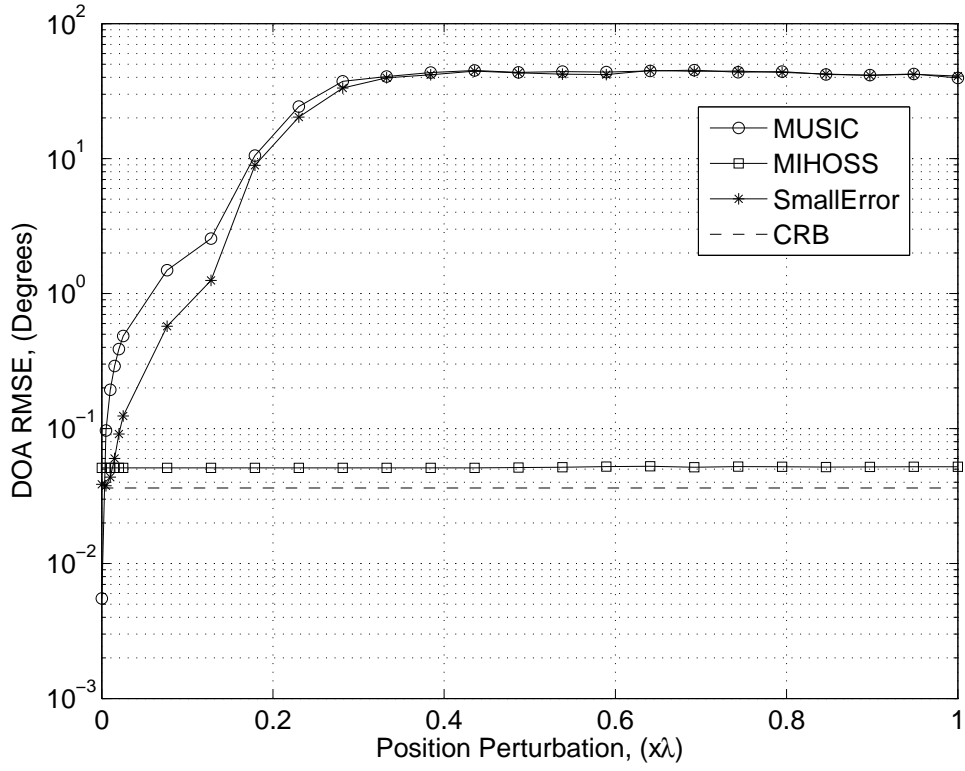


(a)

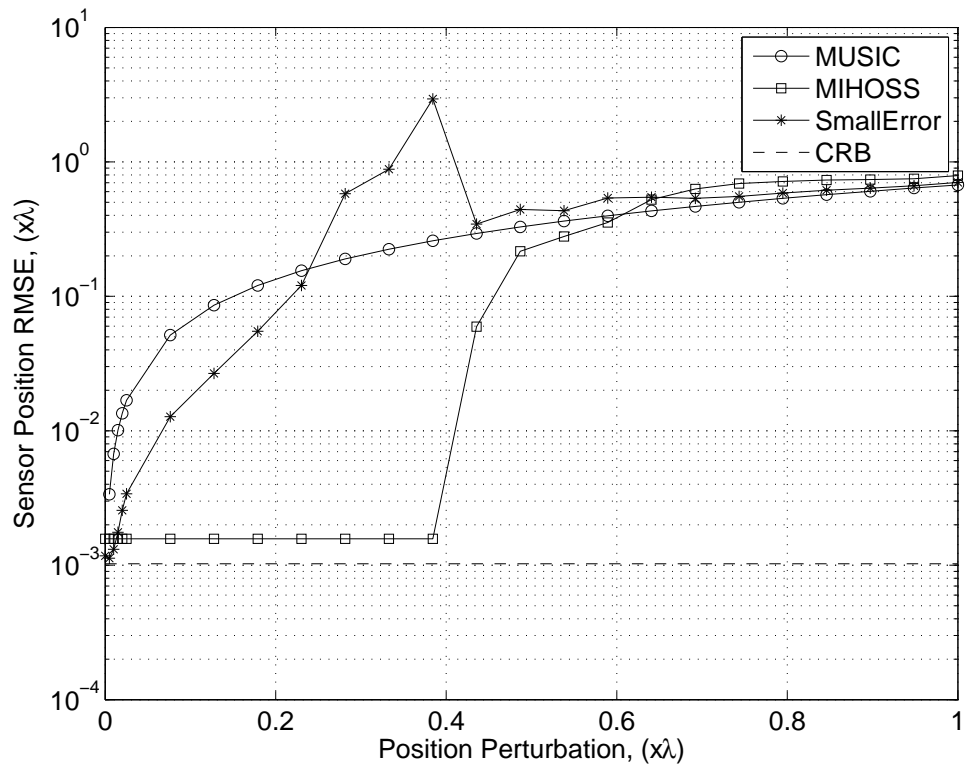


(b)

Figure 3.3: (a) DOA and (b) position estimation RMSE values for different SNR values and sensor position perturbation of  $0.1\lambda$ .



(a)



(b)

Figure 3.4: (a) DOA and (b) position estimation RMSE values for different sensor position perturbations and SNR = 30 dB.

## CHAPTER 4

### ONLINE CALIBRATION WITH ITERATIVE HOS-SOS ALGORITHM IN THE PRESENCE OF MUTUAL COUPLING AND GAIN/PHASE MISMATCH

In this chapter, the online array calibration problem in the presence of mutual coupling and gain/phase mismatches is investigated. For the solution of this problem, a new method, CIHOSS (Online Calibration with Iterative HOS-SOS) Algorithm, is proposed to estimate the DOA angles of multiple sources, gain/phase and mutual coupling parameters jointly by using HOS and SOS approaches in an iterative manner. The proposed method does not assume a special structure for mutual coupling matrix and therefore it is applicable for any arbitrary but known sensor geometry. It only requires two reference sensors that are perfectly calibrated with known gain/phase mismatches and mutual coupling coefficients and no interaction between the reference sensors and the other sensors. Due to the perfectly calibrated reference sensor assumption, the proposed algorithm can be categorized as partly calibrated subarray [34]. But in [34], the interaction between calibrated subarrays is not considered and the required calibrated sensors are much higher than that of the proposed algorithm in this work. As it is stated in [36] the iterative methods suffer from the poor initial estimates for the DOA angles and calibration parameters. In CIHOSS, the initial guesses for DOA angles as well as gain/phase mismatches and mutual coupling coefficients are estimated directly from the sensor outputs using HOS approach. In [30], it is shown that HOS can effectively be used for the joint estimation of DOA angles, gain/phase mismatches and mutual coupling coefficients when the source signals are statistically independent. In this work, the source signals are not assumed to be statistically independent and the performance degradation of the HOS approach is compensated by applying iterative SOS approach to improve the initial estimates.

SOS approach is more accurate for the statistical estimation especially for the small number of samples. Performance results show the effectiveness of the CIHOSS algorithm.

#### 4.1 Problem Statement

A planar array with two reference sensors and  $K - 2$  randomly deployed sensors is assumed. The reference sensors are perfectly calibrated and there is no interaction between the reference sensors and the remaining sensors. Therefore, mutual coupling coefficients between the reference sensors and  $K - 2$  sensors are zero. The magnitude of the mutual coupling between sensors is inversely proportional with the distance between sensors and may become negligible if the distance exceeds a few wavelengths [29]. Hence, it is assumed that the distance between the reference and remaining sensors is greater than the operating wavelength,  $\lambda$ . The reference sensors are placed at  $(0, 0)$  and  $(\Delta, 0)$  coordinates in  $x - y$  plane without loss of generality where  $\Delta \leq \lambda/2$ . Sources are in the same plane as the sensors. The array model for CIHOSS algorithm is illustrated in Fig. 4.1 It is also assumed that different number of

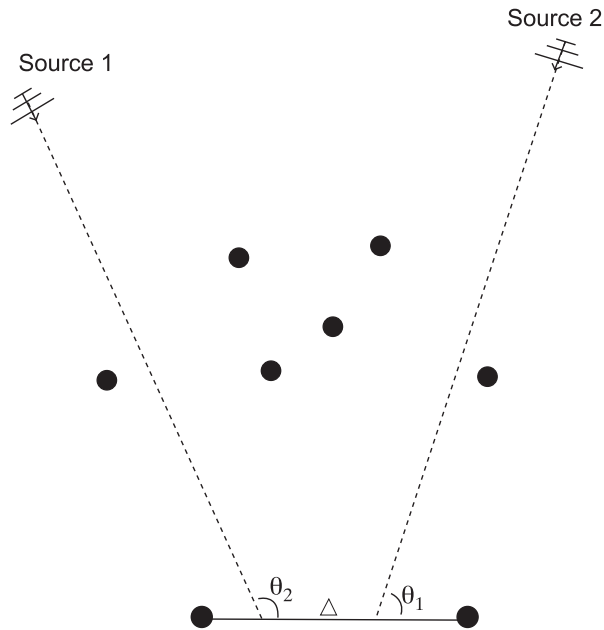


Figure 4.1: Array model for CIHOSS algorithm. There are mutual coupling effects between sensors.

sources exist at different time slots. Hence,  $L$  number of sources are observed at  $H$  different

time slots, i.e.,

$$L = \sum_{h=1}^H L_h \quad (4.1)$$

where  $L_h$  is the number of sources at time slot  $h$ . It is assumed that the source signals have a non-Gaussian distribution. Narrowband model is assumed and the array output vector for the  $h^{th}$  time slot,  $\mathbf{x}^{(h)}(t) = [x_1^{(h)}(t), \dots, x_K^{(h)}(t)]^T$ , can be written as,

$$\begin{aligned} \mathbf{x}^{(h)}(t) &= \mathbf{\Gamma} \mathbf{A}^{(h)}(\Theta^{(h)}) \mathbf{s}^{(h)}(t) + \mathbf{v}^{(h)}(t), \quad t = 1, 2, \dots, N_h \\ &= \bar{\mathbf{A}}^{(h)}(\Theta^{(h)}) \mathbf{s}^{(h)}(t) + \mathbf{v}^{(h)}(t) \end{aligned} \quad (4.2)$$

where,  $N_h$  is the number of snapshots received at the  $h^{th}$  time slot,  $\mathbf{s}^{(h)}(t) = [s_1^{(h)}(t), \dots, s_{L_h}^{(h)}(t)]^T$  is the  $L_h \times 1$  vector of  $L_h$  sources,  $\mathbf{v}^{(h)}(t) = [v_1^{(h)}(t), \dots, v_K^{(h)}(t)]^T$  is the  $K \times 1$  vector of Gaussian noise.  $\mathbf{A}^{(h)}(\Theta^{(h)})$  and  $\bar{\mathbf{A}}^{(h)}(\Theta^{(h)})$  are the nominal and actual array steering matrices for the  $h^{th}$  time slot, respectively.  $\Theta^{(h)} = [\theta_1^{(h)}, \dots, \theta_{L_h}^{(h)}]$  is the DOA angles of  $L_h$  sources received at time slot  $h$ .  $\mathbf{\Gamma}$  is the array distortion matrix which is the product of  $K \times K$  complex mutual coupling matrix,  $\mathbf{M}$ , and  $K \times K$  diagonal gain/phase mismatch matrix,  $\mathbf{T}$ , i.e.,

$$\mathbf{\Gamma} = \mathbf{M} \mathbf{T} \quad (4.3)$$

It is assumed that the total observation time, i.e.,  $N = \sum_{h=1}^H N_h$  is short enough so that the array distortion matrix parameters do not change for different time slots. The matrices  $\mathbf{A}^{(h)}(\Theta^{(h)})$ ,  $\mathbf{M}$  and  $\mathbf{T}$  are defined as

$$\mathbf{A}^{(h)}(\Theta^{(h)}) = \begin{bmatrix} 1 & \dots & 1 \\ e^{j\frac{2\pi}{\lambda} \Delta \cos(\theta_1^{(h)})} & \dots & e^{j\frac{2\pi}{\lambda} \Delta \cos(\theta_{L_h}^{(h)})} \\ e^{j\frac{2\pi}{\lambda} \mathbf{p}_3 \mathbf{u}(\theta_1^{(h)})} & \dots & e^{j\frac{2\pi}{\lambda} \mathbf{p}_3 \mathbf{u}(\theta_{L_h}^{(h)})} \\ \vdots & & \\ e^{j\frac{2\pi}{\lambda} \mathbf{p}_K \mathbf{u}(\theta_1^{(h)})} & \dots & e^{j\frac{2\pi}{\lambda} \mathbf{p}_K \mathbf{u}(\theta_{L_h}^{(h)})} \end{bmatrix} \quad (4.4)$$

$$\mathbf{M} = \begin{bmatrix} 1 & m_{12} & 0 & 0 & 0 & \dots & 0 \\ m_{21} & 1 & 0 & 0 & 0 & \dots & 0 \\ 0 & 0 & 1 & m_{34} & m_{35} & \dots & m_{3K} \\ 0 & 0 & m_{43} & 1 & m_{45} & \dots & m_{4K} \\ 0 & 0 & m_{53} & m_{54} & 1 & \dots & m_{5K} \\ \vdots & \vdots & \vdots & \vdots & \vdots & \ddots & \vdots \\ 0 & 0 & m_{K3} & m_{K4} & m_{K5} & \dots & 1 \end{bmatrix} \quad (4.5)$$

$$\mathbf{T} = \text{diag} \left( 1 \ 1 \ \alpha_3 e^{j\beta_3} \ \dots \ \alpha_K e^{j\beta_K} \right) \quad (4.6)$$

where  $\mathbf{p}_m = [p_{m,x}, p_{m,y}]$  is the 2D position of the  $m^{\text{th}}$  sensor,  $\theta_l^{(h)}$  is the direction-of-arrival of  $l^{\text{th}}$  source in azimuth at time slot  $h$  and  $\mathbf{u}(\theta_l^{(h)}) = [\cos(\theta_l^{(h)}), \sin(\theta_l^{(h)})]^T$  is the unit direction vector of the  $l^{\text{th}}$  source at time slot  $h$ .  $m_{i,j}$  is the complex mutual coupling coefficient between sensor  $i$  and  $j$ .  $\alpha_i$  and  $\beta_i$  are the gain and phase errors of the  $i^{\text{th}}$  sensor, respectively. Since the reference sensors are assumed to be perfectly calibrated,  $m_{12}$  and  $m_{21}$  are known and the mutual coupling between the reference sensors and the other sensors are zero, as in (4.5). Note that most of the works in literature assume that the mutual coupling matrix is symmetric due to the reciprocity theorem [43]. On the other hand, nonreciprocal structures are investigated in some works [44], [45]. Therefore, in order to deal with the most general case, we consider the mutual coupling matrix to be non-symmetric in this thesis.

The goal in this work is to estimate both the DOAs of  $L$  sources,  $\{\theta_l^{(h)}\}_{h=1, l=1}^{H, L_h}$ , and the unknown parameters in  $\mathbf{M}$  and  $\mathbf{T}$  matrices,  $\{m_{i,j}, \alpha_i, \beta_i\}_{i,j=3}^K$  for a given sensor positions, sensor outputs and the mutual coupling coefficients of the two reference sensors,  $m_{12}$  and  $m_{21}$ . One important feature of the above model is that the lower right matrix for  $\mathbf{M}$  is unstructured corresponding to a randomly deployed sensor array.

## 4.2 Cumulant Matrix

Due to the presence of mutual coupling and gain/phase mismatches, the Cumulant matrix derived in Section 2.2.1 can not be directly used for the problem defined in Section 4.1. Note also that in IHOSS and MIHOSS algorithms single cumulant matrix constructed from the reference sensors 1 and 2. On the other hand CIHOSS algorithm uses multiple cumulant matrices constructed from different sensor pairs. Therefore, the cumulant matrix, which is different from the one in IHOSS and MIHOSS algorithms is introduced in this section.

When sensors  $i$  and  $j$  are selected as the sensor pairs, the cumulant matrix composed of the fourth-order cumulants for the time slot  $h$  is written as [30],

$$\mathbf{C}_{ij}^{(h)}(k, l) = \begin{bmatrix} \text{Cum}(x_i^{(h)}(t), x_i^{(h)*}(t), x_k^{(h)}(t), x_l^{(h)*}(t)) & \text{Cum}(x_j^{(h)}(t), x_i^{(h)*}(t), x_k^{(h)}(t), x_l^{(h)*}(t)) \\ \text{Cum}(x_i^{(h)}(t), x_j^{(h)*}(t), x_k^{(h)}(t), x_l^{(h)*}(t)) & \text{Cum}(x_j^{(h)}(t), x_j^{(h)*}(t), x_k^{(h)}(t), x_l^{(h)*}(t)) \end{bmatrix} \quad (4.7)$$

where  $x_i^{(h)}(t)$  is the output signal of the  $i^{\text{th}}$  sensor at time slot  $h$ . For the Gaussian noise

assumption with the cumulant properties in [12], the cumulant matrix is simplified as,

$$\mathbf{C}_{ij}^{(h)} = \begin{bmatrix} \left( \overline{\mathbf{A}}^{(h)} \otimes \overline{\mathbf{a}}_{ri}^{(h)*} \right) \mathbf{C}_s^{(h)} \left( \overline{\mathbf{A}}^{(h)} \otimes \overline{\mathbf{a}}_{ri}^{(h)*} \right)^H & \left( \overline{\mathbf{A}}^{(h)} \otimes \overline{\mathbf{a}}_{ri}^{(h)*} \right) \mathbf{C}_s^{(h)} \left( \overline{\mathbf{A}}^{(h)} \otimes \overline{\mathbf{a}}_{rj}^{(h)*} \right)^H \\ \left( \overline{\mathbf{A}}^{(h)} \otimes \overline{\mathbf{a}}_{rj}^{(h)*} \right) \mathbf{C}_s^{(h)} \left( \overline{\mathbf{A}}^{(h)} \otimes \overline{\mathbf{a}}_{ri}^{(h)*} \right)^H & \left( \overline{\mathbf{A}}^{(h)} \otimes \overline{\mathbf{a}}_{rj}^{(h)*} \right) \mathbf{C}_s^{(h)} \left( \overline{\mathbf{A}}^{(h)} \otimes \overline{\mathbf{a}}_{rj}^{(h)*} \right)^H \end{bmatrix} \quad (4.8)$$

where  $\overline{\mathbf{a}}_{ri}^{(h)}$  is the  $i^{\text{th}}$  row of the actual array steering matrix  $\overline{\mathbf{A}}^{(h)}$  in (4.2) and  $\mathbf{C}_s^{(h)}$  is the  $L_h^2 \times L_h^2$  source cumulant matrix [28] at time slot  $h$  as defined in (2.18).

When the source signals are statistically independent, there are only  $L_h$  nonzero elements in the source cumulant matrix as defined in (2.20). Substituting (2.20) into (4.8) simplifies the relation as

$$\mathbf{C}_{ij}^{(h)} = \begin{bmatrix} \overline{\mathbf{A}}^{(h)} \mathbf{D}_{\overline{\mathbf{a}}_{ri}}^{(h)H} \mathbf{R}_s^{(h)HOS} \mathbf{D}_{\overline{\mathbf{a}}_{ri}}^{(h)} \overline{\mathbf{A}}^{(h)H} & \overline{\mathbf{A}}^{(h)} \mathbf{D}_{\overline{\mathbf{a}}_{ri}}^{(h)H} \mathbf{R}_s^{(h)HOS} \mathbf{D}_{\overline{\mathbf{a}}_{rj}}^{(h)} \overline{\mathbf{A}}^{(h)H} \\ \overline{\mathbf{A}}^{(h)} \mathbf{D}_{\overline{\mathbf{a}}_{rj}}^{(h)H} \mathbf{R}_s^{(h)HOS} \mathbf{D}_{\overline{\mathbf{a}}_{ri}}^{(h)} \overline{\mathbf{A}}^{(h)H} & \overline{\mathbf{A}}^{(h)} \mathbf{D}_{\overline{\mathbf{a}}_{rj}}^{(h)H} \mathbf{R}_s^{(h)HOS} \mathbf{D}_{\overline{\mathbf{a}}_{rj}}^{(h)} \overline{\mathbf{A}}^{(h)H} \end{bmatrix} \quad (4.9)$$

where  $\mathbf{R}_s^{(h)HOS}$  and  $\mathbf{D}_{\overline{\mathbf{a}}_{ri}}^{(h)}$  are  $L_h \times L_h$  diagonal matrices.  $\mathbf{R}_s^{(h)HOS}$  is defined in (2.25) and  $\mathbf{D}_{\overline{\mathbf{a}}_{ri}}^{(h)}$  is defined as

$$\mathbf{D}_{\overline{\mathbf{a}}_{ri}}^{(h)} = \text{diag} \left( \overline{\mathbf{a}}_{ri}^{(h)}(1), \overline{\mathbf{a}}_{ri}^{(h)}(2), \dots, \overline{\mathbf{a}}_{ri}^{(h)}(L_h) \right) \quad (4.10)$$

Using the same approach in Section 2.2.1, the estimate of the desired cumulant matrix,  $\mathbf{C}_{ij}^{(h)}$ , is found as

$$\hat{\mathbf{C}}_{ij}^{(h)} = \sum_{l=1}^{L_h} \begin{bmatrix} \left( \mathbf{Q}_l^{(h)} \otimes \mathbf{q}_{l,i}^{(h)*} \right) \mathbf{C}_x^{(h)} \left( \mathbf{Q}_l^{(h)} \otimes \mathbf{q}_{l,i}^{(h)*} \right)^H & \left( \mathbf{Q}_l^{(h)} \otimes \mathbf{q}_{l,i}^{(h)*} \right) \mathbf{C}_x^{(h)} \left( \mathbf{Q}_l^{(h)} \otimes \mathbf{q}_{l,j}^{(h)*} \right)^H \\ \left( \mathbf{Q}_l^{(h)} \otimes \mathbf{q}_{l,j}^{(h)*} \right) \mathbf{C}_x^{(h)} \left( \mathbf{Q}_l^{(h)} \otimes \mathbf{q}_{l,i}^{(h)*} \right)^H & \left( \mathbf{Q}_l^{(h)} \otimes \mathbf{q}_{l,j}^{(h)*} \right) \mathbf{C}_x^{(h)} \left( \mathbf{Q}_l^{(h)} \otimes \mathbf{q}_{l,j}^{(h)*} \right)^H \end{bmatrix} \quad (4.11)$$

where  $\mathbf{C}_x^{(h)}$  is the  $K^2 \times K^2$  cumulant matrix which contains all the cumulants of the array output, i.e.,

$$\mathbf{C}_x = \left( \overline{\mathbf{A}}^{(h)} \otimes \overline{\mathbf{A}}^{(h)*} \right) \mathbf{C}_s \left( \overline{\mathbf{A}}^{(h)} \otimes \overline{\mathbf{A}}^{(h)*} \right)^H \quad (4.12)$$

and  $\mathbf{q}_{l,j}^{(h)*}$  is the complex conjugate of the  $j^{\text{th}}$  row of the matrix  $\mathbf{Q}_l^{(h)}$ , that is defined as,

$$\mathbf{Q}_l^{(h)} = \mathbf{I} - \hat{\overline{\mathbf{A}}}^{(h)} \mathbf{Z}_l^{(h)} \left( \hat{\overline{\mathbf{A}}}^{(h)} \right)^\dagger \quad (4.13)$$

$\mathbf{Z}_l^{(h)}$  is the  $L_h \times L_h$  diagonal matrix whose diagonal elements are one except the  $l^{\text{th}}$  element and  $\hat{\overline{\mathbf{A}}}^{(h)}$  is the estimate of the actual array steering matrix,  $\overline{\mathbf{A}}^{(h)}$ . When  $\hat{\overline{\mathbf{A}}}^{(h)} = \overline{\mathbf{A}}^{(h)}$ , the cumulant matrices in (4.9) and (4.11) are identical [28], i.e.,  $\hat{\mathbf{C}}_{ij}^{(h)} = \mathbf{C}_{ij}^{(h)}$ . In this chapter, cumulant matrix estimate in (4.11) is used for parameter estimation.

Before presenting the mathematical expressions for CIHOSS algorithm in the following subsections we introduced a lemma that is used in the derivations of the expressions, i.e.,

**Lemma-3:** Let  $\mathbf{X}$  be a  $K \times L$  matrix,  $\mathbf{Y}$  be an  $L \times M$  matrix and  $\mathbf{Z}$  be a  $K \times M$  matrix. Then, the following equality is valid,

$$\|\mathbf{Z} - \mathbf{XY}\|_F^2 = \|\text{vect}(\mathbf{Z}) - (\mathbf{I}_M \otimes \mathbf{X}) \text{vect}(\mathbf{Y})\|^2 \quad (4.14)$$

The proof of Lemma-3 is given in Appendix G.

### 4.3 CIHOSS Algorithm

In this section, a new online calibration algorithm, CIHOSS, is introduced for a solution to the problem described in Section 4.1. CIHOSS algorithm uses both HOS and SOS approaches in an iterative manner in order to take advantages of both approaches. Due to the perfectly calibrated two reference sensors HOS approach can find the DOA angle estimates without being affected by the unknown mutual coupling and gain/phase mismatch parameters. Furthermore, the actual array steering matrix can be estimated directly from the sensor outputs. Then, it is possible to find the mutual coupling and gain/phase mismatch parameters with a closed form expression. When the source signals are statistically independent, it is shown in [30] that HOS approach can effectively be used for the joint estimation of DOA angles, gain/phase mismatch and mutual coupling parameters without requiring any iteration. Since in this work, it is not assumed that the source signals are statistically independent, the parameter estimation performance will be degraded due to the errors in cumulant matrix estimates as in (4.11) and (4.13). To improve the parameter estimation, we propose an iterative HOS approach that updates the cumulant matrix estimates in (4.11) using the estimated actual array steering matrix. The details of the iteration method for HOS approach are explained in Section 4.3.1.4. We also propose to use SOS approach to improve the estimations of HOS approach since SOS approach is more robust to statistical estimation errors especially for the small number of samples. Therefore, in CIHOSS algorithm HOS approach is used for the initial estimation of the DOA angles, gain/phase mismatch and mutual coupling parameters directly from the sensor outputs and SOS approach is used to improve the initial parameter estimates with more accurate statistical information. The details of HOS and SOS approaches are explained in the following subsections.

### 4.3.1 HOS Approach

The first step of the CIHOSS algorithm is to find the initial estimates of DOA angles, gain/phase mismatches and mutual coupling coefficients using HOS approach. In HOS approach, the cumulant matrices composed of the fourth-order cumulants are used. In Section 4.2, it is shown that different sensor pairs ( $1 \leq i, j \leq K, i \neq j$ ) result different cumulant matrices,  $\mathbf{C}_{ij}^{(h)}$  as in (4.9). The DOA angles and actual array steering matrix are estimated by using the relations between the cumulant matrices for different sensor pairs. Total of  $K(K-1)$  distinct cumulant matrices can be obtained for all possible sensor pairs, but  $2K-3$  of them is sufficient for the DOA angles and actual array steering matrix estimations. The selection of cumulant matrices is explained in the following subsections. After finding the DOA angles the nominal array steering matrix is obtained as in (4.4) and then the gain/phase mismatches and mutual coupling coefficients are estimated using the relation between the actual and nominal array steering matrices.

The relations between cumulant matrices for the DOA and actual array steering matrix estimates is obtained from the eigenvalue decomposition of the cumulant matrices  $\mathbf{C}_{ij}^{(h)}$ , i.e.,

$$\begin{bmatrix} \overline{\mathbf{A}}^{(h)} \mathbf{D}_{\overline{\mathbf{a}}_{ri}}^{(h)H} \mathbf{R}_s^{(h)HOS} \mathbf{D}_{\overline{\mathbf{a}}_{ri}}^{(h)} \overline{\mathbf{A}}^{(h)H} & \overline{\mathbf{A}}^{(h)} \mathbf{D}_{\overline{\mathbf{a}}_{ri}}^{(h)H} \mathbf{R}_s^{(h)HOS} \mathbf{D}_{\overline{\mathbf{a}}_{rj}}^{(h)} \overline{\mathbf{A}}^{(h)H} \\ \overline{\mathbf{A}}^{(h)} \mathbf{D}_{\overline{\mathbf{a}}_{rj}}^{(h)H} \mathbf{R}_s^{(h)HOS} \mathbf{D}_{\overline{\mathbf{a}}_{ri}}^{(h)} \overline{\mathbf{A}}^{(h)H} & \overline{\mathbf{A}}^{(h)} \mathbf{D}_{\overline{\mathbf{a}}_{rj}}^{(h)H} \mathbf{R}_s^{(h)HOS} \mathbf{D}_{\overline{\mathbf{a}}_{rj}}^{(h)} \overline{\mathbf{A}}^{(h)H} \end{bmatrix} \begin{bmatrix} \mathbf{B}_1^{(h)} \\ \mathbf{B}_2^{(h)} \end{bmatrix} = \begin{bmatrix} \mathbf{B}_1^{(h)} \\ \mathbf{B}_2^{(h)} \end{bmatrix} \Lambda_s^{(h)} \quad (4.15)$$

where  $\Lambda_s^{(h)}$  is the diagonal matrix composed of the  $L_h$  largest eigenvalues of the matrix  $\mathbf{C}_{ij}^{(h)}$  and  $2K \times L_h$  matrix  $\mathbf{B}^{(h)} = \begin{bmatrix} \mathbf{B}_1^{(h)T} & \mathbf{B}_2^{(h)T} \end{bmatrix}^T$  is composed of the eigenvectors corresponding to these eigenvalues.  $\mathbf{B}_1^{(h)}$  and  $\mathbf{B}_2^{(h)}$  are both  $K \times L_h$  matrices. From (4.15), the relations for matrices  $\mathbf{B}_1^{(h)}$  and  $\mathbf{B}_2^{(h)}$  can be written as

$$\overline{\mathbf{A}}^{(h)} \mathbf{D}_{\overline{\mathbf{a}}_{ri}}^{(h)H} \Phi^{(h)} = \mathbf{B}_1^{(h)} \quad (4.16)$$

$$\overline{\mathbf{A}}^{(h)} \mathbf{D}_{\overline{\mathbf{a}}_{rj}}^{(h)H} \Phi^{(h)} = \mathbf{B}_2^{(h)} \quad (4.17)$$

where  $L_h \times L_h$  matrix  $\Phi^{(h)}$  is defined as

$$\Phi^{(h)} = \left( \mathbf{R}_s^{(h)HOS} \mathbf{D}_{\overline{\mathbf{a}}_{ri}}^{(h)} \overline{\mathbf{A}}^{(h)H} \mathbf{B}_1^{(h)} + \mathbf{R}_s^{(h)HOS} \mathbf{D}_{\overline{\mathbf{a}}_{rj}}^{(h)} \overline{\mathbf{A}}^{(h)H} \mathbf{B}_2^{(h)} \right) \Lambda_s^{(h)-1} \quad (4.18)$$

Using (4.16) and (4.17), the following relation is obtained, i.e.,

$$\begin{aligned} \mathbf{B}_2^{(h)} &= \mathbf{B}_1^{(h)} \Phi^{(h)-1} \left( \mathbf{D}_{\overline{\mathbf{a}}_{ri}}^{(h)H} \right)^{-1} \mathbf{D}_{\overline{\mathbf{a}}_{rj}}^{(h)H} \Phi^{(h)} \\ \mathbf{B}_1^{(h)\dagger} \mathbf{B}_2^{(h)} \Phi^{(h)-1} &= \Phi^{(h)-1} \mathbf{D}_{ij}^{(h)H} \end{aligned} \quad (4.19)$$

Above equation is simply the eigenvalue decomposition of the matrix  $\mathbf{B}_1^{(h)\dagger} \mathbf{B}_2^{(h)}$ .  $\Phi^{(h)-1}$  is the  $L_h \times L_h$  matrix whose columns are composed of the eigenvectors and the corresponding eigenvalues are in the  $L_h \times L_h$  diagonal matrix  $\mathbf{D}_{ij}^{(h)}$  which is defined as

$$\begin{aligned} \mathbf{D}_{ij}^{(h)} &= \mathbf{D}_{\bar{\mathbf{a}}_{rj}^{(h)} \bar{\mathbf{a}}_{ri}^{(h)}}^{(h)-1} \\ &= \text{diag}(\mathbf{d}_{i,j}^{(h)}) \end{aligned} \quad (4.20)$$

where

$$\mathbf{d}_{i,j}^{(h)} = \left[ \frac{\bar{\mathbf{a}}_{rj}^{(h)}(1)}{\bar{\mathbf{a}}_{ri}^{(h)}(1)}, \frac{\bar{\mathbf{a}}_{rj}^{(h)}(2)}{\bar{\mathbf{a}}_{ri}^{(h)}(2)}, \dots, \frac{\bar{\mathbf{a}}_{rj}^{(h)}(L_h)}{\bar{\mathbf{a}}_{ri}^{(h)}(L_h)} \right] \quad (4.21)$$

Note that as it is seen from (4.21), the ratios of  $i^{\text{th}}$  and  $j^{\text{th}}$  rows of the actual array steering matrix can be found from the eigenvalue decomposition of the cumulant matrix  $\mathbf{C}_{ij}^{(h)}$  using the relations (4.15) - (4.21). DOA angles and the actual array steering matrix estimates can be found by using the cumulant matrices for different sensor pairs  $(i, j)$ . The details of the sensor pair selection and estimating DOA angles and the actual array steering matrix are explained in the following subsections.

#### 4.3.1.1 DOA Estimation with HOS Approach

Since the reference sensors, specifically sensor 1 and sensor 2, are perfectly calibrated with known gain/phase mismatch and mutual coupling coefficients, the cumulant matrix for the sensor pairs 1 and 2,  $\mathbf{C}_{12}^{(h)}$ , is used for the DOA angle estimations. The eigenvalue decomposition of matrix  $\mathbf{C}_{12}^{(h)}$  gives the ratios of the first and second rows of the actual array steering matrix as in (4.21). After substituting (4.3) - (4.6) into (4.2), the first and the second rows of the actual array steering matrix are written as

$$\bar{\mathbf{a}}_{r1}^{(h)} = \left[ 1 + m_{12} e^{j\frac{2\pi}{\lambda} \Delta \cos(\theta_1^{(h)})} \quad 1 + m_{12} e^{j\frac{2\pi}{\lambda} \Delta \cos(\theta_2^{(h)})} \quad \dots \quad 1 + m_{12} e^{j\frac{2\pi}{\lambda} \Delta \cos(\theta_{L_h}^{(h)})} \right] \quad (4.22)$$

$$\bar{\mathbf{a}}_{r2}^{(h)} = \left[ m_{21} + e^{j\frac{2\pi}{\lambda} \Delta \cos(\theta_1^{(h)})} \quad m_{21} + e^{j\frac{2\pi}{\lambda} \Delta \cos(\theta_2^{(h)})} \quad \dots \quad m_{21} + e^{j\frac{2\pi}{\lambda} \Delta \cos(\theta_{L_h}^{(h)})} \right] \quad (4.23)$$

Then, since  $m_{12}$  and  $m_{21}$  are assumed to be known, DOA angle corresponding to the  $k^{\text{th}}$  column of actual array steering matrix is found by substituting (4.22) and (4.23) into (4.21) for  $i = 1$  and  $j = 2$ , i.e.,

$$\begin{aligned} \mathbf{d}_{12}^{(h)}(k) &= \frac{m_{21} + e^{j\frac{2\pi}{\lambda} \Delta \cos(\theta_k^{(h)})}}{1 + m_{12} e^{j\frac{2\pi}{\lambda} \Delta \cos(\theta_{k1}^{(h)})}} \\ \theta_k^{(h)} &= \cos^{-1} \left( \frac{\lambda}{2\pi \Delta} \arg \left( \frac{\mathbf{d}_{12}^{(h)}(k) - m_{21}}{1 - \mathbf{d}_{12}^{(h)}(k) m_{12}} \right) \right) \end{aligned} \quad (4.24)$$

where  $\mathbf{d}_{12}^{(h)}(k)$  is the  $k^{\text{th}}$  element of vector  $\mathbf{d}_{12}^{(h)}$ . Note that the distance between the reference sensors,  $\Delta$ , is assumed to be less than  $\lambda/2$ , and there is no ambiguity problem in DOA angle estimation in (4.24). It is also important to note that the DOA angle estimations are not affected from the unknown gain/phase mismatches and mutual coupling coefficients.

#### 4.3.1.2 Actual Steering Matrix Estimation with HOS Approach

Once the DOA angles are estimated as in (4.24), the first and second rows of the actual array steering matrix are found by substituting (4.24) into (4.22) and (4.23), respectively. Then, the  $j^{\text{th}}$  row of the actual array steering matrix can be estimated by finding  $\mathbf{d}_{1,j}^{(h)}$  using the cumulant matrix for sensor pair  $(1, j)$ ,  $\mathbf{C}_{1j}^{(h)}$ , from the expressions (4.15) - (4.21) and multiplying it with the estimated  $\bar{\mathbf{a}}_{r1}^{(h)}$ , i.e.,  $\bar{\mathbf{a}}_{rj}^{(h)} = \mathbf{d}_{1,j}^{(h)} \odot \bar{\mathbf{a}}_{r1}^{(h)}$ . It is important to note that since there is no a priori information to guarantee that the  $p^{\text{th}}$  eigenvalue corresponds to the  $p^{\text{th}}$  source in the eigenvalue decomposition process, the vector  $\mathbf{d}_{1,j}^{(h)}$  has a permutation ambiguity. In other words the ratios of the  $j^{\text{th}}$  row and first row of the actual array steering matrix can be arbitrary ordered in the vector  $\mathbf{d}_{1,j}^{(h)}$ . Therefore, before finding the  $j^{\text{th}}$  row of the actual array steering matrix, the ordering of the elements in vector  $\mathbf{d}_{1,j}^{(h)}$  should be aligned with the order in  $\bar{\mathbf{a}}_{r1}^{(h)}$ . The alignment process can be performed by searching the minimum value of the following cost function for  $3 \leq j \leq K$ , i.e.,

$$\{\hat{\mathbf{P}}_{1j}, \hat{\mathbf{P}}_{2j}\} = \arg \min_{\{\mathbf{P}_{1j}, \mathbf{P}_{2j}\}} \left\| (\mathbf{d}_{2,j}^{(h)} \mathbf{P}_{2j}) \odot \bar{\mathbf{a}}_{r2}^{(h)} - (\mathbf{d}_{1,j}^{(h)} \mathbf{P}_{1j}) \odot \bar{\mathbf{a}}_{r1}^{(h)} \right\|^2 \quad (4.25)$$

where  $\mathbf{P}_{1j}$  and  $\mathbf{P}_{2j}$  are the permutation matrices for arrangement and  $\hat{\mathbf{P}}_{1j}$  and  $\hat{\mathbf{P}}_{2j}$  are the estimated versions. Note that the ordering of the elements in vectors  $\bar{\mathbf{a}}_{r1}^{(h)}$  and  $\bar{\mathbf{a}}_{r2}^{(h)}$  in (4.25) are the same since they are found from the estimated DOA angles using (4.22) and (4.23). Then, the actual array steering matrix is constructed by using (4.25) for  $3 \leq j \leq K$ , i.e.,

$$\bar{\mathbf{A}}^{(h)} = \begin{bmatrix} \bar{\mathbf{a}}_{r1}^{(h)} \\ \bar{\mathbf{a}}_{r2}^{(h)} \\ (\mathbf{d}_{1,3}^{(h)} \hat{\mathbf{P}}_{13}) \odot \bar{\mathbf{a}}_{r1}^{(h)} \\ \vdots \\ (\mathbf{d}_{1,K}^{(h)} \hat{\mathbf{P}}_{1K}) \odot \bar{\mathbf{a}}_{r1}^{(h)} \end{bmatrix} \quad (4.26)$$

The details of the permutation ambiguity problem and the aligning process for the actual array steering matrix estimation are explained in Appendix H.

### 4.3.1.3 Calibration Parameter Estimation with HOS Approach

After finding the DOA angles,  $\{\theta_k^{(h)}\}_{k=1}^{L_h}$ , as in (4.24) and the actual array steering matrix estimate,  $\overline{\mathbf{A}}^{(h)}$ , as in (4.26), the calibration parameters can be found from the relation between actual and nominal array steering matrices given in (4.2), i.e.,

$$\overline{\mathbf{A}}^{(h)} = \mathbf{\Gamma} \mathbf{A}^{(h)} \quad (4.27)$$

Since the sensor positions are known the nominal array steering matrix estimate,  $\mathbf{A}^{(h)}$ , is found by substituting (4.24) into (4.4) with the same column order as actual array steering matrix estimate. Since it is assumed that the calibration parameters are not changed for the different time slots, the calibration parameters are found using the relation in (4.27) for the time slots  $1 \leq h \leq H$  in least square sense by minimizing the following cost function, i.e.,

$$\zeta = \|\mathbf{\Gamma} \mathbf{A} - \overline{\mathbf{A}}\|_F^2 \quad (4.28)$$

where

$$\mathbf{A} = \begin{bmatrix} \mathbf{A}^{(1)} & \mathbf{A}^{(2)} & \dots & \mathbf{A}^{(H)} \end{bmatrix} \quad (4.29)$$

$$\overline{\mathbf{A}} = \begin{bmatrix} \overline{\mathbf{A}}^{(1)} & \overline{\mathbf{A}}^{(2)} & \dots & \overline{\mathbf{A}}^{(H)} \end{bmatrix} \quad (4.30)$$

Using Lemma-3, the cost function in (4.28) can be rewritten as

$$\zeta = \left\| \left( \mathbf{I}_K \otimes \mathbf{A}^T \right) \mathbf{z} - \overline{\mathbf{a}} \right\|^2 \quad (4.31)$$

where  $\mathbf{z} = \text{vect}(\mathbf{\Gamma}^T)$  and  $\overline{\mathbf{a}} = \text{vect}(\overline{\mathbf{A}}^T)$ .

The cost function in (4.31) can be solved more effectively by considering the known parameters of array distortion matrix,  $\mathbf{\Gamma}$ , as seen from (4.5) and (4.6). Let  $\mathbf{z}_k$  and  $\mathbf{z}_u$  are the column vectors composed of the known and unknown elements of vector  $\mathbf{z}$ , respectively. Then,  $\mathbf{z}_u$  can be found in least squares sense as

$$\widehat{\mathbf{z}}_u = \mathbf{F}_u^\dagger (\overline{\mathbf{a}} - \mathbf{F}_k \mathbf{z}_k) \quad (4.32)$$

where  $\mathbf{F}_k$  and  $\mathbf{F}_u$  are the  $KL \times U_k$  and  $KL \times (K^2 - U_k)$  matrices composed of the columns of matrix  $(\mathbf{I}_K \otimes \mathbf{A}^T)$  corresponding to the indices of known and unknown elements of vector  $\mathbf{z}$ .  $U_k$  is the number of known array distortion parameters.

After finding the unknown parameters in array distortion matrix,  $\mathbf{\Gamma}$ , the matrices  $\mathbf{T}$  and  $\mathbf{M}$  can be found as

$$\mathbf{T} = \text{diag}(\mathbf{\Gamma}) \quad (4.33)$$

$$\mathbf{M} = \mathbf{\Gamma}\mathbf{T}^{-1} \quad (4.34)$$

The relation in (4.33) and (4.34) is written since the matrix  $\mathbf{T}$  is diagonal and the diagonal entries of matrix  $\mathbf{M}$  is all one as given in (4.5) and (4.6).

#### 4.3.1.4 HOS Iteration

As explained in the previous subsections HOS approach uses multiple cumulant matrices defined for different sensor pairs to estimate both the DOA angles and calibration parameters. For the given cumulant matrices, all the parameters are estimated directly, without requiring any iteration. In CIHOSS, the cumulant matrices are estimated as in (4.11) and they depend on the actual array steering matrix estimation. It is shown in [28] that the optimum cumulant matrix can be obtained when the actual array steering matrix is known accurately. In CIHOSS, we propose an iterative method for the HOS approach that updates the estimate of actual array steering matrix as in (4.26) to increase the accuracy of the parameter estimations. Since there is no a-priori information for the actual array steering matrix, we start with the zero matrix and iteratively update. To guarantee the convergence, a cost function in (4.40) is evaluated for each iteration and the iterative process is stopped when the cost function starts to increase. The cost function used in the iterative process is defined in Section 4.3.2. The HOS iteration process is summarized in Algorithm 4.1.

#### 4.3.2 CIHOSS Cost Function

Since the statistical information can be estimated more accurately in SOS approach, SOS based cost function is selected for the iterative process in CIHOSS. The covariance matrix for the sensor output at time slot  $h$ , assuming zero mean signals, is

$$\begin{aligned} \mathbf{R}^{(h)} &= E\{\mathbf{x}^{(h)}(t)(\mathbf{x}^{(h)}(t))^H\} \\ &= \mathbf{M}\mathbf{T}\mathbf{A}^{(h)}\mathbf{R}_s^{(h)}(\mathbf{A}^{(h)})^H\mathbf{T}^H\mathbf{M}^H + \sigma_v^{(h)2}\mathbf{I}_K \end{aligned} \quad (4.35)$$

---

**Algorithm 4.1:** Pseudocode for Iteration Process of HOS Approach.

---

- 1 Set the iteration counter to zero, i.e.,  $k = 0$ ;
  - 2 Initialize the gain/phase mismatch and mutual coupling matrices as identity matrix, i.e.,  $\mathbf{T}_0 = \mathbf{I}$  and  $\mathbf{M}_0 = \mathbf{I}$ . Initialize the actual array steering matrix,  $\hat{\mathbf{A}}_0^{(h)}$ , as zero matrix for all time slots  $h$ ,  $1 \leq h \leq H$ ;
  - 3 Compute the initial value of the cost function,  $Q_0$ , as in (4.49);
  - 4 **for**  $h = 1$  to  $H$  **do**
    - 5 Find the cumulant matrix estimate,  $\hat{\mathbf{C}}_{ij}^{(h)}$  using the actual array steering matrix estimate at  $k^{\text{th}}$  iteration,  $\hat{\mathbf{A}}_k^{(h)}$ , as in (4.11) and (4.13) for  $1 \leq i \leq 2$  and  $i + 1 \leq j \leq K$ ;
    - 6 Find the eigenvectors of  $\hat{\mathbf{C}}_{ij}^{(h)}$  corresponds to the  $L_h$  largest eigenvalues and construct matrices  $\mathbf{B}_1^{(h)}$  and  $\mathbf{B}_2^{(h)}$  as in (4.15);
    - 7 Find the eigenvalues of  $\mathbf{B}_1^{(h)\dagger} \mathbf{B}_2^{(h)}$  and construct the vector  $\mathbf{d}_{i,j}^{(h)}$  as in (4.20);
    - 8 Find the updated DOA angles,  $\theta_{l,\text{upd}}^{(h)}|_{l=1}^{L_h}$ , using  $\mathbf{d}_{12}^{(h)}$  as in (4.24) and construct the nominal array steering matrix,  $\mathbf{A}^{(h)}$  using updated DOA angles as in (4.4);
    - 9 Find the permutation matrix  $\hat{\mathbf{P}}_{1j}$  using the cost function in (4.25) and construct the updated actual array steering matrix estimate,  $\bar{\mathbf{A}}_{\text{upd}}^{(h)}$  as in (4.26);
  - 10 **end**
  - 11 Construct the whole nominal and actual array steering matrices,  $\mathbf{A}$ ,  $\bar{\mathbf{A}}$  using  $\mathbf{A}^{(h)}$  and  $\bar{\mathbf{A}}_{\text{upd}}^{(h)}$  for  $1 \leq h \leq H$  as in (4.29) and (4.30), respectively;
  - 12 Find the updated calibration parameters,  $\mathbf{T}_{\text{upd}}$  and  $\mathbf{M}_{\text{upd}}$ , using the relation between the actual and nominal array steering matrix using the equations (4.32) - (4.34);
  - 13 Compute the matrix  $\mathbf{S}_k$  as in (4.46) using  $\mathbf{M}_{\text{upd}}$ ,  $\mathbf{T}_{\text{upd}}$  and  $\mathbf{A}$ ;
  - 14 Find the value of the cost function in (4.28) using the updated parameters,  $\mathbf{T}_{\text{upd}}$ ,  $\mathbf{M}_{\text{upd}}$ ,  $\mathbf{A}$ ,  $\bar{\mathbf{A}}$  i.e.,  $Q_k = \|\mathbf{E}_s - \mathbf{M}_{\text{upd}} \mathbf{T}_{\text{upd}} \mathbf{A} \mathbf{S}_k\|_F^2$ ;
  - 15 **if**  $Q_k < Q_{k-1}$  **then**
    - 16 Increment the iteration counter, i.e.,  $k = k + 1$ ;
    - 17 Set the parameter estimates at  $k^{\text{th}}$  iteration, i.e.,  $\theta_{l,k}^{(h)}|_{l=1}^{L_h} = \theta_{l,\text{upd}}^{(h)}|_{l=1}^{L_h}$ ,  $\hat{\mathbf{A}}_k^{(h)} = \bar{\mathbf{A}}_{\text{upd}}^{(h)}$ ,  $\mathbf{T}_k = \mathbf{T}_{\text{upd}}$ ,  $\mathbf{M}_k = \mathbf{M}_{\text{upd}}$ , for  $1 \leq h \leq H$ ;
    - 18 Go to Step 4;
  - 19 **else**
    - 20 Set the final parameter estimates to the estimates at  $(k - 1)^{\text{st}}$  iteration, i.e.,  $\Theta^{\text{HOS}} = [\theta_{1,k-1}^{(1)}, \dots, \theta_{L_1,k-1}^{(1)}, \dots, \theta_{L_H,k-1}^{(H)}]$ ,  $\mathbf{T}^{\text{HOS}} = \mathbf{T}_{k-1}$ ,  $\mathbf{M}^{\text{HOS}} = \mathbf{M}_{k-1}$ ;
  - 21 **end**
-

where  $\sigma_v^{(h)2}$  is the noise variance at time slot  $h$ ,  $\mathbf{R}_s^{(h)} = E\{\mathbf{s}^{(h)}(t)(\mathbf{s}^{(h)}(t))^H\}$  is the covariance matrix of the source signals at time slot  $h$  and  $\mathbf{I}_K$  is the  $K \times K$  identity matrix. Eigenvalue decomposition of the matrix  $\mathbf{R}^{(h)}$  gives the following relation for the signal subspace, i.e.,

$$\mathbf{R}^{(h)}\mathbf{E}_s^{(h)} = \mathbf{E}_s^{(h)}\mathbf{\Lambda}_s^{(h)} \quad (4.36)$$

where  $\mathbf{\Lambda}_s$  is the  $L_h \times L_h$  diagonal matrix composed of the eigenvalues of the signal space and  $\mathbf{E}_s^{(h)}$  is the  $K \times L_h$  matrix whose columns are composed of the eigenvectors corresponding to the signal space. Substituting (4.35) into (4.36) results the following relation, i.e.,

$$\mathbf{E}_s^{(h)} = \mathbf{M}\mathbf{T}\mathbf{A}^{(h)}\mathbf{S}^{(h)} \quad (4.37)$$

where  $L_h \times L_h$  matrix  $\mathbf{S}^{(h)}$  is defined as,

$$\mathbf{S}^{(h)} = \mathbf{R}_s^{(h)} \left( \mathbf{A}^{(h)} \right)^H \mathbf{T}^H \mathbf{M}^H \mathbf{E}_s^{(h)} \left( \mathbf{\Lambda}_s^{(h)} - \sigma_v^{(h)2} \mathbf{I}_{L_h} \right)^{-1} \quad (4.38)$$

and  $\mathbf{I}_{L_h}$  is the  $L_h \times L_h$  identity matrix. Note that, although the matrix  $\mathbf{S}^{(h)}$  has closed form expression that contains the known and unknown parameters, we do not use this expression in the estimation process. The reason for this fact is that using the closed form expression of matrix  $\mathbf{S}^{(h)}$  makes the expressions more complex to solve analytically. Therefore, we assume the matrix  $\mathbf{S}^{(h)}$  as an arbitrary  $L_h \times L_h$  matrix for simplicity.

A nonlinear least-squares problem for the time slot  $h$  can be formulated as the following cost function, i.e.,

$$Q^{(h)} = \left\| \mathbf{E}_s^{(h)} - \mathbf{M}\mathbf{T}\mathbf{A}^{(h)}\mathbf{S}^{(h)} \right\|_F^2 \quad (4.39)$$

Considering all the cost functions for time slot  $1 \leq h \leq H$ , and using the addition property of norms, the overall cost function can be written as,

$$\begin{aligned} Q &= \sum_{h=1}^H Q^{(h)} \\ &= \left\| \mathbf{E}_s - \mathbf{M}\mathbf{T}\mathbf{A}\mathbf{S} \right\|_F^2 \end{aligned} \quad (4.40)$$

where

$$\mathbf{E}_s = \begin{bmatrix} \mathbf{E}_s^{(1)} & \mathbf{E}_s^{(2)} & \dots & \mathbf{E}_s^{(H)} \end{bmatrix} \quad (4.41)$$

$$\mathbf{A} = \begin{bmatrix} \mathbf{A}^{(1)} & \mathbf{A}^{(2)} & \dots & \mathbf{A}^{(H)} \end{bmatrix} \quad (4.42)$$

$$\mathbf{S} = \begin{bmatrix} \mathbf{S}^{(1)} & \mathbf{0}_{L_1 \times L_2} & \dots & \mathbf{0}_{L_1 \times L_H} \\ \mathbf{0}_{L_2 \times L_1} & \mathbf{S}^{(2)} & \dots & \mathbf{0}_{L_2 \times L_H} \\ \vdots & \vdots & \ddots & \vdots \\ \mathbf{0}_{L_H \times L_1} & \mathbf{0}_{L_H \times L_2} & \dots & \mathbf{S}^{(H)} \end{bmatrix} \quad (4.43)$$

where  $\mathbf{0}_{i \times j}$  is the zero matrix with  $i$  rows and  $j$  columns. Note that, the matrix  $\mathbf{S}$  includes the unknown parameters and they are computed from either an initial value at the beginning or from the values computed at the previous iteration.

The estimation of complex matrix  $\mathbf{S}$  is found by minimizing the cost function in (4.40) with respect to the parameters in matrix  $\mathbf{S}$  and the last estimates of the parameters in matrices  $\mathbf{M}$ ,  $\mathbf{T}$  and  $\mathbf{A}$  are kept fixed during the minimization. Using the fact in Lemma-3, the cost function in (4.40) can be rewritten as,

$$Q = \|\bar{\mathbf{e}}_s - (\mathbf{I}_L \otimes \mathbf{MTA}) \mathbf{s}\|^2 \quad (4.44)$$

where  $\bar{\mathbf{e}}_s = \text{vect}(\mathbf{E}_s)$  and  $\mathbf{s} = \text{vect}(\mathbf{S})$ . As it is seen from (4.43),  $L^2 - \sum_{h=1}^H L_h^2$  number of parameters of complex matrix  $\mathbf{S}$  are zero. By considering these known parameters, (4.44) can be rewritten as

$$Q = \|\bar{\mathbf{e}}_s - \mathbf{Y} \mathbf{s}_u\|^2 \quad (4.45)$$

where  $\mathbf{s}_u$  is  $\left(\sum_{h=1}^H L_h^2\right) \times 1$  column vector composed of the unknown elements of vector  $\mathbf{s}$  and  $\mathbf{Y}$  is the  $KL \times \left(\sum_{h=1}^H L_h^2\right)$  matrix composed of the columns of the matrix  $(\mathbf{I}_L \otimes \mathbf{MTA})$  corresponding to the indices of unknown elements of vector  $\mathbf{s}$ . The unknown parameters in matrix  $\mathbf{S}$  are estimated in least squares sense as

$$\mathbf{s}_u = \mathbf{Y}^\dagger \bar{\mathbf{e}}_s \quad (4.46)$$

Then, the estimate of the matrix  $\mathbf{S}$  can easily be constructed from  $\mathbf{s}_u$  and known indices of zero elements in matrix  $\mathbf{S}$ . After the matrix  $\mathbf{S}$  is estimated, the cost value for the current iteration is found by using the estimated matrices,  $\mathbf{M}$ ,  $\mathbf{T}$ ,  $\mathbf{A}$  and  $\mathbf{S}$  in (4.40).

For the initial cost value, the nominal array steering matrix is estimated using MUSIC spectrum [1] with identity matrix for gain/phase mismatch and mutual coupling matrices, i.e.,

$$\Omega(\theta^{(h)}) = \frac{1}{\mathbf{a}^H(\theta^{(h)})\mathbf{G}^{(h)}\mathbf{G}^{(h)H}\mathbf{a}(\theta^{(h)})} \quad (4.47)$$

where  $\mathbf{a}(\theta^{(h)})$  is the nominal array steering vector for the source DOA angle of  $\theta^{(h)}$  and  $\mathbf{G}^{(h)}$  is the  $K \times (K - L_h)$  matrix whose columns are composed of the eigenvectors corresponding to the noise space of covariance matrix for sensor output at time slot  $h$ . Then, the initial value of the nominal array steering matrix for time slot  $h$  is computed as

$$\mathbf{A}_0^{(h)} = \left[ \mathbf{a}(\hat{\theta}_1^{(h,spc)}) \quad \mathbf{a}(\hat{\theta}_2^{(h,spc)}) \quad \dots \quad \mathbf{a}(\hat{\theta}_{L_h}^{(h,spc)}) \right] \quad (4.48)$$

where  $\hat{\theta}_i^{(h,spc)}$ , for  $1 \leq i \leq L_h$  is the DOA angle estimates corresponding to the  $L_h$  largest peaks in MUSIC spectrum,  $\Omega(\theta^{(h)})$ . The initial cost value is computed as

$$Q_0 = \|\mathbf{E}_s - \mathbf{M}_0\mathbf{T}_0\mathbf{A}_0\mathbf{S}_0\|_F^2 \quad (4.49)$$

where  $\mathbf{A}_0 = \left[ \mathbf{A}_0^{(1)} \quad \mathbf{A}_0^{(2)} \quad \dots \quad \mathbf{A}_0^{(H)} \right]$  and  $\mathbf{S}_0$  is the initial value of matrix  $\mathbf{S}$  computed from (4.46) using  $\mathbf{M}_0$ ,  $\mathbf{T}_0$  and  $\mathbf{A}_0$ .

### 4.3.3 SOS Approach

As explained in Section 4.3.1, HOS approach gives a direct solution for the DOA angles, gain/phase mismatch and mutual coupling parameter estimations as given in (4.24), (4.33) and (4.34), respectively. It is important to note that the accuracy of the Cumulant matrix estimation (4.11) used in the HOS approach is affected by the dependency between source signals and the accuracy of the actual array steering matrix estimation as in (4.13). Since there is no a priori information about the actual array steering matrix, zero matrix is used as the initial estimate of the actual array steering matrix in (4.13). As compared with the HOS approach, SOS approach can estimate the second order statistics more accurately for finite length signals. Therefore, in CIHOSS we propose to apply SOS approach to improve the initial parameter estimations obtained in HOS approach. Iterative use of HOS and SOS approaches is repeated until the minimum value of a cost function is obtained. Note that, at each iteration the value of the cost function is evaluated and whenever the cost function increases, the iteration is stopped. Therefore, CIHOSS is guaranteed to converge.

In SOS approach, the cost function,  $Q$ , in (4.40) is minimized for each parameter separately to improve the parameter estimations obtained from the HOS approach given in Section 4.3.1. While minimizing the cost function  $Q$  with respect to one of the parameters, the last estimates of the other parameters are used as constants. The minimization steps are repeated iteratively to obtain the minimum value of the cost function. Note that, at each iteration the value of the cost function is evaluated and whenever the cost function increases, the iteration is stopped and the parameters corresponding to the minimum cost function are used as the final parameter estimations. Therefore, the iterative approach used in SOS is guaranteed to converge. The details of each parameter estimation are explained in the following subsections.

#### 4.3.3.1 DOA Estimation with SOS Approach

In this step, the DOA estimations are found by minimizing the cost function in (4.40) with respect to the DOA angles and the last estimates of the parameters,  $\mathbf{M}$ ,  $\mathbf{T}$  and  $\mathbf{S}$  are kept fixed during the minimization. Since minimizing the cost function with respect to the DOA angles is a nonlinear optimization problem, Newton method [32] is used to update the last DOA angle estimates, i.e.,

$$\Theta_{j+1} = \Theta_j - \mu \mathbf{H}_j^{-1} \mathbf{g}_j \quad (4.50)$$

where  $\mu \geq 0$  is the step size and  $\mathbf{H}_j$  and  $\mathbf{g}_j$  are the Hessian matrix and gradient vector for the DOA angles at iteration  $j$ ,  $\Theta_j$ , respectively.  $L \times 1$  column vector  $\Theta$  is defined as

$$\Theta = \left[ \theta_1^{(1)} \quad \theta_2^{(1)} \quad \dots \quad \theta_{L_1}^{(1)} \quad \theta_1^{(2)} \quad \dots \quad \theta_{L_2}^{(2)} \quad \dots \quad \theta_{L_H}^{(H)} \right]^T \quad (4.51)$$

Derivations of Hessian matrix and the gradient vector are given in Appendix F. Note that  $\Theta_0$  is the initial estimate of the DOA angles and they are obtained from the HOS approach as given in (4.24) for  $1 \leq h \leq H$ .

#### 4.3.3.2 Gain/Phase Mismatch Parameter Estimation with SOS Approach

In this step, the gain/phase mismatch matrix,  $\mathbf{T}$ , is estimated by minimizing the cost function in (4.40) with respect to parameters in matrix  $\mathbf{T}$  and the last estimates of the parameters in matrices  $\mathbf{M}$ ,  $\mathbf{A}$  and  $\mathbf{S}$  are kept fixed during the minimization. The cost function in (4.40) can

be rewritten as,

$$\begin{aligned}
Q &= \sum_{l=1}^L (\mathbf{e}_l - \mathbf{M}\mathbf{T}\mathbf{A}\mathbf{s}_l)^H (\mathbf{e}_l - \mathbf{M}\mathbf{T}\mathbf{A}\mathbf{s}_l) \\
&= \sum_{l=1}^L \|\mathbf{e}_l\|^2 - \mathbf{e}_l^H \mathbf{M}\mathbf{T}\mathbf{A}\mathbf{s}_l - \mathbf{s}_l^H \mathbf{A}^H \mathbf{T}^H \mathbf{M}^H \mathbf{e}_l + \mathbf{s}_l^H \mathbf{A}^H \mathbf{T}^H \mathbf{M}^H \mathbf{M}\mathbf{T}\mathbf{A}\mathbf{s}_l
\end{aligned} \quad (4.52)$$

where  $K \times 1$  vectors  $\mathbf{e}_l$  and  $\mathbf{s}_l$  are the  $l^{\text{th}}$  column of matrices  $\mathbf{E}_s$  and  $\mathbf{S}$ , respectively. Since the gain/phase mismatch matrix,  $\mathbf{T}$ , is a diagonal matrix, using the Lemma 1 in [29], (4.52) is simplified as,

$$\begin{aligned}
Q &= \sum_{l=1}^L \|\mathbf{e}_l\|^2 - \mathbf{e}_l^H \mathbf{M}\mathbf{D}_l \mathbf{t} - \mathbf{t}^H \mathbf{D}_l^H \mathbf{M}^H \mathbf{e}_l + \mathbf{t}^H \mathbf{D}_l^H \mathbf{M}^H \mathbf{M}\mathbf{D}_l \mathbf{t} \\
&= z_0 - \mathbf{z}_1^H \mathbf{t} - \mathbf{t}^H \mathbf{z}_1 + \mathbf{t}^H \mathbf{Z}_2 \mathbf{t}
\end{aligned} \quad (4.53)$$

where  $\mathbf{D}_l$  is the  $K \times K$  diagonal matrix whose diagonal elements are composed of the elements of the vector  $\mathbf{A}\mathbf{s}_l$ ,  $\mathbf{t}$  is the  $K \times 1$  column vector whose elements are composed of the diagonal elements of gain/phase mismatch matrix  $\mathbf{T}$  and

$$z_0 = \sum_{l=1}^L \|\mathbf{e}_l\|^2 \quad (4.54)$$

$$\mathbf{z}_1 = \sum_{l=1}^L \mathbf{D}_l^H \mathbf{M}^H \mathbf{e}_l \quad (4.55)$$

$$\mathbf{Z}_2 = \sum_{l=1}^L \mathbf{D}_l^H \mathbf{M}^H \mathbf{M}\mathbf{D}_l \quad (4.56)$$

Since the gain/phase mismatch parameters of the sensor 1 and sensor 2 are fixed to 1 as in (4.6), the vector  $\mathbf{t}$  can be rewritten as

$$\mathbf{t} = \begin{bmatrix} \mathbf{1}_{2 \times 1} \\ \mathbf{t}_u \end{bmatrix} \quad (4.57)$$

where  $\mathbf{t}_u$  is the  $(K - 2) \times 1$  column vector whose elements are composed of the unknown gain/phase mismatch parameters and  $\mathbf{1}_{2 \times 1}$  is the  $2 \times 1$  column vector with all one. Substituting (4.57) into (4.53), further simplifies the cost function, i.e.,

$$Q = \bar{z}_0 - \bar{\mathbf{z}}_1^H \mathbf{t}_u - \mathbf{t}_u^H \bar{\mathbf{z}}_1 + \mathbf{t}_u^H \mathbf{Z}_{2,3} \mathbf{t}_u \quad (4.58)$$

where

$$\bar{z}_0 = z_0 - \mathbf{z}_{1,1}^H \mathbf{1}_{2 \times 1} - \mathbf{1}_{2 \times 1}^T \mathbf{z}_{1,1} + \mathbf{1}_{2 \times 1}^T \mathbf{Z}_{2,1} \mathbf{1}_{2 \times 1} \quad (4.59)$$

$$\bar{\mathbf{z}}_1 = \mathbf{z}_{1,2} - \mathbf{Z}_{2,2}^H \mathbf{1}_{2 \times 1} \quad (4.60)$$

and  $\mathbf{z}_{1,1}$  is the  $2 \times 1$  column vector,  $\mathbf{z}_{1,2}$  is the  $(K - 2) \times 1$  column vector,  $\mathbf{Z}_{2,1}$  is the  $2 \times 2$  matrix,  $\mathbf{Z}_{2,2}$  is the  $2 \times (K - 2)$  matrix and  $\mathbf{Z}_{2,3}$  is the  $(K - 2) \times (K - 2)$  matrix defined as

$$\mathbf{z}_1 = \begin{bmatrix} \mathbf{z}_{1,1} \\ \mathbf{z}_{1,2} \end{bmatrix} \quad (4.61)$$

$$\mathbf{Z}_2 = \begin{bmatrix} \mathbf{Z}_{2,1} & \mathbf{Z}_{2,2} \\ \mathbf{Z}_{2,2}^H & \mathbf{Z}_{2,3} \end{bmatrix} \quad (4.62)$$

Then, the unknown gain/phase mismatch parameters,  $\mathbf{t}_u$  can be found by taking the derivative of the cost function in (4.58) with respect to  $\mathbf{t}_u$  and setting it to zero, i.e.,

$$\begin{aligned} \frac{\partial Q}{\partial \mathbf{t}_u} &= -\bar{\mathbf{z}}_1 + \mathbf{Z}_{2,3} \mathbf{t}_u = 0 \\ \mathbf{t}_u &= \mathbf{Z}_{2,3}^{-1} \bar{\mathbf{z}}_1 \end{aligned} \quad (4.63)$$

Then, the estimate of the gain/phase mismatch matrix can easily be constructed from (4.63) and (4.57).

#### 4.3.3.3 Mutual Coupling Parameter Estimation with SOS Approach

In this step, the mutual coupling matrix estimate,  $\mathbf{M}$ , is found by minimizing the cost function in (4.40) with respect to the parameters in matrix  $\mathbf{M}$  and the last estimates of the parameters in matrices  $\mathbf{T}$ ,  $\mathbf{A}$  and  $\mathbf{S}$  are kept fixed during the minimization. Using the fact in Lemma-3, the cost function in (4.40) can be rewritten as,

$$Q = \left\| \mathbf{e}_s - (\mathbf{I}_K \otimes \mathbf{S}^T \mathbf{A}^T \mathbf{T}^T) \mathbf{m} \right\|^2 \quad (4.64)$$

where  $\mathbf{e}_s = \text{vect}(\mathbf{E}_s^T)$  and  $\mathbf{m} = \text{vect}(\mathbf{M}^T)$ . As given in (4.5), some elements of the matrix  $\mathbf{M}$  are known a priori. Considering these known elements, (4.64) can be solved more effectively. Let  $\mathbf{m}_k$  and  $\mathbf{m}_u$  are the column vectors composed of the known and unknown elements of vector  $\mathbf{m}$ , respectively. Then, (4.64) can be rewritten as

$$Q = \left\| \mathbf{e}_s - \mathbf{G}_k \mathbf{m}_k - \mathbf{G}_u \mathbf{m}_u \right\|^2 \quad (4.65)$$

where  $\mathbf{G}_k$  and  $\mathbf{G}_u$  are the  $KL \times (KL - V_u)$  and  $KL \times V_u$  matrices composed of the columns of matrix  $(\mathbf{I}_K \otimes \mathbf{S}^T \mathbf{A}^T \mathbf{T}^T)$  corresponding to the indices of known and unknown elements of vector  $\mathbf{m}$ .  $V_u$  is the number of unknown mutual coupling parameters. The unknown mutual coupling parameters are then estimated in least squares sense as

$$\mathbf{m}_u = \mathbf{G}_u^\dagger (\mathbf{e}_s - \mathbf{G}_k \mathbf{m}_k) \quad (4.66)$$

Then, the estimate of the mutual coupling matrix can easily be constructed from (4.66).

#### 4.3.3.4 SOS Iteration

As explained in the previous subsections, SOS approach updates the three parameter estimates sequentially by minimizing the cost function defined in (4.40). In the updating process only one parameter is changed while the others are kept fixed. All the parameter estimates except the DOA angle estimates, are found using a linear set of equations. Due to the nonlinearity of DOA angle estimate equation, Newton method is used to update the DOA angle estimates. To guarantee the convergence, the cost function in (4.40) is evaluated for the updated parameter estimates and the iteration is stopped when the cost function starts to increase. Since only the DOA angles are updated using a nonlinear set of equations the convergence time depends only on the selected stepsize in Newton method. The stepsize in DOA estimation is dynamically selected to decrease the convergence time. The SOS iteration process is summarized in Algorithm 4.2.

#### 4.3.4 Solvability

CIHOSS algorithm iteratively solves different types of equations for each parameter estimation. The relation between the number of sensors and the number of sources required to have a solution changes for each equation. In this section, the solvability criterion of the CIHOSS algorithm is investigated and the relation between the number of sources and the number of sensors as well as the number of unknowns is determined.

##### 4.3.4.1 Solvability of HOS approach

In HOS approach the DOA angles at each time slot are estimated from the eigenvalue decomposition of the matrix  $\mathbf{C}_{ij}^{(h)}$  in (4.9). As it is seen in (4.19), for the solution of the DOA angle estimations, the  $L_h \times L_h$  matrix  $\mathbf{\Phi}^{(h)}$  defined in (4.18) is required to be nonsingular or in other words the rank of  $\mathbf{\Phi}^{(h)}$  should be equal to  $L_h$ . Since the matrices  $\mathbf{R}_s^{(h)HOS}$ ,  $\mathbf{D}_{\mathbf{a}_i}^{(h)}$ ,  $\mathbf{D}_{\mathbf{a}_j}^{(h)}$  and  $\mathbf{\Lambda}_s^{(h)}$  are all  $L_h \times L_h$  diagonal matrices whose diagonal elements are non-zero, their ranks are  $L_h$ . The rank of the  $K \times L_h$  matrices  $\overline{\mathbf{A}}^{(h)}$ ,  $\mathbf{B}_1^{(h)}$  and  $\mathbf{B}_2^{(h)}$  are  $\min(K, L_h)$ . Using these facts and the rank properties, the solvability criterion for DOA angle estimates with HOS approach

---

**Algorithm 4.2:** Pseudocode for Iteration Process of SOS Approach.

---

- 1 Set the iteration counter to zero, i.e.,  $k = 0$  and set the initial value of the cost function,  $Q_0$ , to the last cost function obtained from HOS approach;
  - 2 Set the initial DOA angle estimates to the estimates found from HOS approach,  $\Theta^{HOS}$ , defined in Table 4.1, i.e.,  $\Theta_0 = \Theta^{HOS}$ , and find the initial nominal array steering matrix,  $\mathbf{A}_0$ , using  $\Theta_0$ ;
  - 3 Set the initial gain/phase and mutual coupling matrices as  $\mathbf{T}_0 = \mathbf{T}^{HOS}$  and  $\mathbf{M}_0 = \mathbf{M}^{HOS}$ , respectively;
  - 4 Find the initial complex matrix  $\mathbf{S}_0$  as in (4.46) using  $\mathbf{A}_0$  and the parameters  $\mathbf{M}_0, \mathbf{T}_0$  found from the HOS approach;
  - 5 Find the Hessian matrix,  $\mathbf{H}_k$ , defined in (F.6) and gradient vector,  $\mathbf{g}_k$ , defined in (F.1) using the DOA angle estimates at  $k^{th}$  iteration and find the delta update of DOA angles, i.e.,  

$$\Delta_{\Theta_k} = \mathbf{H}_k^{-1} \mathbf{g}_k;$$
  - 6 Define the minimum and maximum values of the step size using  $\Delta_{\Theta_k}$ .  $\mu_{min}$  is selected as 0 and  $\mu_{max}$  is selected as  $\frac{3}{\max_{1 \leq l \leq L} \Delta_{\Theta_k}(l)}$ ;
  - 7 **for**  $\mu = \mu_{min}$  **to**  $\mu_{max}$  **do**
  - 8     Find the updated DOA angles as  $\Theta_{upd}(\mu) = \Theta_k - \mu \Delta_{\Theta_k}$  and construct the updated nominal array steering matrix,  $\mathbf{A}_{upd}(\mu)$ , using  $\Theta_{upd}(\mu)$  and sensor positions as in (4.4);
  - 9     Find the updated gain/phase mismatch matrix,  $\mathbf{T}_{upd}(\mu)$ , as in (4.63) using  $\mathbf{A}_{upd}(\mu), \mathbf{M}_k$  and  $\mathbf{S}_k$ ;
  - 10     Find the updated mutual coupling matrix,  $\mathbf{M}_{upd}(\mu)$ , as in (4.66) using  $\mathbf{A}_{upd}(\mu), \mathbf{T}_{upd}(\mu)$  and  $\mathbf{S}_k$ ;
  - 11     Find the updated matrix  $\mathbf{S}$ ,  $\mathbf{S}_{upd}(\mu)$ , as in (4.46) using  $\mathbf{A}_{upd}(\mu), \mathbf{T}_{upd}(\mu)$  and  $\mathbf{M}_{upd}(\mu)$ ;
  - 12     Evaluate the cost function in (4.40) and find  

$$\gamma(\mu) = \|\mathbf{E}_s - \mathbf{M}_{upd}(\mu) \mathbf{T}_{upd}(\mu) \mathbf{A}_{upd}(\mu) \mathbf{S}_{upd}(\mu)\|_F^2$$
  - 13 **end**
  - 14 Find the optimum value of the stepsize that results minimum cost value, i.e.,  $\mu_{opt} = \arg \min_{\mu} \gamma(\mu)$  and find the cost value at  $k^{th}$  iteration,  $Q_k = \gamma(\mu_{opt})$ ;
  - 15 **if**  $Q_k < Q_{k-1}$  **then**
  - 16     Set the parameter estimates at  $k^{th}$  iteration, i.e.,  $\Theta_{k+1} = \Theta_k - \mu_{opt} \Delta_{\Theta_k}, \mathbf{M}_{k+1} = \mathbf{M}_{upd}(\mu_{opt}),$   

$$\mathbf{T}_{k+1} = \mathbf{T}_{upd}(\mu_{opt});$$
  - 17     Increment the iteration counter; i.e.,  $k = k + 1$ ;
  - 18     Go to Step 5;
  - 19 **else**
  - 20     Set the final parameter estimates to the estimates at  $(k - 1)^{st}$  iteration, i.e.,  $\Theta^{SOS} = \Theta_{k-1},$   

$$\mathbf{M}^{SOS} = \mathbf{M}_{k-1} \text{ and } \mathbf{T}^{SOS} = \mathbf{T}_{k-1};$$
  - 21 **end**
-

is obtained as

$$\begin{aligned} 2 \min(K, L_h) &\geq \text{rank}(\mathbf{\Phi}^{(h)}) \\ 2 \min(K, L_h) &\geq L_h \end{aligned} \quad (4.67)$$

The inequality in (4.67) is satisfied when the number of sensors is greater than the number of sources at time slot  $h$ , i.e.,  $K \geq L_h$ , which is the condition for the DOA estimation in SOS approach. Due to the virtual sensors, HOS approach can find the DOA angles that is larger than the number of sensors. The minimum number of sensors required to find  $L_h$  number of DOA angles can be found from (4.67), as

$$K \geq \frac{L_h}{2} \quad (4.68)$$

The elements of the array distortion matrix,  $\mathbf{\Gamma}$ , are estimated from (4.32). As it is seen in (4.32) for a valid solution,  $KL \times (K^2 - U_k)$  matrix  $\mathbf{F}_u$  should be full column rank, which requires  $KL \geq (K^2 - U_k)$ . From (4.3), (4.5) and (4.6), it can be easily found that the minimum value of  $U_k$  is  $4K - 4$ . Therefore, the following relation should be satisfied to have a solution for the array distortion matrix, i.e.,

$$L \geq \frac{(K - 2)^2}{K} \quad (4.69)$$

#### 4.3.4.2 Solvability of CIHOSS

For the problem defined in Section 4.1, there are  $L$  number of unknowns for DOA angles,  $K - 2$  number of complex unknowns for gain/phase mismatch parameters,  $K^2 - 5K + 6$  number of complex unknowns for mutual coupling parameters and  $\sum_{h=1}^H L_h^2$  number of complex unknowns for parameters of the matrix  $\mathbf{S}$ . Therefore, there are  $L + 2(K - 2)^2 + 2 \sum_{h=1}^H L_h^2$  total number of real unknown parameters. These unknown parameters are estimated by minimizing the cost function in (4.40), which results  $2KL$  number of real equations. Then, the condition for the solvability of these equations is

$$KL \geq \frac{L}{2} + (K - 2)^2 + \sum_{h=1}^H L_h^2 \quad (4.70)$$

Even though the condition in (4.70) is not satisfied, a valid solution for the parameter estimations in HOS and SOS approaches can be found depending on the solvability conditions

of each parameter. But in this case there are infinitely many solutions since the overall set of equations is underdetermined. Therefore, to obtain the solvability criterion for the parameter estimations in CIHOSS algorithm the condition for each parameter estimation in HOS and SOS approaches and the condition for the overall set of equations in (4.70) should be considered together. Note that in SOS approach, the different types of parameters are estimated by minimizing the same cost function in (4.40) with respect to the selected parameter. While minimizing the cost function with respect to one of the parameters, the last estimates of the other parameters are used as known quantities in the equations. Hence, the condition in (4.70) also satisfies the solvability conditions of each parameter in SOS approach and the conditions in (4.68) and (4.69) since both  $K$  and  $L$  are positive quantities. Therefore, substituting (4.1) into (4.70) gives the condition for the solvability of CIHOSS algorithm as

$$\sum_{h=1}^H L_h \geq \frac{(K-2)^2}{K-\frac{1}{2}} + \frac{\sum_{h=1}^H L_h^2}{K-\frac{1}{2}} \quad (4.71)$$

Note that when  $L_h = 1$  for  $h = 1, 2, \dots, H$ , the condition in (4.71) is always satisfied when  $L \geq K - 2$ .

#### 4.4 Cramér Rao Bound

In this section, the Cramér Rao bound (CRB) expressions are given for the defined problem in Section 4.1. The signal waveforms are considered to be deterministic unknown process and the noise is assumed to be temporally uncorrelated complex Gaussian process. In this section, CRB expressions are derived by considering a non-circular complex Gaussian distribution for the noise with unknown covariance matrix. The modification for circular case is also given. Noise may be spatially correlated. The unknown parameter set is defined as

$$\Omega = \left\{ \theta_l, m_{g,ij}, m_{p,ij}, \alpha_i, \beta_i, \Re(s_{l_h}^{(h)}(t)), \Im(s_{l_h}^{(h)}(t)), \mathbf{R}^{(h)} \right\} \quad (4.72)$$

for  $1 \leq l \leq L$ ,  $3 \leq i \leq K$ ,  $3 \leq j \leq K$ ,  $1 \leq t \leq N$  and  $1 \leq h \leq H$ .  $m_{g,ij}$  and  $m_{p,ij}$  are the gain and phase terms of mutual coupling coefficient,  $m_{ij}$ , respectively. Then, the CRB for the

DOA and calibration parameters are given by

$$CRB_{\Theta} = \frac{1}{L} \sum_{i=1}^L \mathbf{F}_{i,i}^{-1} \quad (4.73)$$

$$CRB_{m_g} = \frac{1}{K^2 - 5K + 6} \sum_{i=L+1}^{L+K^2-5K+6} \mathbf{F}_{i,i}^{-1} \quad (4.74)$$

$$CRB_{m_p} = \frac{1}{K^2 - 5K + 6} \sum_{i=L+1+K^2-5K+6}^{L+2K^2-10K+12} \mathbf{F}_{i,i}^{-1} \quad (4.75)$$

$$CRB_{\alpha} = \frac{1}{K-2} \sum_{i=L+1+2K^2-10K+12}^{L+2K^2-9K+10} \mathbf{F}_{i,i}^{-1} \quad (4.76)$$

$$CRB_{\beta} = \frac{1}{K-2} \sum_{i=L+2K^2-9K+11}^{L+2K^2-8K+8} \mathbf{F}_{i,i}^{-1} \quad (4.77)$$

where  $\mathbf{F}_{i,i}^{-1}$  is the  $i^{th}$  row and  $i^{th}$  column of the inverse of Fisher Information matrix,  $\mathbf{F}$ , defined as

$$\mathbf{F} = \begin{bmatrix} \mathbf{F}_{\Theta,\Theta} & \mathbf{F}_{\Theta,m_g} & \mathbf{F}_{\Theta,m_p} & \mathbf{F}_{\Theta,\alpha} & \mathbf{F}_{\Theta,\beta} & \mathbf{F}_{\Theta,s} & \mathbf{0}_{L \times 4K^2} \\ \mathbf{F}_{\Theta,m_g}^T & \mathbf{F}_{m_g,m_g} & \mathbf{F}_{m_g,m_p} & \mathbf{F}_{m_g,\alpha} & \mathbf{F}_{m_g,\beta} & \mathbf{F}_{m_g,s} & \mathbf{0}_{V_u \times 4K^2} \\ \mathbf{F}_{\Theta,m_p}^T & \mathbf{F}_{m_g,m_p}^T & \mathbf{F}_{m_p,m_p} & \mathbf{F}_{m_p,\alpha} & \mathbf{F}_{m_p,\beta} & \mathbf{F}_{m_p,s} & \mathbf{0}_{V_u \times 4K^2} \\ \mathbf{F}_{\Theta,\alpha}^T & \mathbf{F}_{m_g,\alpha}^T & \mathbf{F}_{m_p,\alpha}^T & \mathbf{F}_{\alpha,\alpha} & \mathbf{F}_{\alpha,\beta} & \mathbf{F}_{\alpha,s} & \mathbf{0}_{(K-2) \times 4K^2} \\ \mathbf{F}_{\Theta,\beta}^T & \mathbf{F}_{m_g,\beta}^T & \mathbf{F}_{m_p,\beta}^T & \mathbf{F}_{\alpha,\beta}^T & \mathbf{F}_{\beta,\beta} & \mathbf{F}_{\beta,s} & \mathbf{0}_{(K-2) \times 4K^2} \\ \mathbf{F}_{\Theta,s}^T & \mathbf{F}_{m_g,s}^T & \mathbf{F}_{m_p,s}^T & \mathbf{F}_{\alpha,s}^T & \mathbf{F}_{\beta,s}^T & \mathbf{F}_{s,s} & \mathbf{0}_{2L \times 4K^2} \\ \mathbf{0}_{4K^2 \times L} & \mathbf{0}_{4K^2 \times V_u} & \mathbf{0}_{4K^2 \times V_u} & \mathbf{0}_{4K^2 \times (K-2)} & \mathbf{0}_{4K^2 \times (K-2)} & \mathbf{0}_{4K^2 \times 2L} & \mathbf{F}_{R,R} \end{bmatrix} \quad (4.78)$$

where  $\mathbf{0}_{i \times j}$  is the zero matrix with  $i$  row and  $j$  column and  $V_u = (K^2 - 5K + 6)$  is the number of unknown mutual coupling parameters.

$L \times L$  Fisher Information submatrix corresponding to the DOA angles,  $\mathbf{F}_{\Theta,\Theta}$ , is defined as

$$\mathbf{F}_{\Theta,\Theta} = \sum_{h=1}^H \sum_{t_h=1}^{N_h} \mathbf{F}_{\Theta}^T(h, t_h) \mathbf{R}^{(h)-1} \mathbf{F}_{\Theta}(h, t_h) \quad (4.79)$$

where  $2K \times 2K$  matrix  $\mathbf{R}^{(h)}$  is the real covariance matrix of the noise for the time slot  $h$ , i.e.,

$$\mathbf{R}^{(h)} = \sum_{t_h=1}^{N_h} \begin{bmatrix} \Re \{ \mathbf{v}^{(h)}(t_h) \} \\ \Im \{ \mathbf{v}^{(h)}(t_h) \} \end{bmatrix} \begin{bmatrix} \Re \{ \mathbf{v}^{(h)}(t_h) \} \\ \Im \{ \mathbf{v}^{(h)}(t_h) \} \end{bmatrix}^T \quad (4.80)$$

and  $2K \times L$  matrix  $\mathbf{F}_{\Theta}(h, t_h)$  is found as

$$\mathbf{F}_{\Theta}(h, t_h) = \begin{bmatrix} \mathbf{f}_{\theta_1^{(1)}}(t_h) & \mathbf{f}_{\theta_2^{(1)}}(t_h) & \dots & \mathbf{f}_{\theta_{L_1}^{(1)}}(t_h) & \mathbf{f}_{\theta_1^{(2)}}(t_h) & \dots & \mathbf{f}_{\theta_{L_H}^{(H)}}(t_h) \end{bmatrix} \quad (4.81)$$

and  $2K \times 1$  vector  $\mathbf{f}_{\theta_n^{(h)}}(t_h)$  for  $1 \leq n \leq L_h$  is defined as

$$\mathbf{f}_{\theta_n^{(h)}}(t_h) = \begin{bmatrix} -\Re \{\mathbf{MT}\} \mathbf{D}_{n,h} \Im \{s_n^{(h)}(t_h) \mathbf{a}_n^{(h)}\} - \Im \{\mathbf{MT}\} \mathbf{D}_{n,h} \Re \{s_n^{(h)}(t_h) \mathbf{a}_n^{(h)}\} \\ \Re \{\mathbf{MT}\} \mathbf{D}_{n,h} \Re \{s_n^{(h)}(t_h) \mathbf{a}_n^{(h)}\} - \Im \{\mathbf{MT}\} \mathbf{D}_{n,h} \Im \{s_n^{(h)}(t_h) \mathbf{a}_n^{(h)}\} \end{bmatrix} \quad (4.82)$$

where  $\mathbf{a}_n^{(h)}$  is the  $n^{\text{th}}$  column of the nominal array steering matrix in time slot  $h$ ,  $\mathbf{A}^{(h)}$  in (4.4) and  $K \times K$  diagonal matrix  $\mathbf{D}_{n,h}$  is defined as

$$\mathbf{D}_{n,h} = \frac{2\pi}{\lambda} \text{diag} \left( -p_{1,x} \sin(\theta_n^{(h)}) + p_{1,y} \cos(\theta_n^{(h)}) \quad \dots \quad -p_{K,x} \sin(\theta_n^{(h)}) + p_{K,y} \cos(\theta_n^{(h)}) \right) \quad (4.83)$$

$L \times (K^2 - 5K + 6)$  matrix  $\mathbf{F}_{\Theta, m_g}$  corresponding to DOA angles and gain terms of mutual coupling is defined as

$$\mathbf{F}_{\Theta, m_g} = \sum_{h=1}^H \sum_{t_h=1}^{N_h} \mathbf{F}_{\Theta}^T(h, t_h) \mathbf{R}^{(h)-1} \mathbf{F}_{m_g}(h, t_h) \quad (4.84)$$

where  $2K \times (K^2 - 5K + 6)$  matrix  $\mathbf{F}_{m_g}(h, t_h)$  is found as

$$\mathbf{F}_{m_g}(h, t_h) = \begin{bmatrix} \mathbf{f}_{m_g,34}(h, t_h) & \dots & \mathbf{f}_{m_g,3K}(h, t_h) & \mathbf{f}_{m_g,43}(h, t_h) & \mathbf{f}_{m_g,45}(h, t_h) & \dots & \mathbf{f}_{m_g,K(K-1)}(h, t_h) \end{bmatrix} \quad (4.85)$$

where  $2K \times 1$  vector  $\mathbf{f}_{m_g,ij}(h, t_h)$  is defined as

$$\mathbf{f}_{m_g,ij}(h, t_h) = \begin{bmatrix} \mathbf{0}_{(i-1) \times 1} \\ \Re \{ \mathbf{t}_j \mathbf{A}^{(h)} e^{jm_g,ij} \mathbf{s}^{(h)}(t_h) \} \\ \mathbf{0}_{(K-1) \times 1} \\ \Im \{ \mathbf{t}_j \mathbf{A}^{(h)} e^{jm_g,ij} \mathbf{s}^{(h)}(t_h) \} \\ \mathbf{0}_{(K-i) \times 1} \end{bmatrix} \quad (4.86)$$

and  $\mathbf{t}_j$  is the  $j^{\text{th}}$  row of gain/phase mismatch matrix  $\mathbf{T}$  in (4.6).

$L \times (K^2 - 5K + 6)$  Fisher Information submatrix corresponding to DOA angles and phase terms of mutual coupling coefficients,  $\mathbf{F}_{\Theta, m_p}$ , is defined as

$$\mathbf{F}_{\Theta, m_p} = \sum_{h=1}^H \sum_{t_h=1}^{N_h} \mathbf{F}_{\Theta}^T(h, t_h) \mathbf{R}^{(h)-1} \mathbf{F}_{m_p}(h, t_h) \quad (4.87)$$

where  $2K \times (K^2 - 5K + 6)$  matrix  $\mathbf{F}_{m_p}(h, t_h)$  is found as

$$\mathbf{F}_{m_p}(h, t_h) = \begin{bmatrix} \mathbf{f}_{m_p,34}(h, t_h) & \dots & \mathbf{f}_{m_p,3K}(h, t_h) & \mathbf{f}_{m_p,43}(h, t_h) & \mathbf{f}_{m_p,45}(h, t_h) & \dots & \mathbf{f}_{m_p,K(K-1)}(h, t_h) \end{bmatrix} \quad (4.88)$$

where  $2K \times 1$  vector  $\mathbf{f}_{m_p,ij}(h, t_h)$  is defined as

$$\mathbf{f}_{m_p,ij}(h, t_h) = \begin{bmatrix} \mathbf{0}_{(i-1) \times 1} \\ -\Im \left\{ \mathbf{t}_{r_j} \mathbf{A}^{(h)} m_{ij} \mathbf{s}^{(h)}(t_h) \right\} \\ \mathbf{0}_{(K-1) \times 1} \\ \Re \left\{ \mathbf{t}_{r_j} \mathbf{A}^{(h)} m_{ij} \mathbf{s}^{(h)}(t_h) \right\} \\ \mathbf{0}_{(K-i) \times 1} \end{bmatrix} \quad (4.89)$$

$L \times (K - 2)$  Fisher Information submatrix corresponding to DOA angles and gain mismatch parameters,  $\mathbf{F}_{\Theta, \alpha}$ , is defined as

$$\mathbf{F}_{\Theta, \alpha} = \sum_{h=1}^H \sum_{t_h=1}^{N_h} \mathbf{F}_{\Theta}^T(h, t_h) \mathbf{R}^{(h)-1} \mathbf{F}_{\alpha}(h, t_h) \quad (4.90)$$

where  $2K \times (K - 2)$  matrix  $\mathbf{F}_{\alpha}(h, t_h)$  is found as

$$\mathbf{F}_{\alpha}(h, t_h) = \begin{bmatrix} \mathbf{f}_{\alpha_3} & \mathbf{f}_{\alpha_4} & \dots & \mathbf{f}_{\alpha_K} \end{bmatrix} \quad (4.91)$$

$$\mathbf{f}_{\alpha_i} = \begin{bmatrix} \Re \left\{ e^{j\beta_i} \mathbf{m}_i \mathbf{a}_{r_i}^{(h)} \mathbf{s}^{(h)}(t_h) \right\} \\ \Im \left\{ e^{j\beta_i} \mathbf{m}_i \mathbf{a}_{r_i}^{(h)} \mathbf{s}^{(h)}(t_h) \right\} \end{bmatrix} \quad (4.92)$$

where  $\mathbf{m}_i$  is the  $i^{\text{th}}$  column of mutual coupling matrix,  $M$ , and  $\mathbf{a}_{r_i}^{(h)}$  is the  $i^{\text{th}}$  row of the nominal array steering matrix at time slot  $h$ ,  $\mathbf{A}^{(h)}$ .

$L \times (K - 2)$  Fisher Information submatrix corresponding to DOA angles and phase mismatch parameters,  $\mathbf{F}_{\Theta, \beta}$ , is defined as

$$\mathbf{F}_{\Theta, \beta} = \sum_{h=1}^H \sum_{t_h=1}^{N_h} \mathbf{F}_{\Theta}^T(h, t_h) \mathbf{R}^{(h)-1} \mathbf{F}_{\beta}(h, t_h) \quad (4.93)$$

where  $2K \times (K - 2)$  matrix  $\mathbf{F}_{\beta}(h, t_h)$  is found as

$$\mathbf{F}_{\beta}(h, t_h) = \begin{bmatrix} \mathbf{f}_{\beta_3} & \mathbf{f}_{\beta_4} & \dots & \mathbf{f}_{\beta_K} \end{bmatrix} \quad (4.94)$$

$$\mathbf{f}_{\beta_i} = \begin{bmatrix} -\Im \left\{ \alpha_i e^{j\beta_i} \mathbf{m}_i \mathbf{a}_{r_i}^{(h)} \mathbf{s}^{(h)}(t_h) \right\} \\ \Re \left\{ \alpha_i e^{j\beta_i} \mathbf{m}_i \mathbf{a}_{r_i}^{(h)} \mathbf{s}^{(h)}(t_h) \right\} \end{bmatrix} \quad (4.95)$$

$L \times 2L$  Fisher Information submatrix corresponding to DOA angles and source signals,  $\mathbf{F}_{\Theta, s}$ , is defined as

$$\mathbf{F}_{\Theta, s} = \sum_{h=1}^H \sum_{t_h=1}^{N_h} \mathbf{F}_{\Theta}^T(h, t_h) \mathbf{R}^{(h)-1} \mathbf{F}_s(h, t_h) \quad (4.96)$$

where  $2K \times 2L$  matrix  $\mathbf{F}_s(h, t_h)$  is found as

$$\mathbf{F}_s(h, t_h) = \begin{bmatrix} \mathbf{0}_{K \times z_1} & \Re \{ \mathbf{MTA}^{(h)} \} & \mathbf{0}_{K \times z_2} & -\Im \{ \mathbf{MTA}^{(h)} \} & \mathbf{0}_{K \times z_3} \\ \mathbf{0}_{K \times z_1} & \Im \{ \mathbf{MTA}^{(h)} \} & \mathbf{0}_{K \times z_2} & \Re \{ \mathbf{MTA}^{(h)} \} & \mathbf{0}_{K \times z_3} \end{bmatrix} \quad (4.97)$$

where  $z_1 = \sum_{i=1}^{h-1} L_i$ ,  $z_2 = L - L_h$  and  $z_3 = \sum_{i=h+1}^H L_i$ .

$4K^2 \times 4K^2$  Fisher Information submatrix corresponding to noise covariance elements,  $\mathbf{F}_{R,R}$ , is defined as

$$\mathbf{F}_{R,R} = \begin{bmatrix} \mathbf{F}_{R^{(1)}} & \mathbf{0}_{4K^2 \times 4K^2} & \dots & \mathbf{0}_{4K^2 \times 4K^2} \\ \mathbf{0}_{4K^2 \times 4K^2} & \mathbf{F}_{R^{(2)}} & \dots & \mathbf{0}_{4K^2 \times 4K^2} \\ \vdots & \vdots & \ddots & \vdots \\ \mathbf{0}_{4K^2 \times 4K^2} & \mathbf{0}_{4K^2 \times 4K^2} & \dots & \mathbf{F}_{R^{(H)}} \end{bmatrix} \quad (4.98)$$

$$\mathbf{F}_{R^{(h)}} = \begin{bmatrix} \mathbf{R}^{(h)-T} \otimes \bar{\mathbf{r}}_1^{(h)} & \mathbf{R}^{(h)-T} \otimes \bar{\mathbf{r}}_2^{(h)} & \dots & \mathbf{R}^{(h)-T} \otimes \bar{\mathbf{r}}_K^{(h)} \end{bmatrix} \quad (4.99)$$

where  $\bar{\mathbf{r}}_i^{(h)}$  is the  $i^{\text{th}}$  column of matrix  $\mathbf{R}^{(h)-1}$ .

## 4.5 Performance Results

The performance of CIHOSS algorithm is evaluated for the DOA, gain/phase mismatch and mutual coupling coefficient parameter estimations. Mutual coupling coefficients are complex valued. Since to the best of our knowledge, there is no online calibration algorithm in the literature for the defined problem in Section 4.1, the CRB expressions in (4.73) - (4.77) are used to show the effectiveness of the CIHOSS algorithm.

It is assumed that there are  $K = 6$  sensors and  $L = 6$  far field sources. The number of sources at each time slot is selected by satisfying the condition in (4.71).  $K - 2$  sensor positions are randomly selected from a uniform distribution in the deployment area of  $2\lambda \times 2\lambda$ . The distance between the two reference sensors is adjusted to be  $\lambda/2$ .  $N = 1000$  snapshots are collected for each time slot. The performance results are averaged over 100 trials. At each trial, source signals, noise, the sensor positions, the gain/phase mismatch and mutual coupling parameters and the DOA angles of source signals are changed randomly. The DOA angles are selected randomly in the range of  $[10, 170]$  degrees and the difference between the DOA angles of the source signals is set to 30 degrees. The phase terms of gain/phase mismatch and mutual coupling coefficients are selected randomly in the range of  $[-60, 60]$  degrees. The gain terms

of gain/phase mismatch and mutual coupling coefficients are selected randomly in the range of  $[0.8, 1.2]$  and  $[0.1, 0.3]$ , respectively. The simulation parameters are summarized in Table 4.1.

Table 4.1: Simulation parameters for CIHOSS algorithm.

Number of sensors	$K = 6$
Total number of sources	$L = 6$
Number of snapshots	$N_h = 1000, \forall h$
Wavelength	$\lambda = 30$ meters
Deployment area	$[2\lambda \times 2\lambda]$
Distance between reference sensors	$\Delta = \lambda/2$
DOA range	$[10^\circ, 170^\circ]$
Separation of source DOAs	$30^\circ$
Phase terms of gain/phase mismatch	$[-60^\circ, 60^\circ]$
Phase terms of mutual coupling coefficients	$[-60^\circ, 60^\circ]$
Gain terms of gain/phase mismatch	$[0.8, 1.2]$
Gain terms of mutual coupling coefficients	$[0.1, 0.3]$
Number of trials	100

Two different scenarios are evaluated for the performance of CIHOSS algorithm. In the first scenario, there are  $H = 4$  time slots and the number of the sources at each time slot is selected as,  $\{L_1 = 1, L_2 = 2, L_3 = 2, L_4 = 1\}$ . In the second scenario, it is assumed that there are  $H = 6$  time slots and the number of sources at each time slot is selected as  $L_h = 1$ , for  $h = 1, 2, 3, 4, 5, 6$ .

The DOA estimation performance of CIHOSS algorithm is presented in Fig. 4.2.

The performance of the CIHOSS algorithm for estimating the gain/phase mismatch parameters is presented in Fig. 4.3 for the two scenarios. In Fig. 4.3-a, the estimation performance for the gain terms is presented while Fig. 4.3-b is for the phase terms.

Fig. 4.4 shows the performance of the CIHOSS algorithm for estimating the mutual coupling coefficients. The estimation performance of the gain terms of the mutual coupling coefficients is shown in Fig. 4.4-a, while the performance of the phase terms is shown in Fig. 4.4-b.

As it can be seen from Fig. 4.2 - Fig. 4.4, CIHOSS estimates all the unknown parameters accurately after  $SNR = 5$  dB for both scenarios. It is also seen that, the performance of

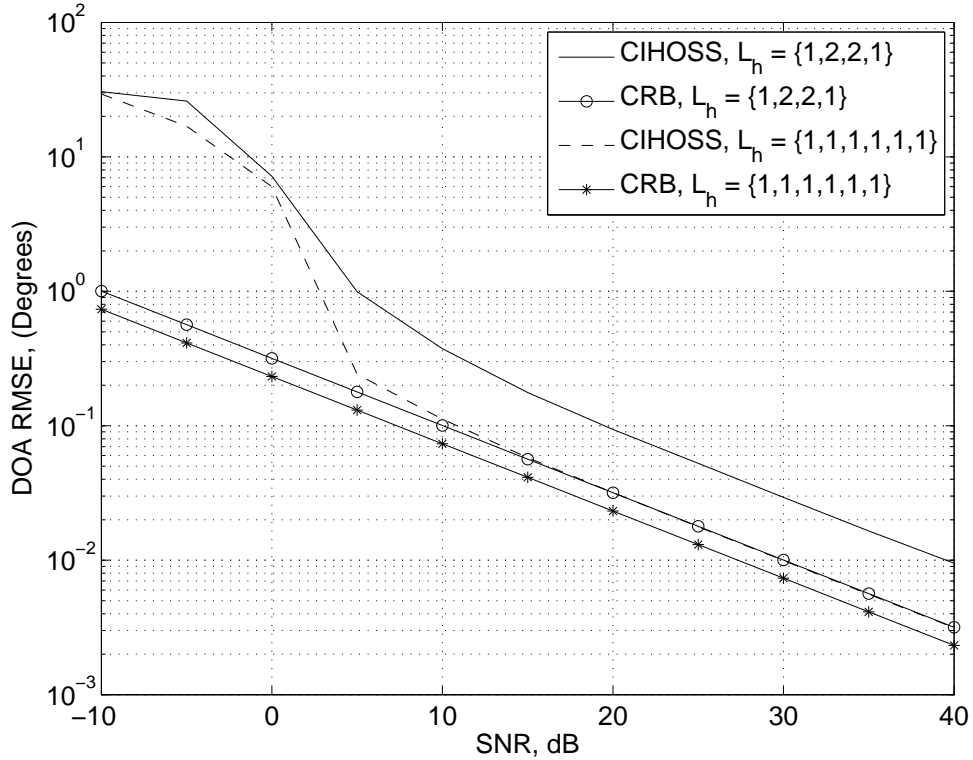


Figure 4.2: SNR performance for the DOA estimation.

the CIHOSS algorithm in scenario-2 is better than the performance in scenario-1, which is consistent with the performance of CRBs. There are mainly two reasons for this fact. The first reason is, since the same number of sources are observed at more time slots, the total number of unknowns in scenario-2 is less than the unknowns in scenario-1. The second reason is that the accuracy of the estimation in HOS approach decreases as the number of sources received in the same time slot increases, which can be seen in Fig. 4.5. In Fig. 4.5-a, the values of the cost function in (4.40) for the iterations are given for scenario-1 and Fig. 4.5-b shows the values for scenario-2. As it is seen from these figures, the cost function values are decreased more rapidly and reach the final cost value with less number of iterations in scenario-2 than that of scenario-1, since the initial estimates in HOS approach is more accurate in scenario-2.

The effectiveness of the HOS approach for the initial estimate is shown in Figs. 4.6 - 4.9. We compare the CIHOSS algorithm with the algorithm proposed in [32] and labeled as Abramovich in the figures. For the fair comparison we assume that only the DOA angles and mutual coupling coefficients are unknown and mutual coupling matrix,  $\mathbf{M}$ , is symmetric

and satisfies the constraints in (4.5). In Fig. 4.6 and Fig. 4.7, “Large Error” is used for the mutual coupling coefficients whose gain terms are in the range of  $[0, 0.5]$  and the phase terms are in the range of  $[-60^\circ, 60^\circ]$ . “Small Error” is used for the mutual coupling coefficients whose gain terms are in the range of  $[0, 0.05]$  and the phase terms are in the range of  $[-5^\circ, 5^\circ]$  in Fig. 4.8 and Fig. 4.9, respectively. In [32], the initial mutual coupling matrix is assumed to be identity matrix and the initial DOA angles are estimated with Bartlett spectrum using the initial mutual coupling matrix. Then, the DOA angles and the calibration parameters are iteratively updated similar to SOS approach in CIHOSS algorithm. The results of this algorithm is shown as “Abramovich with Bartlett” in the legend of the figures. Therefore, comparing CIHOSS with the algorithm in [32] shows the effect of using HOS approach in the calibration. As it is seen from these figures, the algorithm in [32] can not be used effectively for the online array calibration. We modified the algorithm in [32] to find the initial DOA estimates from MUSIC spectrum and its performances are given with legend “Abramovich with MUSIC”. As it is seen from Fig. 4.8 and Fig. 4.9, using MUSIC spectrum instead of Bartlett spectrum can improve the performance of the algorithm in [32]. However, as it is seen from Fig. 4.6 and Fig. 4.7, when the mutual coupling coefficients are large, it can not provide a solution even for large SNR values. On the other hand, CIHOSS algorithm can effectively be used for small and large mutual coupling coefficients.

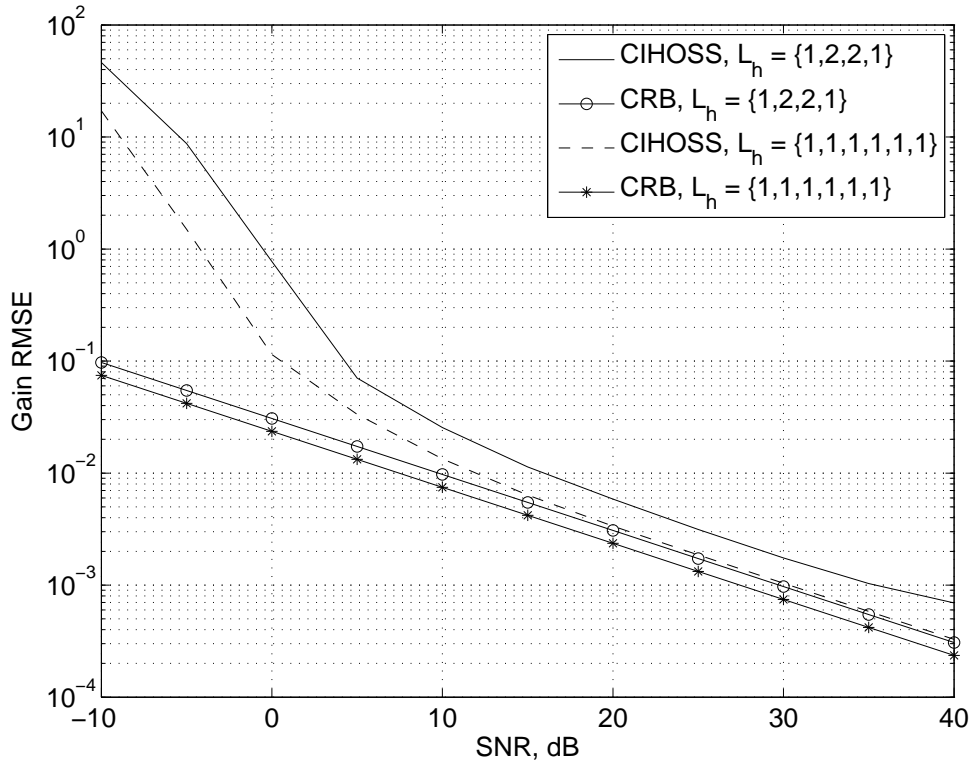
#### 4.6 Advantages of CIHOSS Algorithm

The advantages of the CIHOSS algorithm can be summarized as follows:

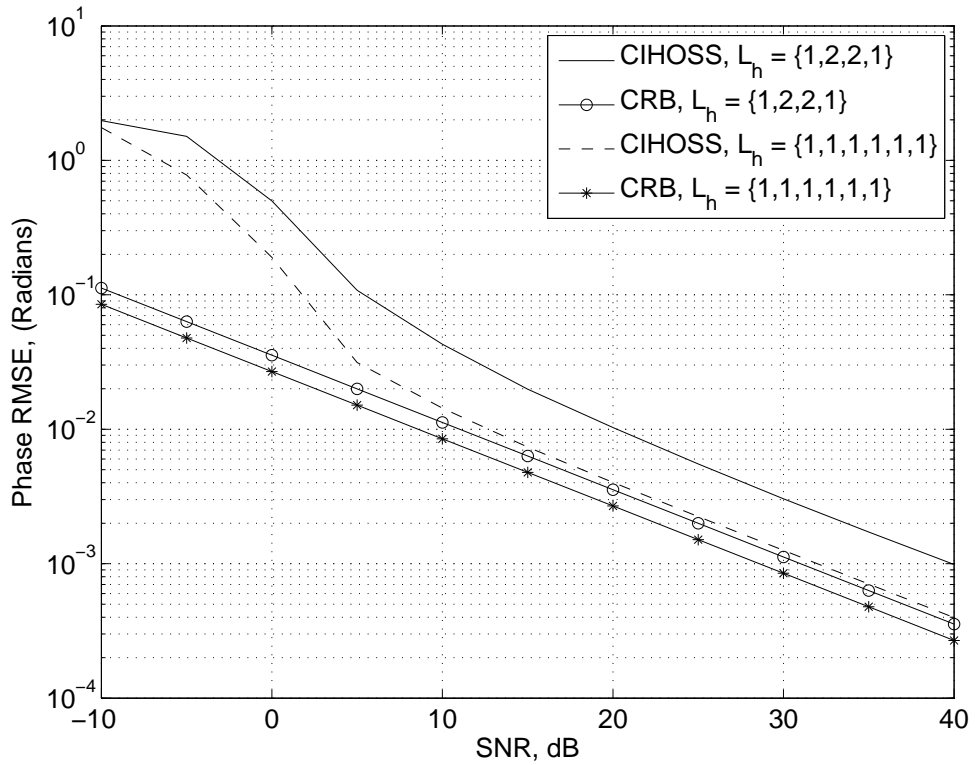
- CIHOSS algorithm jointly estimates the DOA angles, gain/phase mismatches and mutual coupling coefficients when the sensor positions are known and the two reference sensors are perfectly calibrated.
- CIHOSS algorithm does not assume any special structure for mutual coupling matrix and therefore CIHOSS algorithm is applicable to any sensor geometry.
- CIHOSS algorithm does not need initial estimate of gain/phase mismatch and mutual coupling coefficients, since these parameters are estimated directly from the sensor

outputs by using HOS approach.

- CIHOSS can accurately estimates the parameters even for large errors in gain/phase mismatches and mutual coupling coefficients.
  - 0.016 degrees accuracy in DOA estimation is achieved at SNR = 30 dB.
  - 0.0013 accuracy in the gain mismatches and gain terms of mutual coupling coefficients is achieved at SNR = 30 dB.
  - 0.09 degrees accuracy in the phase mismatch is achieved at SNR = 30 dB
  - 0.36 degrees accuracy in the phase terms of mutual coupling coefficients is achieved at SNR = 30 dB.

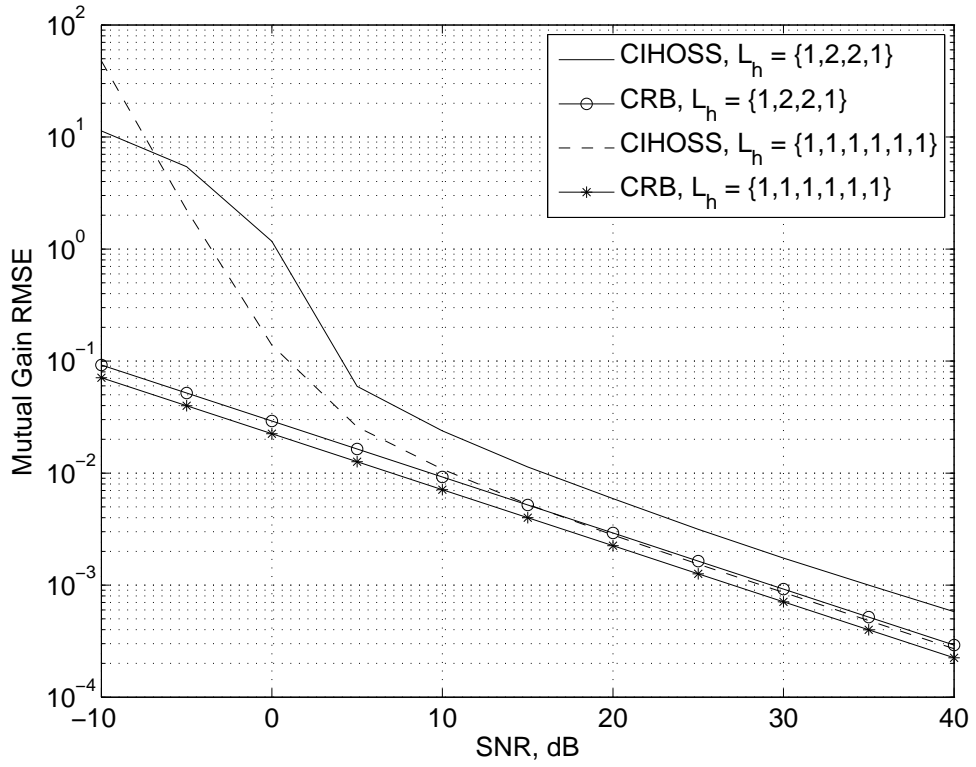


(a)

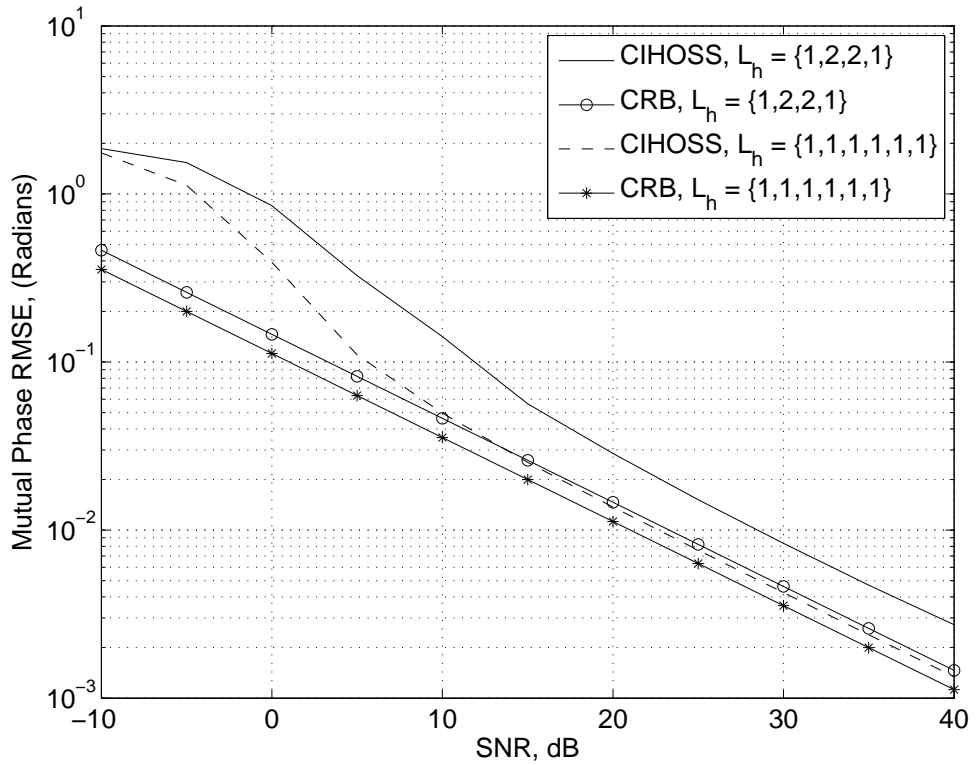


(b)

Figure 4.3: SNR performance for the estimation of the (a) gain and (b) phase terms of the gain/phase mismatch parameters.

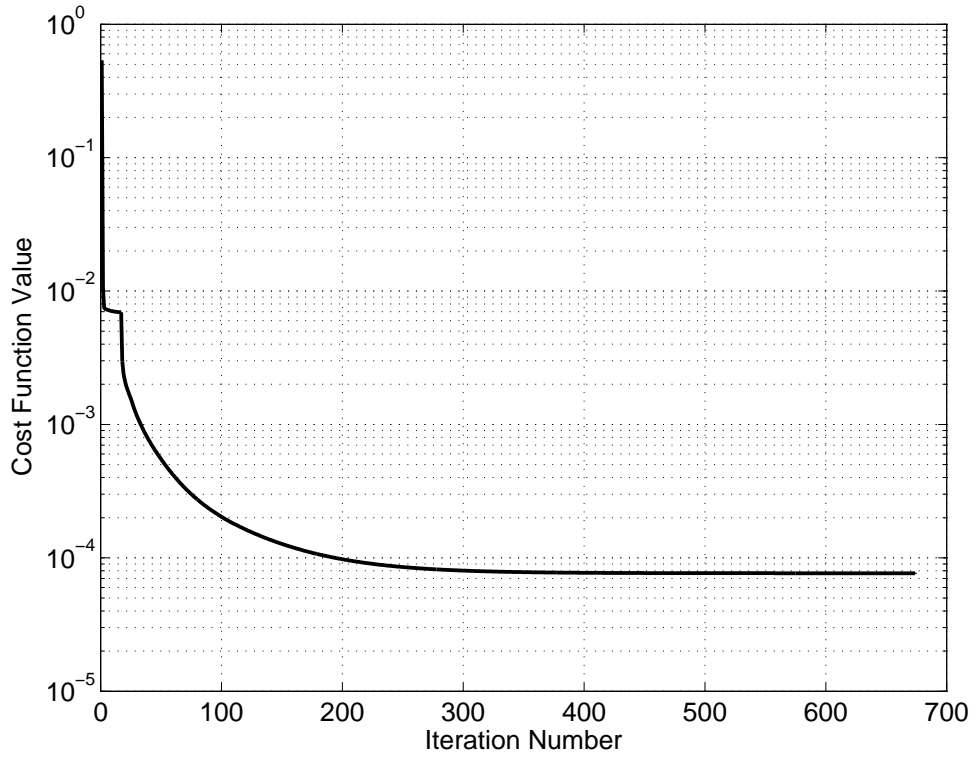


(a)

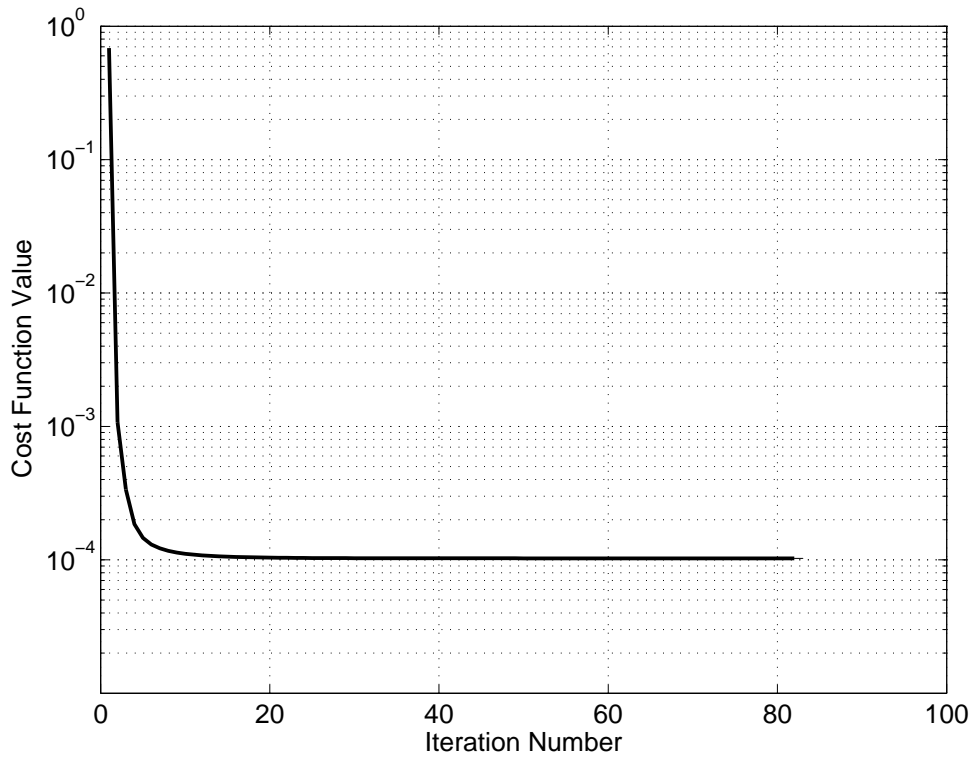


(b)

Figure 4.4: SNR performance for the estimation of the (a) gain and (b) phase terms of the mutual coupling coefficients.



(a)



(b)

Figure 4.5: Cost function values in iteration for cluster distribution of (a)  $L_h = \{1, 2, 2, 1\}$  and (b)  $L_h = \{1, 1, 1, 1, 1, 1\}$  at SNR = 15 dB.

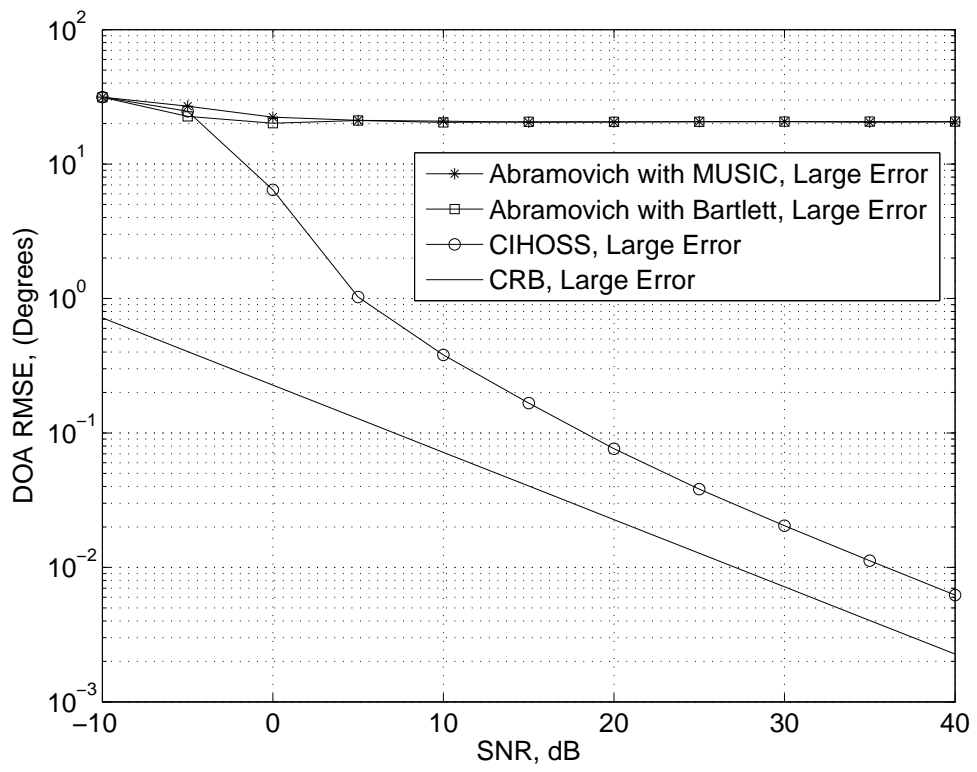
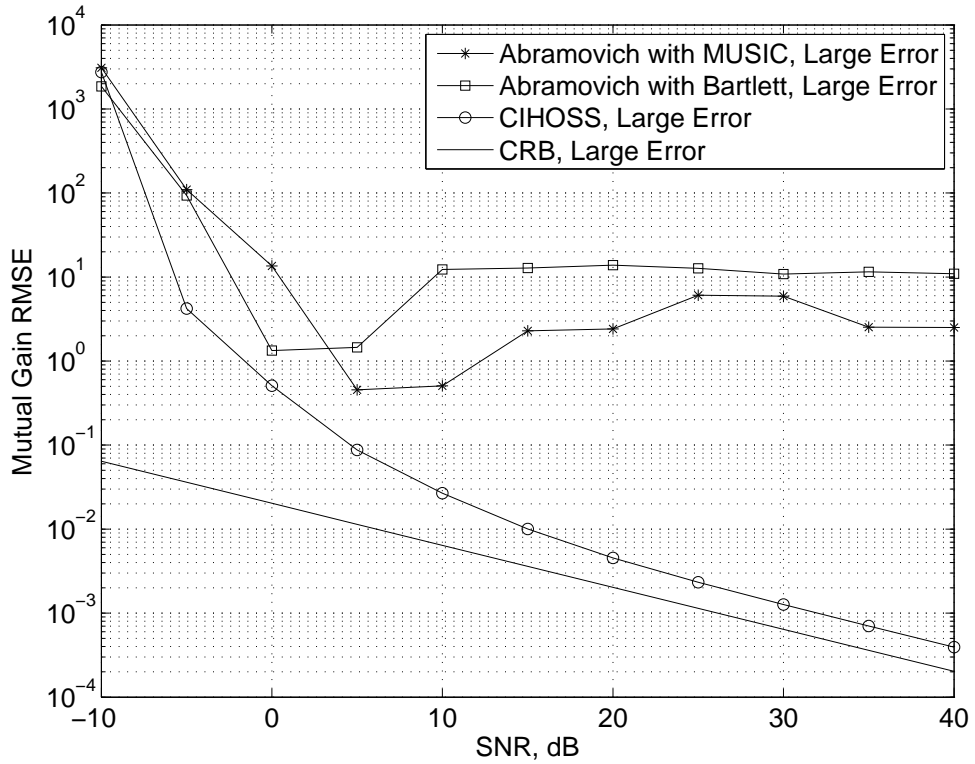
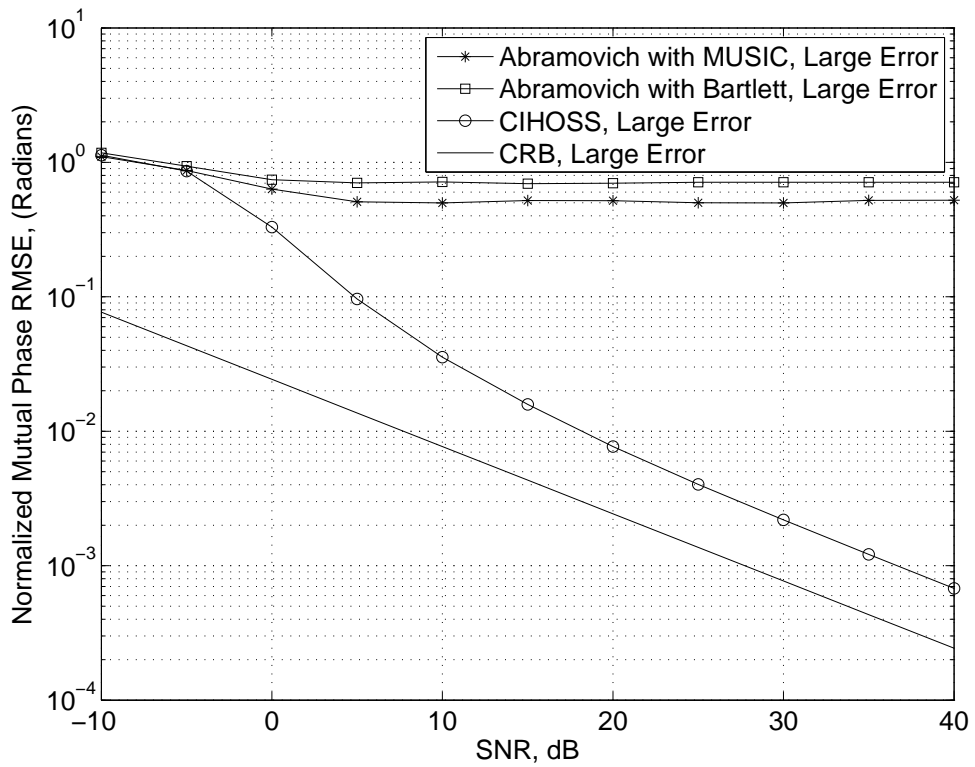


Figure 4.6: SNR performance for the DOA estimation for “Large Error” in mutual coupling coefficients.



(a)



(b)

Figure 4.7: SNR performance for the estimation of the (a) gain and (b) phase terms of the mutual coupling coefficients for “Large Error” in mutual coupling coefficients.

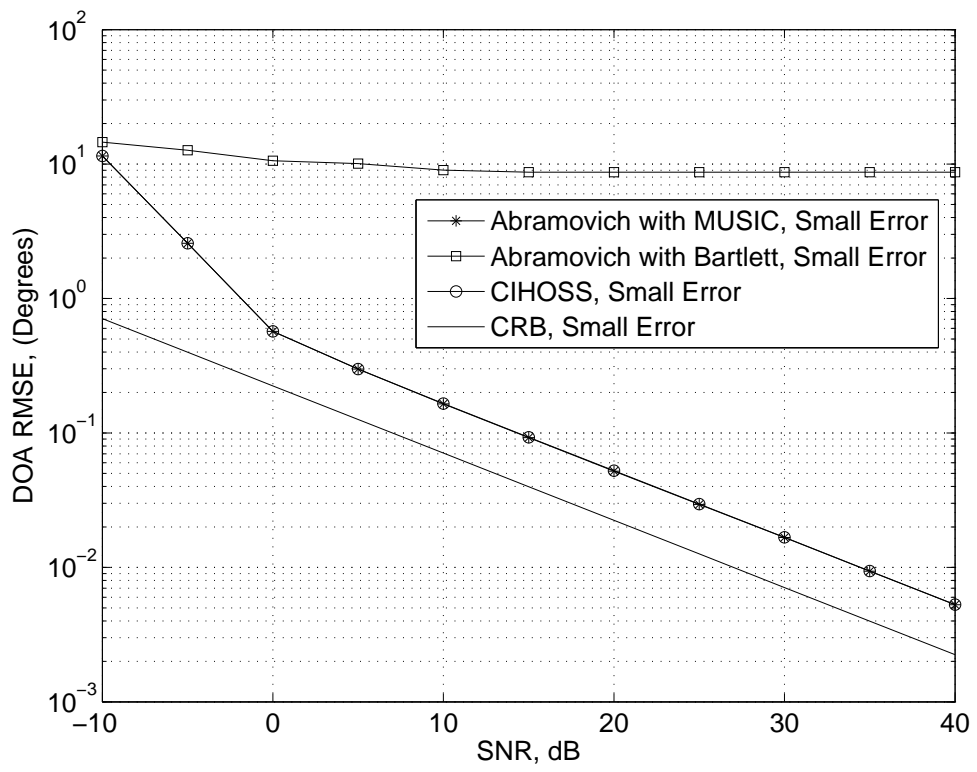
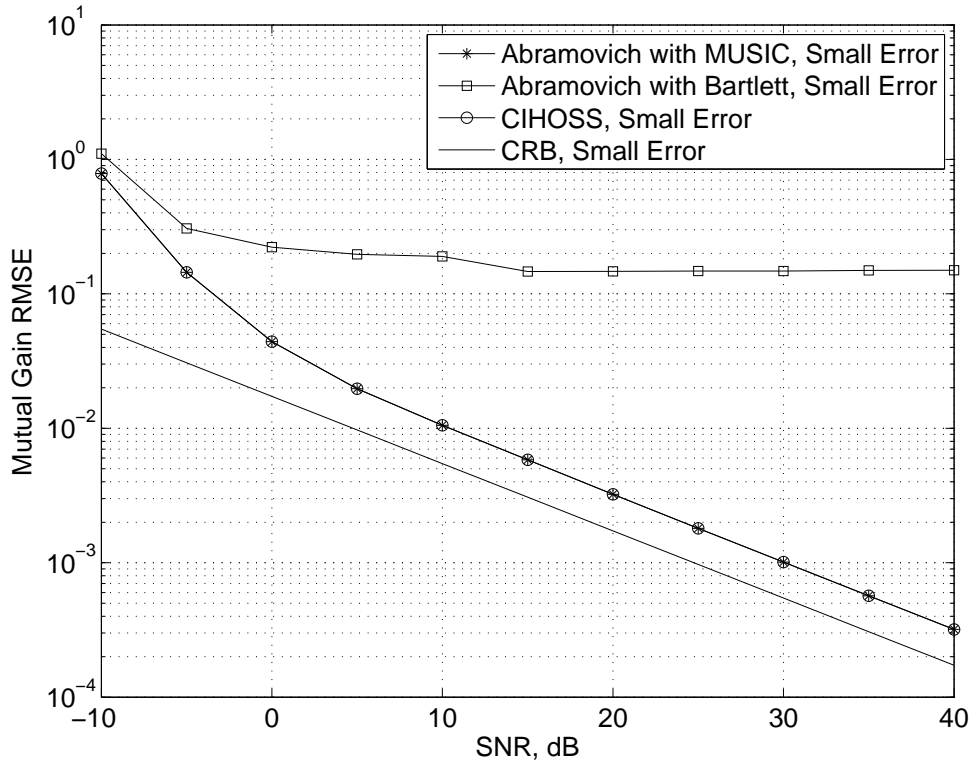
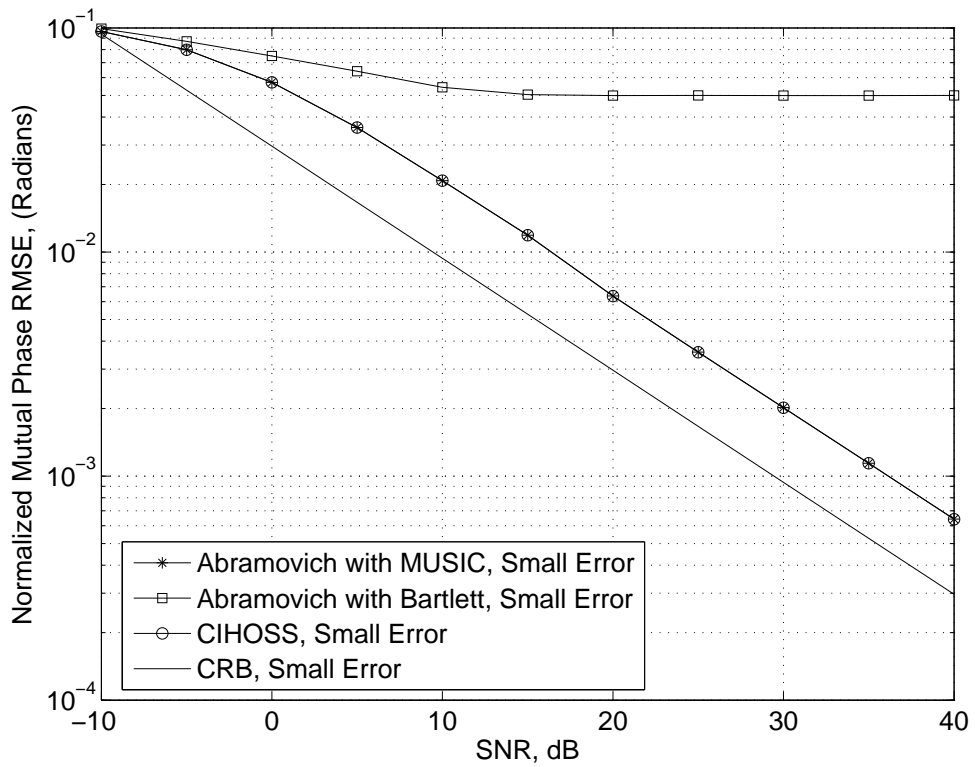


Figure 4.8: SNR performance for the DOA estimation for “Small Error” in mutual coupling coefficients.



(a)



(b)

Figure 4.9: SNR performance for the estimation of the (a) gain and (b) phase terms of the mutual coupling coefficients for “Small Error” in mutual coupling coefficients.

## CHAPTER 5

### CONCLUSION

Calibration is an important process for any device. Sensor arrays usually require a calibration process in order to correct several imperfections. Some of the main sources of error are the sensor position errors, gain/phase imperfections and mutual coupling between antennas. Calibration can be performed online or offline. In this thesis, online sensor array calibration problem is investigated where the calibration is performed during the parameter estimation.

A new online array calibration approach that uses both Higher-Order-Statistics (HOS) and Second-Order-Statistics (SOS) iteratively to estimate the unknown calibration parameters has been presented. The proposed approach exploits the advantages of both HOS and SOS approaches for the parameter estimation. HOS approach is used to obtain an initial parameter estimate, since it can estimate the DOA angles without being affected by the unknown calibration parameters. In addition, it can be used to find the array steering matrix estimate directly from the sensor outputs even for the multi-source case. A new cumulant matrix estimate has been proposed for the effective implementation of the HOS approach when the source signals are statistically dependent. This cumulant matrix estimate can be seen as a generalization of the approaches known in the literature. SOS approach is used to improve the initial estimates obtained from the HOS approach, since it is more robust to the statistical estimation errors for finite length observations. In the proposed online array calibration approach, it is assumed that the two reference sensors are perfectly calibrated with known positions, gain/phase mismatch and mutual coupling. Proposed iterative approach is guaranteed to converge since the cost function is non-negative and improved at each iteration. The proposed approach has been applied for three different online array calibration problems and new algorithms for each of these problems have been introduced.

In the first problem, joint DOA and sensor position estimation when the sensor positions are unknown except the two reference sensors has been investigated and a new algorithm, IHOSS, has been presented. IHOSS eliminates the need to know the nominal sensor positions for the online array calibration in the presence of errors in sensor positions. In this respect, IHOSS is the first algorithm in the literature which finds the DOA and sensor position estimations in case of randomly deployed sensors with unknown coordinates. The ambiguity problem in sensor position estimation due to the wrap around in array steering matrix phase terms has been considered in the IHOSS algorithm and a new method for unambiguous sensor position estimation has been proposed. The proposed method solves the ambiguity problem in sensor position estimation by observing the source signals at least in two different frequencies. Hence, IHOSS algorithm is applicable for wideband signals.

In the second problem, the online array calibration in the presence of errors in sensor positions has been investigated for narrowband signals and a new algorithm, MIHOSS, has been presented. The sensor position estimation method in IHOSS algorithm has been modified for the narrowband signals. In this case, it is assumed that the nominal sensor positions are known and there are perturbations in sensor positions. The upper bound of perturbations in sensor positions for unambiguous sensor position estimation has been presented. It has been shown that the upper bound for the perturbations to achieve parameter estimations is much higher than the alternatives in the literature. Therefore, MIHOSS algorithm can handle both small and large errors in sensor positions.

In the last problem, the effect of gain/phase mismatch and mutual coupling on the DOA estimation performance has been investigated and a new algorithm, CIHOSS, has been proposed for the joint parameter estimation. In this problem, the sensor positions are assumed to be known. It is also assumed that the two reference sensors are perfectly calibrated and placed far away from the other sensors. Therefore, there is no interaction between the reference sensors and the other sensors. The proposed algorithm does not assume a special structure for the mutual coupling matrix and therefore, it is applicable for arbitrary sensor geometries. CIHOSS uses multiple cumulant matrices generated by different sensor pairs to estimate the calibration parameters. The ambiguity problem in the permutation of columns of the actual array steering matrix estimate has been considered and an alignment technique has been introduced to order the elements of rows of the actual array steering matrix.

Deterministic CRB expressions for the DOA and array calibration parameter estimations have been derived. Several simulations have been done and it has been shown that all the proposed algorithms perform well for multiple sources and closely follow the CRB for both DOA and calibration parameters at high SNR.

Some of the future works for this research can be summarized as follows:

- The proposed algorithms in this thesis require two reference sensors that are perfectly calibrated. The effects of the errors in parameters of the reference sensors can be investigated and the proposed algorithms can be improved to be robust to these errors.
- In this thesis, it is assumed that the source signals are non-Gaussian, since the fourth-order cumulants are zero for Gaussian signals. Although this fact is true asymptotically, for the finite length signals it is not always satisfied. In other words, the fourth-order cumulant of the finite length signals generated from the Gaussian distribution may be non-zero. Using this fact, a method can be found to modify the received source signals such that the fourth order cumulants are not zero. We can select a subset of the received signals to be used in the HOS approach such that the fourth-order cumulants of these modified signals are not zero. Transforming the received signals into a new frame by preserving the relations between sensor outputs may also be the solution of using Gaussian signals in HOS approach.

## REFERENCES

- [1] R. Schmidt, *Multiple emitter location and signal parameter estimation*, Proc. RADC Spectrum Estimation Workshop, pp. 243–258, 1979.
- [2] R. Roy and T. Kailath, *ESPRIT - Estimation of Signal Parameters Via Rotational Invariance Techniques*, IEEE Trans. on Acoustics, Speech, and Signal Processing, Vol. 37, No. 7, pp. 984–995, July 1989.
- [3] P. Stoica and A. Nehorai, *MUSIC, maximum likelihood, and Cramer-Rao bound: Further results and comparisons*, IEEE Trans. Acoust., Speech, Signal Process., Vol. 38, No. 12, pp. 2140–2150, December 1990.
- [4] B. Ottersten, M. Viberg and T. Kailath, *Performance analysis of the total least squares ESPRIT algorithm*, IEEE Trans. on Signal Proc., Vol. 39, No. 5, pp. 1122–1135, May 1991.
- [5] M. Aktaş and T. E. Tuncer, *Iterative HOS-SOS (IHOSS) Based Sensor Localization and Direction-Of-Arrival Estimation*, IEEE International Conference on Acoustics, Speech, and Signal Processing, ICASSP-2010, March 2010.
- [6] A. J. Weiss and B. Friedlander, *Array Shape Calibration Using Sources in Unknown Locations - A Maximum Likelihood Approach*, IEEE Trans on Acoustics, Speech and Signal Processing, Vol. 37, No. 12, pp. 1958–1966, December 1989.
- [7] B. P. Flanagan and K. L. Bell, *Array Self Calibration with Large Sensor Position Errors*, Proc. of 33<sup>rd</sup> IEEE Asilomar Conf. On Sig. Syst. and Comp., pp. 258–261, Oct. 1999.
- [8] C. S. See and B. Poh, *Parametric Sensor Array Calibration Using Measured Steering Vectors of Uncertain Locations*, IEEE Trans. on Signal Processing, Vol. 47, No. 4, pp. 1133–1137, April 1999.
- [9] Y. Rockah and P. M. Schulthesis, *Array Shape Calibration Using Sources in Unknown Locations - Part I: Far-Field Sources*, IEEE Trans. on Acoustics, Speech and Signal Processing, Vol. ASSP-35, No. 3, pp. 286–299, March 1987.
- [10] H. S. Mir, J. D. Sahr, G. F. Hatke, and C. M. Keller, *Passive Source Localization Using an Airborne Sensor Array in the Presence of Manifold Perturbations*, IEEE Trans. on Signal Processing, Vol. 55, No. 6, pp. 2486–2496, June 2007.
- [11] M. Lanne, A. Lundgren and M. Viberg, *Optimized Beamforming Calibration In The Presence of Array Imperfections*, IEEE International Conference on Acoustics, Speech and Signal Processing, ICASSP 2007, Vol. 2, pp. 973–976, April 2007.
- [12] M. C. Dogan and J. M. Mendel, *Applications of Cumulants to Array Processing - Part I: Aperture Extension and Array Calibration*, IEEE Trans. on Signal Proc., Vol. 43, No. 5, pp. 1200–1216, May 1995.

- [13] N. Yuen and B. Friedlander, *Asymptotic Performance Analysis of ESPRIT, Higher Order ESPRIT, and Virtual ESPRIT Algorithms*, IEEE Trans. on Signal Proc., Vol. 44, No. 10, pp. 2537–2550, October 1996.
- [14] E. Gönen, J. M. Mendel and M. C. Dogan, *Applications of Cumulants to Array Processing-Part IV: Direction Finding in Coherent Signals Case*, IEEE Trans. on Signal Proc., Vol. 45, No. 9, pp. 2265–2276, September 1997.
- [15] T. E. Tuncer and B. Friedlander, *Classical and Modern Direction-of-Arrival Estimation*, Academic Press, 2009.
- [16] T. E. Tuncer and M. T. Özgen, *No-Search Algorithm For Direction Of Arrival Estimation*, Radio Science, Vol.44, pp. 1–14, September 30, 2009.
- [17] M. G. Amin, *Sufficient Conditions for Alias-Free Direction of Arrival Estimation in Periodic Spatial Spectra*, IEEE Trans. on Antenna and Propagation, Vol. 41, No. 4, pp. 508–511, April 1993.
- [18] P. Chevalier, L. Albera, A. Ferrol, and P. Comon, *On the Virtual Array Concept for Higher Order Array Processing*, IEEE Trans. on Signal Proc., Vol. 53, No. 4, pp. 1254–1271, April 2005.
- [19] B. Picinbono, *Second-Order Complex Random Vectors and Normal Distributions*, IEEE Trans. on Signal Proc., Vol. 44, No. 10, pp. 2637–2640, October 1996.
- [20] J. Delmas and H. Abeida, *Stochastic Cramér-Rao Bound for Noncircular Signals with Application to DOA Estimation*, IEEE Trans. on Signal Proc., Vol. 52, No. 11, pp. 3192–3199, November 2004.
- [21] S. M. Kay, *Fundamentals of Statistical Signal Processing: Estimation Theory*, Upper Saddle River, NJ: Prentice-Hall, 1993.
- [22] M. Pesavento and A. B. Gershman, *Maximum-Likelihood Direction-of-Arrival Estimation in the Presence of Unknown Nonuniform Noise*, IEEE Trans. on Signal Proc., Vol. 49, No. 7, pp. 1310–1324, July 2001.
- [23] P. Stoica and A. Nehorai, *Performance Study of Conditional and Unconditional Direction-of-Arrival Estimation*, IEEE Trans. on Signal Proc., Vol. 38, No. 10, pp. 1783–1795, October 1990.
- [24] A. J. Weiss and B. Friedlander, *On the Cramér-Rao Bound for Direction Finding of Correlated Signals*, IEEE Trans. on Signal Proc., Vol. 41, No. 1, pp. 495–499, January 1993.
- [25] P. Stoica and R. Moses, *Spectral Analysis of Signals*, Prentice Hall, 2005.
- [26] H. L. Van Trees, *Optimum Array Processing*, Wiley-Interscience, New York, NY, USA, 2002.
- [27] A. J. Weiss and B. Friedlander, *DOA and Steering Vector Estimation Using a Partially Calibrated Array*, IEEE Trans. on Aerospace and Electronic Systems, Vol. 32, pp. 1047–1057, 1996.

- [28] M. Aktaş, and T. E. Tuncer, *Iterative HOS-SOS (IHOSS) Algorithm for Direction-of-Arrival Estimation and Sensor Localization*, IEEE Trans. on Signal Proc., Vol. 58, pp. 6181–6194, Dec. 2010.
- [29] B. Friedlander, and A. J. Weiss, *Direction Finding in the Presence of Mutual Coupling*, IEEE Trans. on Antennas and Propagation, Vol. 39, pp. 273–284, March 1991.
- [30] M. Aktaş and T. E. Tuncer, *HOS Based Online Calibration*, European Signal Processing Conference (EUSIPCO-2011), Barcelona, Aug. 31, 2011.
- [31] M. Aktaş and T. E. Tuncer, *Array Calibration with Modified Iterative HOS-SOS (MI-HOSS) Algorithm*, European Signal Processing Conference (EUSIPCO-2011), pp. 614–618, Barcelona, Aug. 31, 2011.
- [32] I. S. D. Solomon, D. A. Gray, Y. I. Abramovich, and S. J. Anderson, *Receiver Array Calibration Using Disparate Sources*, IEEE Trans. on Antennas and Propagation, Vol. 47, pp. 496–505, March 1999.
- [33] Z. Ye, and C. Liu, *2-D DOA Estimation in the Presence of Mutual Coupling*, IEEE Trans. on Antennas and Propagation, Vol. 56, pp. 3150–3158, October 2008.
- [34] C. M. S. See, and A. B. Gershman, *Direction-of-Arrival Estimation in Partly Calibrated Subarray-Based Sensor Arrays*, IEEE Trans. on Signal Proc., Vol. 52, pp. 329–338, February 2004.
- [35] F. Sellone, and A. Serra, *A Novel Online Mutual Coupling Compensation Algorithm for Uniform and Linear Arrays*, IEEE Trans. on Signal Proc., Vol. 55, No. 2, pp. 560–573, February 2007.
- [36] S. Henault and Y.M.M. Antar, *Limitations of Online Calibration Methods in Antenna Arrays*, IEEE, Antennas and Propagation Society International Symposium (APSURSI), pp. 1–4, July 2010.
- [37] M. Lin and L. Yang, *Blind Calibration and DOA Estimation With Uniform Circular Arrays in the Presence of Mutual Coupling*, IEEE Antennas and Wireless Propagation Letters, Vol. 5, pp. 315–318, December 2006.
- [38] W. Biao and C. Hui, *Performance Analysis of self-Calibration Algorithm for L-shaped Array*, International Conference on Measuring Technology and Mechatronics Automation, Vol. 3, pp. 798–802, April 2009.
- [39] W. Biao and C. Hui, *DOA estimation and self-calibration algorithm for Yshaped array in the presence of mutual coupling*, 2nd International Congress on Image and Signal Processing, CISP '09, pp. 1–5, October 2009.
- [40] L. Xiang et al, *Direction of arrival estimation for uniform circular array based on fourth-order cumulants in the presence of unknown mutual coupling*, IET Microwaves, Antennas and Propagation, Vol. 2, pp. 281–287, April 2008.
- [41] A. J. Weiss and B. Friedlander, *Array shape calibration using eigenstructure methods*, Twenty-Third Asilomar Conference on Signals, Systems and Computers, Vol. 2, pp. 925–929, 1989
- [42] B. P. Flanagan and K. L. Bell, *Array self-calibration with large sensor position errors*, Elsevier Science Signal Processing, pp. 2201–2214, 2001.

- [43] D. M. Pozar, *Microwave Engineering*, John Wiley & Sons, Inc., 2011.
- [44] P. K. Amiri, et al., *Nonreciprocal spin wave spectroscopy of thin Ni–Fe stripes*, Appl. Phys. Lett. 91, 062502 (2007).
- [45] T. Kodera, D. L. Sounas and C. Caloz, *Nonreciprocal Magnetless CRLH Leaky-Wave Antenna Based on a Ring Metamaterial Structure*, IEEE Antennas and Wireless Propagation Letters, Vol. 10, pp. 1551–1554, 2011.

## APPENDIX A

### Proof of Lemma-1

By substituting (2.26) and (2.25) into (2.23), the desired cumulant matrix,  $\mathbf{C}^d$ , is rewritten as,

$$\mathbf{C}^d = \sum_{i=1}^L \begin{bmatrix} \gamma_i \mathbf{a}_i \mathbf{a}_i^H & \gamma_i d_i \mathbf{a}_i \mathbf{a}_i^H \\ \gamma_i d_i^* \mathbf{a}_i \mathbf{a}_i^H & \gamma_i \mathbf{a}_i \mathbf{a}_i^H \end{bmatrix} \quad (\text{A.1})$$

where  $\mathbf{a}_i$  is the  $i^{\text{th}}$  column of array steering matrix,  $\mathbf{A}$  and  $d_i$  is the  $i^{\text{th}}$  diagonal element of matrix  $\mathbf{D}$  in (2.26). When it is assumed that only the  $i^{\text{th}}$  source is received, the cumulant matrix for the array output is written as in the same form of (2.17), i.e.,

$$\begin{aligned} \mathbf{C}^{(i)} &= \begin{bmatrix} \mathbf{C}_{xx}^{(i)} & \mathbf{C}_{xy}^{(i)} \\ \mathbf{C}_{xy}^{(i)H} & \mathbf{C}_{xx}^{(i)} \end{bmatrix} \\ \mathbf{C}_{xx}^{(i)}(k, l) &= \text{Cum}(x_1^{(i)}(t), x_1^{(i)*}(t), x_k^{(i)}(t), x_l^{(i)*}(t)) \\ \mathbf{C}_{xy}^{(i)}(k, l) &= \text{Cum}(x_2^{(i)}(t), x_1^{(i)*}(t), x_k^{(i)}(t), x_l^{(i)*}(t)) \end{aligned} \quad (\text{A.2})$$

where  $x_m^{(i)}(t) = a_{m,i} s_i(t) + v_m(t)$  is the  $m^{\text{th}}$  sensor output for the  $i^{\text{th}}$  source.  $a_{j,i}$  is the  $j^{\text{th}}$  row and  $i^{\text{th}}$  column of array steering matrix,  $\mathbf{A}$ . It is assumed that the noise is Gaussian and independent with the source signals. Using this fact and the cumulant properties [CP1] and [CP4] in [12], the matrix elements in (A.2) can be rewritten in a more compact form by substituting (4.4), (2.26), and (2.20) into (A.2) such as,

$$\begin{aligned} \mathbf{C}_{xx}^{(i)}(k, l) = a_{k,i} a_{l,i}^* \gamma_i &\Rightarrow \mathbf{C}_{xx}^{(i)} = \mathbf{a}_i \mathbf{a}_i^H \gamma_i \\ \mathbf{C}_{xy}^{(i)}(k, l) = d_i a_{k,i} a_{l,i}^* \gamma_i &\Rightarrow \mathbf{C}_{xy}^{(i)} = d_i \mathbf{a}_i \mathbf{a}_i^H \gamma_i \end{aligned} \quad (\text{A.3})$$

Substituting (A.3) into (A.2) and summing up for all of the sources gives us the desired cumulant matrix in (A.1).

## APPENDIX B

### Derivation of (2.32)

The cumulants corresponding to the  $i^{th}$  source are found by substituting (2.30) into (A.2), i.e.,

$$\begin{aligned}\hat{\mathbf{C}}_{xx}^{(i)}(k, l) &= Cum(\bar{x}_1^{(i)}(t), (\bar{x}_1^{(i)}(t))^*, \bar{x}_k^{(i)}(t), (\bar{x}_l^{(i)}(t))^*) \\ \hat{\mathbf{C}}_{xy}^{(i)}(k, l) &= Cum(\bar{x}_2^{(i)}(t), (\bar{x}_1^{(i)}(t))^*, \bar{x}_k^{(i)}(t), (\bar{x}_l^{(i)}(t))^*)\end{aligned}\quad (\text{B.1})$$

where  $\bar{x}_k^{(i)}(t) = \sum_{m=1}^M q_{km}^{(i)} x_m(t)$  and  $q_{kl}^{(i)}$  is the  $k^{th}$  row and  $l^{th}$  column of matrix  $\mathbf{Q}_i$  in (2.30). From the cumulant properties [CP1], [CP2] and [CP4] in [12],  $\hat{\mathbf{C}}_{xx}^i$  and  $\hat{\mathbf{C}}_{xy}^i$  in (B.1) can be written as,

$$\begin{aligned}\hat{\mathbf{C}}_{xx}^i &= (\mathbf{Q}_i \otimes \mathbf{q}_1^{(i)*}) \mathbf{C}_x (\mathbf{Q}_i \otimes \mathbf{q}_1^{(i)*})^H \\ \hat{\mathbf{C}}_{xy}^i &= (\mathbf{Q}_i \otimes \mathbf{q}_1^{(i)*}) \mathbf{C}_x (\mathbf{Q}_i \otimes \mathbf{q}_2^{(i)*})^H\end{aligned}\quad (\text{B.2})$$

where  $\mathbf{q}_j^{(i)*}$  is the complex conjugate of the  $j^{th}$  row of the matrix  $\mathbf{Q}_i$  and  $\mathbf{C}_x$  is defined in (2.33). Substituting (B.2) into (A.2) and summing up for all of the incoming sources results (2.32), which is the estimate of desired cumulant matrix in (2.23).

## APPENDIX C

### Proof of Theorem-1 in IHOSS

Let  $\{\hat{k}_{f_j}^{(i)}\}_{j=1}^F$  and  $\{\bar{k}_{f_j}^{(i)}\}_{j=1}^F$  be the correct ambiguity terms for the unambiguous sensor positions and the estimated ambiguity terms as in (2.50) for  $1 \leq i \leq L$ . To resolve the ambiguity in sensor positions, the minimization problem in (2.50) should have unique solution, which is  $\{\bar{k}_{f_j}^{(i)}\}_{j=1}^F = \{\hat{k}_{f_j}^{(i)}\}_{j=1}^F$ .

The minimization in (2.50) is done over the summation of positive terms. Therefore, the uniqueness of only one term of the summation is sufficient for the overall uniqueness. This fact results that (2.50) has a unique solution, if the following inequality is satisfied for at least one of the frequencies,  $f_j$ ,  $j \in \{2, \dots, F\}$  for  $1 \leq i \leq L$ ,

$$\left(K_{m,j}^{(i)}\right)^2 \neq \left(\frac{\vartheta_s}{2\pi f_1} \hat{\xi}_m^{(i)}(f_1) + \frac{\vartheta_s}{f_1} \bar{k}_{f_1}^{(i)} - \frac{\vartheta_s}{2\pi f_j} \hat{\xi}_m^{(i)}(f_j) - \frac{\vartheta_s}{f_j} \bar{k}_{f_j}^{(i)}\right)^2 \quad (\text{C.1})$$

where  $K_{m,j}^{(i)}$  corresponds to the minimum distance between possible dot products of the position vector of the  $m^{\text{th}}$  sensor and the propagation vector of the  $i^{\text{th}}$  source for  $f_1$  and  $f_j$ , i.e.,

$$\begin{aligned} K_{m,j}^{(i)} &= \frac{\vartheta_s}{2\pi f_1} \hat{\xi}_m^{(i)}(f_1) + \frac{\vartheta_s}{f_1} \bar{k}_{f_1}^{(i)} - \frac{\vartheta_s}{2\pi f_j} \hat{\xi}_m^{(i)}(f_j) - \frac{\vartheta_s}{f_j} \bar{k}_{f_j}^{(i)} \\ &= \tau_{m,1}^{(i)} \left(\bar{k}_{f_1}^{(i)}\right) - \tau_{m,j}^{(i)} \left(\bar{k}_{f_j}^{(i)}\right), \quad 1 \leq i \leq L \end{aligned} \quad (\text{C.2})$$

and  $\bar{k}_{f_j}^{(i)}$  is an integer, i.e.,

$$\bar{k}_{f_j}^{(i)} = \bar{k}_{f_j}^{(i)} - g_j^{(i)}, \quad \text{such that } g_j^{(i)} \in \mathcal{Z}, \quad \sum_{j=1}^F |g_j^{(i)}| \neq 0 \quad (\text{C.3})$$

Substituting (C.2) and (C.3) into (C.1) simplifies the inequality and the required condition on the frequencies to satisfy (C.1) for all possible values of  $K_{m,j}^{(i)}$  is found as,

$$\left|\frac{g_j^{(i)}}{f_j} - \frac{g_1^{(i)}}{f_1}\right| > \frac{2}{\vartheta_s} |K_{m,j}^{(i)}|, \quad \forall i \in \{1, \dots, L\} \\ \exists j \in \{2, \dots, F\} \quad (\text{C.4})$$

Note that for the error free case, the dot products for the two frequencies are the same at the correct ambiguity terms,  $\forall j \in \{1, \dots, F\}$ , i.e.,

$$\frac{\vartheta_s}{2\pi f_1} \xi_m^{(i)}(f_1) + \frac{\vartheta_s}{f_1} k_{f_1}^{(i)} = \frac{\vartheta_s}{2\pi f_j} \xi_m^{(i)}(f_j) + \frac{\vartheta_s}{f_j} k_{f_j}^{(i)} \quad (\text{C.5})$$

When there are errors in estimated parameters,  $\hat{\xi}_m^{(i)}(f_j)$ , the equality in (C.5) is not satisfied and a non-zero  $K_{m,j}^{(i)}$  value is obtained. Since the possible values of the dot product are symmetric with the correct ambiguity term, it is found that the maximum value of  $K_{m,j}^{(i)}$  is bounded, i.e.,

$$\beta_j^{(i)} = \frac{\vartheta_s}{f_j} \left| \frac{f_j}{f_1} - \left[ \frac{f_j}{f_1} \right]_r \right| \geq 2 |K_{m,j}^{(i)}| \quad (\text{C.6})$$

The inequality in (C.6) is valid, if the following conditions are satisfied for all values of  $k \in \mathcal{Z} > 1$ ,

$$\beta_j^{(i)} < \begin{cases} \left| \frac{\vartheta_s}{f_1} - k\beta_j^{(i)} \right|, & \text{for } \left[ \frac{f_j}{f_1} \right]_r < \frac{f_j}{f_1} \\ \left| \frac{\vartheta_s}{f_j} - k\beta_j^{(i)} \right|, & \text{for } \left[ \frac{f_j}{f_1} \right]_r > \frac{f_j}{f_1} \end{cases} \quad (\text{C.7})$$

Substituting (C.6) into (C.7) simplifies the inequalities, i.e.,

$$\left[ \frac{f_j}{f_1} \right]_r < \frac{f_j}{f_1} < \frac{k+1}{k} \left[ \frac{f_j}{f_1} \right]_r \quad \text{or} \quad \frac{k}{k+1} \left[ \frac{f_j}{f_1} \right]_r < \frac{f_j}{f_1} < \left[ \frac{f_j}{f_1} \right]_r \quad (\text{C.8})$$

Substituting (C.6) into (C.4) results,

$$\left| g_j^{(i)} - g_1^{(i)} \frac{f_j}{f_1} \right| \geq \left| \frac{f_j}{f_1} - \left[ \frac{f_j}{f_1} \right]_r \right|, \quad \forall i \in \{1, \dots, L\} \\ \exists j \in \{2, \dots, F\} \quad (\text{C.9})$$

Note that the equality in (C.9) is due to the fact that the ambiguity in sensor positions cannot be solved via frequency selection when  $|K_{m,j}^{(i)}| = \frac{1}{2}\beta_j^{(i)}$ . There are two possible ambiguity terms at which  $|K_{m,j}^{(i)}| = \frac{1}{2}\beta_j^{(i)}$  whatever the selected frequencies are, i.e.,

$$\frac{\vartheta_s}{2\pi f_1} \hat{\xi}_m^{(i)}(f_1) + \frac{\vartheta_s}{f_1} k_{f_1}^{(i)} - \frac{\vartheta_s}{2\pi f_j} \hat{\xi}_m^{(i)}(f_j) - \frac{\vartheta_s}{f_j} k_{f_j}^{(i)} = \frac{1}{2} \left( \frac{\vartheta_s}{f_1} - \frac{\vartheta_s}{f_j} \left[ \frac{f_j}{f_1} \right]_r \right) \\ \frac{\vartheta_s}{2\pi f_1} \hat{\xi}_m^{(i)}(f_1) + \frac{\vartheta_s}{f_1} \left( k_{f_1}^{(i)} - 1 \right) - \frac{\vartheta_s}{2\pi f_j} \hat{\xi}_m^{(i)}(f_j) - \frac{\vartheta_s}{f_j} \left( k_{f_j}^{(i)} - \left[ \frac{f_j}{f_1} \right]_r \right) = \frac{1}{2} \left( \frac{\vartheta_s}{f_j} \left[ \frac{f_j}{f_1} \right]_r - \frac{\vartheta_s}{f_1} \right) \quad (\text{C.10})$$

This problem can be solved by constraining  $K_{m,j}^{(i)}$ . In this case, there is no two ambiguity terms which return the same  $|K_{m,j}^{(i)}|$  terms. This constraint which guarantees the correct ambiguity resolution is given as,

$$|K_{m,j}^{(i)}| < \frac{1}{2}\beta_j^{(i)} = \frac{1}{2} \frac{\vartheta_s}{f_j} \left| \frac{f_j}{f_1} - \left[ \frac{f_j}{f_1} \right]_r \right| \quad (\text{C.11})$$

Since the value of  $K_{m,j}^{(i)}$  is determined by the errors of the estimated parameters in (2.50), to satisfy the condition in (C.11), the estimation errors should also be bounded. For this case,

the term that is tried to be minimized in (2.50) can be written for the correct ambiguity term by substituting (2.56) into (2.50), i.e.,

$$K = \sum_{j=2}^F \left( \frac{\vartheta_s}{2\pi f_1} (\xi_m^{(i)}(f_1) + \Delta \xi_m^{(i)}(f_1)) + \frac{\vartheta_s}{f_1} k_{f_1}^{(i)} - \frac{\vartheta_s}{2\pi f_j} (\xi_m^{(i)}(f_j) + \Delta \xi_m^{(i)}(f_j)) - \frac{\vartheta_s}{f_j} k_{f_j}^{(i)} \right)^2 \quad (C.12)$$

Using the relation in (C.5), (C.12) can be simplified as,

$$K = \sum_{j=2}^F \left( \frac{\vartheta_s}{2\pi f_1} \Delta \xi_m^{(i)}(f_1) - \frac{\vartheta_s}{2\pi f_j} \Delta \xi_m^{(i)}(f_j) \right)^2 \quad (C.13)$$

For the unique solution of (2.50) to be the correct ambiguity term, i.e.,  $\{\bar{k}_{f_j}^{(i)}\}_{j=1}^F = \{k_{f_j}^{(i)}\}_{j=1}^F$ ,  $K$  should be equal to the solution of the minimization problem in (2.50), i.e.,  $K = \sum_{j=2}^F (K_{m,j}^{(i)})^2$ . Using (C.11) and (C.13) in this relation simplifies the conditions on estimation errors for unambiguous sensor positions as in (2.54).

To complete the proof, we should specify the possible ranges of  $g_j^{(i)}$  and  $k$ , which depend on the search region for  $k_{f_j}^{(i)}$ . The limiting value for the search region is found from (3.3) by considering the position of the most distant sensor with respect to the reference sensor defined as  $\mathbf{h} = (h_x, h_y)$  in Theorem-1, i.e.,

$$\frac{f_j \bar{h}^{(i)}}{\vartheta_s} - 1 \leq k_{f_j}^{(i)} \leq \frac{f_j \bar{h}^{(i)}}{\vartheta_s}, \quad \forall j \in \{1, \dots, F\} \quad (C.14)$$

where  $\bar{h}^{(i)} = h_x \cos(\theta_i) + h_y \sin(\theta_i)$ . Note that the inequality in (C.14) is based on the fact that (3.3) is in the range of  $[0, 2\pi]$ . The limits of  $k_{f_j}^{(i)}$  satisfied for all values of  $\theta_i$  are found by using simple trigonometric identities for  $j \in \{1, \dots, F\}$ , i.e.,

$$- \left[ \frac{f_j}{\vartheta_s} \sqrt{h_x^2 + h_y^2} + 1 \right] \leq k_{f_j}^{(i)} \leq \left[ \frac{f_j}{\vartheta_s} \sqrt{h_x^2 + h_y^2} \right] \quad (C.15)$$

Then, the possible ranges for  $g_j^{(i)}$ ,  $j \in \{1, \dots, F\}$ , can be found from (C.15) and (C.3) such as,

$$\begin{aligned} - \left[ \frac{f_j}{\vartheta_s} \sqrt{h_x^2 + h_y^2} \right] + \bar{k}_{f_j, \min}^{(i)} \leq g_j^{(i)} \leq \left[ \frac{f_j}{\vartheta_s} \sqrt{h_x^2 + h_y^2} + 1 \right] + \bar{k}_{f_j, \max}^{(i)} \\ -2 \left[ \frac{f_j}{\vartheta_s} \sqrt{h_x^2 + h_y^2} \right] - 1 \leq g_j^{(i)} \leq 2 \left[ \frac{f_j}{\vartheta_s} \sqrt{h_x^2 + h_y^2} \right] + 1 \end{aligned} \quad (C.16)$$

Since conditions in (C.7) should be satisfied for all possible dot product values,  $\tau_{m,j}^{(i)}(k_{f_j}^{(i)})$ , in the deployment area, the maximum value of  $k$  is found from (C.15) as,

$$\max\{k\} = \frac{1}{2 \left[ \frac{1}{\vartheta_s} \max_j(f_j) \sqrt{h_x^2 + h_y^2} \right] + 1} \quad (C.17)$$

Substituting (C.17) into (C.8) gives the condition in (2.52).

## APPENDIX D

### Cramér-Rao Bound

In this section, we derive the general deterministic CRB expressions for the DOA and sensor position estimations. Source signals are assumed to be deterministic unknown processes and noise is temporally uncorrelated zero-mean Gaussian process. It is also assumed that the array output is available at multiple frequencies for the same sources. Noise is uncorrelated for different frequencies. There is no circularity and spatial correlation assumption about the complex Gaussian noise.

The complex valued array output given in (2.4) can be rewritten in terms of real and imaginary parts for  $1 \leq t \leq N$  and  $1 \leq j \leq F$  as,

$$\begin{aligned} \mathbf{x}_{f_j}^{(c)}(t) &= \left[ \mathbf{x}_{f_1}^{(c)T}(1) \quad \dots \quad \mathbf{x}_{f_F}^{(c)T}(1) \quad \dots \quad \mathbf{x}_{f_F}^{(c)T}(N) \right]^T \\ \mathbf{x}_{f_j}^{(c)}(t) &= \mathbf{A}_{f_j}^{(c)} \mathbf{s}_{f_j}^{(c)}(t) + \mathbf{v}_{f_j}^{(c)}(t) \\ \begin{bmatrix} \Re(\mathbf{x}_{f_j}(t)) \\ \Im(\mathbf{x}_{f_j}(t)) \end{bmatrix} &= \begin{bmatrix} \Re(\mathbf{A}_{f_j}) & -\Im(\mathbf{A}_{f_j}) \\ \Im(\mathbf{A}_{f_j}) & \Re(\mathbf{A}_{f_j}) \end{bmatrix} \begin{bmatrix} \Re(\mathbf{s}_{f_j}(t)) \\ \Im(\mathbf{s}_{f_j}(t)) \end{bmatrix} + \begin{bmatrix} \Re(\mathbf{v}_{f_j}(t)) \\ \Im(\mathbf{v}_{f_j}(t)) \end{bmatrix} \end{aligned} \quad (\text{D.1})$$

Then according to the given assumptions, the distribution of  $\mathbf{x}^{(c)}$  can be expressed as Normal distribution,  $N\{\mathbf{m}(\Omega), \mathbf{R}(\Omega)\}$ .  $MNF \times 1$  vector  $\mathbf{m}(\Omega)$  and  $MNF \times MNF$  block diagonal matrix  $\mathbf{R}(\Omega)$  are defined as,

$$\mathbf{m}(\Omega) = \left[ \left( \mathbf{A}_{f_1}^{(c)} \mathbf{s}_{f_1}^{(c)}(1) \right)^T \quad \dots \quad \left( \mathbf{A}_{f_F}^{(c)} \mathbf{s}_{f_F}^{(c)}(1) \right)^T \quad \dots \quad \left( \mathbf{A}_{f_F}^{(c)} \mathbf{s}_{f_F}^{(c)}(N) \right)^T \right]^T \quad (\text{D.2})$$

$$\mathbf{R}(\Omega) = \text{diag}(\mathbf{R}_{f_1}(1), \dots, \mathbf{R}_{f_F}(1), \dots, \mathbf{R}_{f_F}(N)) \quad (\text{D.3})$$

$\mathbf{R}_{f_j}(t)$  is defined for non-circular and circular noise cases in (2.66) and (2.76), respectively.  $\Omega$  is a real-valued parameter vector that completely and uniquely specifies the distribution of  $\mathbf{x}^{(c)}$  and in our case it is defined as,

$$\Omega = \left\{ \theta_i, p_{m_{u,x}}, p_{m_{u,y}}, \Re(s_{i,f_j}(t)), \Im(s_{i,f_j}(t)), \left( \mathbf{R}_{f_j}(t) \right)_{k,l} \right\} \quad (\text{D.4})$$

for,  $m_u \in \{\text{sensor indices with unknown positions}\}$ ,  $1 \leq i \leq L$ ,  $1 \leq t \leq N$ ,  $1 \leq k \leq l \leq 2M$  and  $1 \leq j \leq F$ .  $(\mathbf{R}_{f_j}(t))_{k,l}$  is the  $k^{\text{th}}$  row and  $l^{\text{th}}$  column of the matrix  $\mathbf{R}_{f_j}(t)$ .

Using the definitions in (D.2) and (D.3), the Fisher information matrix corresponding to the distribution of  $\mathbf{x}^{(c)}$  is written as in [20], i.e.,

$$\mathbf{FIM}_{m,k} = \sum_{j=1}^F \sum_{t=1}^N \left\{ \left( \frac{\partial \mathbf{A}_{f_j}^{(c)} \mathbf{s}_{f_j}^{(c)}(t)}{\partial \Omega_m} \right)^T \mathbf{R}_{f_j}^{-1}(t) \frac{\partial \mathbf{A}_{f_j}^{(c)} \mathbf{s}_{f_j}^{(c)}(t)}{\partial \Omega_k} + \frac{1}{2} \text{tr} \left( \mathbf{R}_{f_j}^{-1}(t) \frac{\partial \mathbf{R}_{f_j}(t)}{\partial \Omega_m} \mathbf{R}_{f_j}^{-1}(t) \frac{\partial \mathbf{R}_{f_j}(t)}{\partial \Omega_k} \right) \right\} \quad (\text{D.5})$$

where  $\Omega_i$  denotes the  $i^{\text{th}}$  component of  $\Omega$ .

Note that, since the vector  $\mathbf{A}_{f_j}^{(c)} \mathbf{s}_{f_j}^{(c)}(t)$  is independent of the elements of covariance matrix  $\mathbf{R}_{f_j}(t)$  and  $\mathbf{R}_{f_j}(t)$  is depends on only its elements, the following relations are satisfied,

$$\begin{aligned} \frac{\partial \mathbf{A}_{f_j}^{(c)} \mathbf{s}_{f_j}^{(c)}(t)}{\partial (\mathbf{R}_{f_j}(t))_{k,l}} &= \mathbf{0}; & \frac{\partial \mathbf{R}_{f_j}(t)}{\partial \theta_i} &= \mathbf{0}; & \frac{\partial \mathbf{R}_{f_j}(t)}{\partial p_{m_u,x}} &= \mathbf{0}; \\ \frac{\partial \mathbf{R}_{f_j}(t)}{\partial p_{m_u,y}} &= \mathbf{0}; & \frac{\partial \mathbf{R}_{f_j}(t)}{\partial \Re(s_{i,f_j}(t))} &= \mathbf{0}; & \frac{\partial \mathbf{R}_{f_j}(t)}{\partial \Im(s_{i,f_j}(t))} &= \mathbf{0} \end{aligned} \quad (\text{D.6})$$

When all the unknown parameters in (D.4) are considered with the relations in (D.6), the Fisher Information matrix can be expressed as,

$$\mathbf{FIM} = \begin{bmatrix} \mathbf{FIM}_{\Theta,\Theta} & \mathbf{FIM}_{\Theta,\mathbf{P}} & \mathbf{FIM}_{\Theta,\mathbf{s}} & \mathbf{0} \\ \mathbf{FIM}_{\Theta,\mathbf{P}}^T & \mathbf{FIM}_{\mathbf{P},\mathbf{P}} & \mathbf{FIM}_{\mathbf{P},\mathbf{s}} & \mathbf{0} \\ \mathbf{FIM}_{\Theta,\mathbf{s}}^T & \mathbf{FIM}_{\mathbf{P},\mathbf{s}}^T & \mathbf{FIM}_{\mathbf{s},\mathbf{s}} & \mathbf{0} \\ \mathbf{0} & \mathbf{0} & \mathbf{0} & \mathbf{FIM}_{\mathbf{R},\mathbf{R}} \end{bmatrix} \quad (\text{D.7})$$

$\mathbf{FIM}_{\Theta,\Theta}$  is the Fisher Information sub-matrix corresponding to the DOA angles and obtained by substituting (D.6) into (D.5) for  $\{\Omega_m, \Omega_k\} \in \{\theta_i\}_{i=1}^L$ , i.e.,

$$\mathbf{FIM}_{\Theta,\Theta} = \sum_{j=1}^F \sum_{t=1}^N \mathbf{FIM}_{\Theta}^T(t, f_j) \mathbf{R}_{f_j}^{-1}(t) \mathbf{FIM}_{\Theta}(t, f_j) \quad (\text{D.8})$$

where  $2M \times L$  matrix  $\mathbf{FIM}_{\Theta}(t, f_j)$  is found as,

$$\mathbf{FIM}_{\Theta}(t, f_j) = \begin{bmatrix} \frac{\partial \mathbf{A}_{f_j}^{(c)} \mathbf{s}_{f_j}^{(c)}(t)}{\partial \theta_1} & \dots & \frac{\partial \mathbf{A}_{f_j}^{(c)} \mathbf{s}_{f_j}^{(c)}(t)}{\partial \theta_L} \end{bmatrix} \quad (\text{D.9})$$

Taking the derivative of  $\mathbf{A}_{f_j}^{(c)} \mathbf{s}_{f_j}^{(c)}(t)$  with respect to  $\theta_i$  for  $1 \leq i \leq L$  simplifies the expression in (D.9) as in (2.69).

The Fisher Information sub-matrix corresponding to the DOA angles and unknown sensor positions,  $\mathbf{FIM}_{\Theta,\mathbf{P}}$ , is obtained by substituting (D.6) into (D.5) for  $\Omega_m \in \{\theta_i\}_{i=1}^L$  and  $\Omega_k \in$

$\{p_{m_u,x}, p_{m_u,y}\}_{u=1}^{M_u}$ , i.e.,

$$\mathbf{FIM}_{\Theta,\mathbf{P}} = \sum_{j=1}^F \sum_{t=1}^N \mathbf{FIM}_{\Theta}^T(t, f_j) \mathbf{R}_{f_j}^{-1}(t) \mathbf{FIM}_{\mathbf{P}}(t, f_j) \quad (\text{D.10})$$

where  $M_u$  is the number of sensors with unknown positions and  $2M \times 2M_u$  matrix  $\mathbf{FIM}_{\mathbf{P}}(t, f_j)$  is found as,

$$\mathbf{FIM}_{\mathbf{P}}(t, f_j) = \begin{bmatrix} \frac{\partial \mathbf{A}_{f_j}^{(c)} \mathbf{s}_{f_j}^{(c)}(t)}{\partial p_{m_1,x}} & \dots & \frac{\partial \mathbf{A}_{f_j}^{(c)} \mathbf{s}_{f_j}^{(c)}(t)}{\partial p_{m_{M_u},x}} & \dots & \frac{\partial \mathbf{A}_{f_j}^{(c)} \mathbf{s}_{f_j}^{(c)}(t)}{\partial p_{m_{M_u},y}} \end{bmatrix} \quad (\text{D.11})$$

Taking the derivative of  $\mathbf{A}_{f_j}^{(c)} \mathbf{s}_{f_j}^{(c)}(t)$  with respect to the position of the  $m^{\text{th}}$  sensor for  $m \in \{ \text{sensor indices with unknown positions} \}$  simplifies the expression in (D.11) as in (2.70).

The Fisher Information sub-matrix corresponding to the DOA angles and source signals,  $\mathbf{FIM}_{\Theta,\mathbf{s}}$ , is obtained by substituting (D.6) into (D.5) for  $\Omega_k \in \{ \mathfrak{R}(s_{i,f_j}(t)), \mathfrak{I}(s_{i,f_j}(t)) \}$  and  $\Omega_m \in \{\theta_i\}_{i=1}^L$ ,  $1 \leq i \leq L$  and  $1 \leq j \leq F$ , i.e.,

$$\mathbf{FIM}_{\Theta,\mathbf{s}} = \sum_{j=1}^F \sum_{t=1}^N \mathbf{FIM}_{\Theta}^T(t, f_j) \mathbf{R}_{f_j}^{-1}(t) \mathbf{FIM}_{\mathbf{s}}(t, f_j) \quad (\text{D.12})$$

where  $2M \times 2NLF$  matrix  $\mathbf{FIM}_{\mathbf{s}}(t, f_j)$  is found by taking the derivative of  $\mathbf{A}_{f_j}^{(c)} \mathbf{s}_{f_j}^{(c)}(t)$  with respect to the real and imaginary parts of the source signals at each frequency, i.e.,

$$\mathbf{FIM}_{\mathbf{s}}(t, f_j) = \begin{bmatrix} \mathbf{0}_{(t-1)2LF+(j-1)2L} & \mathbf{A}_{f_j}^{(c)} & \mathbf{0}_{(N-t)2LF+(F-j)2L} \end{bmatrix} \quad (\text{D.13})$$

where  $\mathbf{0}_b$  is the  $2M \times b$  zero matrix. Substituting (D.13) into (D.12) simplifies the relation as in (D.14). In a similar way, the other Fisher Information sub-matrices are obtained as in

(D.15), D.16 and (D.17).

$$\mathbf{FIM}_{\Theta,s} = \begin{bmatrix} \left(\mathbf{FIM}_{\Theta}^T(1, f_1)\mathbf{R}_{f_1}^{-1}(1)\mathbf{A}_{f_1}^{(c)}\right)^T \\ \vdots \\ \left(\mathbf{FIM}_{\Theta}^T(1, f_F)\mathbf{R}_{f_F}^{-1}(1)\mathbf{A}_{f_F}^{(c)}\right)^T \\ \vdots \\ \left(\mathbf{FIM}_{\Theta}^T(N, f_F)\mathbf{R}_{f_F}^{-1}(N)\mathbf{A}_{f_F}^{(c)}\right)^T \end{bmatrix}^T \quad (\text{D.14})$$

$$\mathbf{FIM}_{P,P} = \sum_{j=1}^F \sum_{t=1}^N \mathbf{FIM}_{P}^T(t, f_j)\mathbf{R}_{f_j}^{-1}(t)\mathbf{FIM}_{P}(t, f_j) \quad (\text{D.15})$$

$$\mathbf{FIM}_{P,s} = \begin{bmatrix} \left(\mathbf{FIM}_{P}^T(1, f_1)\mathbf{R}_{f_1}^{-1}(1)\mathbf{A}_{f_1}^{(c)}\right)^T \\ \vdots \\ \left(\mathbf{FIM}_{P}^T(1, f_F)\mathbf{R}_{f_F}^{-1}(1)\mathbf{A}_{f_F}^{(c)}\right)^T \\ \vdots \\ \left(\mathbf{FIM}_{P}^T(N, f_F)\mathbf{R}_{f_F}^{-1}(N)\mathbf{A}_{f_F}^{(c)}\right)^T \end{bmatrix}^T \quad (\text{D.16})$$

$$\mathbf{FIM}_{s,s} = \text{diag}\left(\mathbf{A}_{f_1}^{(c)T}\mathbf{R}_{f_1}^{-1}(1)\mathbf{A}_{f_1}^{(c)}, \dots, \mathbf{A}_{f_F}^{(c)T}\mathbf{R}_{f_F}^{-1}(1)\mathbf{A}_{f_F}^{(c)}, \dots, \mathbf{A}_{f_F}^{(c)T}\mathbf{R}_{f_F}^{-1}(N)\mathbf{A}_{f_F}^{(c)}\right) \quad (\text{D.17})$$

Applying the partitioned matrix inversion formula [21], we can obtain the sub-matrices of inverse Fisher Information matrix corresponding to the DOA and sensor position estimation, i.e.,

$$\mathbf{FIM}_{\Theta}^{-1} = \left(\mathbf{K}_3 - \mathbf{K}_1\mathbf{K}_2^{-1}\mathbf{K}_1^T\right)^{-1} \quad (\text{D.18})$$

$$\mathbf{FIM}_{P}^{-1} = \mathbf{K}_2^{-1} + \mathbf{K}_2^{-1}\mathbf{K}_1^T\mathbf{FIM}_{\Theta}^{-1}\mathbf{K}_1\mathbf{K}_2^{-1} \quad (\text{D.19})$$

where

$$\mathbf{K}_1 = \mathbf{FIM}_{\Theta,P} - \mathbf{FIM}_{\Theta,s}\mathbf{FIM}_{s,s}^{-1}\mathbf{FIM}_{P,s}^T \quad (\text{D.20})$$

$$\mathbf{K}_2 = \mathbf{FIM}_{P,P} - \mathbf{FIM}_{P,s}\mathbf{FIM}_{s,s}^{-1}\mathbf{FIM}_{P,s}^T \quad (\text{D.21})$$

$$\mathbf{K}_3 = \mathbf{FIM}_{\Theta,\Theta} - \mathbf{FIM}_{\Theta,s}\mathbf{FIM}_{s,s}^{-1}\mathbf{FIM}_{\Theta,s}^T \quad (\text{D.22})$$

Substituting (D.8), (D.10), (D.14), (D.15), (D.16) and (D.17) into (D.20), (D.21) and (D.22) results a more compact form of  $\mathbf{K}_1$ ,  $\mathbf{K}_2$  and  $\mathbf{K}_3$  as in (2.63) - (2.65).

## APPENDIX E

### Proof of Lemma-2

To find the best sensor position estimate among the possible sensor position estimates,  $\hat{\mathbf{p}}_m(\mathbf{k}_m) = \hat{\mathbf{p}}_m(\mathbf{k}_m) + \mathbf{p}_m^0$ , unambiguously, it should be guaranteed that the sensor position estimate closest to the nominal sensor position is also closest to the actual sensor position. It is also necessary that there is only one sensor position estimate closest to the nominal sensor position. Let  $\hat{\mathbf{k}}_m^0$  and  $\hat{\mathbf{k}}_m^a$  be the ambiguity terms for which the position estimates are closest to the nominal and actual sensor positions, respectively, i.e,

$$\begin{aligned}\hat{\mathbf{k}}_m^0 &= \arg \min_{\mathbf{k}_m} \|\hat{\mathbf{p}}_m(\mathbf{k}_m) - \mathbf{p}_m^0\|^2 \\ &= \arg \min_{\mathbf{k}_m} \|\hat{\mathbf{p}}_m(\mathbf{k}_m)\|^2\end{aligned}\tag{E.1}$$

$$\begin{aligned}\hat{\mathbf{k}}_m^a &= \arg \min_{\mathbf{k}_m} \|\hat{\mathbf{p}}_m(\mathbf{k}_m) - (\tilde{\mathbf{p}}_m + \mathbf{p}_m^0)\|^2 \\ &= \arg \min_{\mathbf{k}_m} \|\hat{\mathbf{p}}_m(\mathbf{k}_m) - \tilde{\mathbf{p}}_m\|^2\end{aligned}\tag{E.2}$$

Then, the necessary conditions for the best unambiguous sensor position estimate can be expressed as,

$$\hat{\mathbf{k}}_m^0 = \hat{\mathbf{k}}_m^a\tag{E.3}$$

$$\|\hat{\mathbf{p}}_m(\hat{\mathbf{k}}_m^0)\|^2 < \|\hat{\mathbf{p}}_m(\mathbf{k}_m)\|^2, \quad \forall \mathbf{k}_m \neq \hat{\mathbf{k}}_m^0\tag{E.4}$$

The position perturbation of the  $m^{th}$  sensor can be written in polar form as

$$\tilde{\mathbf{p}}_m = \|\tilde{\mathbf{p}}_m\| \mathbf{u}^T(\beta_m)\tag{E.5}$$

where  $\beta_m$  is the angle of direction vector between the actual and nominal positions of the  $m^{th}$  sensor relative to the x-axis, respectively and  $\mathbf{u}(\beta_m)$  is defined as,

$$\mathbf{u}(\beta_m) = \begin{bmatrix} \cos(\beta_m) & \sin(\beta_m) \end{bmatrix}^T\tag{E.6}$$

Substituting (E.5) into (E.2) and considering that all the parameters are real, simplifies the relation as,

$$\begin{aligned}\hat{\mathbf{k}}_m^a &= \arg \min_{\mathbf{k}_m} \left( \|\hat{\mathbf{p}}_m(\mathbf{k}_m)\|^2 + \|\tilde{\mathbf{p}}_m\|^2 - 2\|\tilde{\mathbf{p}}_m\| \hat{\mathbf{p}}_m^T(\mathbf{k}_m) \mathbf{u}(\beta_m) \right) \\ &= \arg \min_{\mathbf{k}_m} \left( \|\hat{\mathbf{p}}_m(\mathbf{k}_m)\|^2 - 2\|\tilde{\mathbf{p}}_m\| \hat{\mathbf{p}}_m^T(\mathbf{k}_m) \mathbf{u}(\beta_m) \right)\end{aligned}\quad (\text{E.7})$$

The necessary condition on ambiguity terms in (E.3) and (E.4) is satisfied when the term that is tried to be minimized in (E.7) takes its minimum value at  $\hat{\mathbf{k}}_m^0$ . This relation can be specified as,

$$2\|\tilde{\mathbf{p}}_m\| \left( \hat{\mathbf{p}}_m(\mathbf{k}_m) - \hat{\mathbf{p}}_m(\hat{\mathbf{k}}_m^0) \right)^T \mathbf{u}(\beta_m) < \|\hat{\mathbf{p}}_m(\mathbf{k}_m)\|^2 - \|\hat{\mathbf{p}}_m(\hat{\mathbf{k}}_m^0)\|^2, \quad \forall \mathbf{k}_m \neq \hat{\mathbf{k}}_m^0 \quad (\text{E.8})$$

Then, for the worst case scenario the upper bound of  $\|\tilde{\mathbf{p}}_m\|$  can be expressed as,

$$\|\tilde{\mathbf{p}}_m\| < \frac{1}{2} \frac{\min_{\mathbf{k}_m} \left( \|\hat{\mathbf{p}}_m(\mathbf{k}_m)\|^2 - \|\hat{\mathbf{p}}_m(\hat{\mathbf{k}}_m^0)\|^2 \right)}{\max_{\mathbf{k}_m, \beta_m} \left( \left( \hat{\mathbf{p}}_m(\mathbf{k}_m) - \hat{\mathbf{p}}_m(\hat{\mathbf{k}}_m^0) \right)^T \mathbf{u}(\beta_m) \right)}, \quad \forall \mathbf{k}_m \neq \hat{\mathbf{k}}_m^0 \quad (\text{E.9})$$

The term in the denominator in (E.9) can be simplified as

$$\begin{aligned}\max_{\mathbf{k}_m, \beta_m} \left( \left( \hat{\mathbf{p}}_m(\mathbf{k}_m) - \hat{\mathbf{p}}_m(\hat{\mathbf{k}}_m^0) \right)^T \mathbf{u}(\beta_m) \right) &= \max_{\mathbf{k}_m, \beta_m, \gamma_m} \left( \|\hat{\mathbf{p}}_m(\mathbf{k}_m) - \hat{\mathbf{p}}_m(\hat{\mathbf{k}}_m^0)\| \mathbf{u}^T(\gamma_m) \mathbf{u}(\beta_m) \right) \\ &= \max_{\mathbf{k}_m} \|\hat{\mathbf{p}}_m(\mathbf{k}_m) - \hat{\mathbf{p}}_m(\hat{\mathbf{k}}_m^0)\| \max_{\beta_m, \gamma_m} \left( \mathbf{u}^T(\gamma_m) \mathbf{u}(\beta_m) \right) \\ &= \max_{\mathbf{k}_m} \|\hat{\mathbf{p}}_m(\mathbf{k}_m) - \hat{\mathbf{p}}_m(\hat{\mathbf{k}}_m^0)\|\end{aligned}\quad (\text{E.10})$$

where  $\gamma_m$  is the angle of the direction vector between  $\hat{\mathbf{p}}_m(\mathbf{k}_m)$  and  $\hat{\mathbf{p}}_m(\hat{\mathbf{k}}_m^0)$  relative to the x-axis and  $\mathbf{u}(\gamma_m)$  is defined as,

$$\mathbf{u}(\gamma_m) = \begin{bmatrix} \cos(\gamma_m) & \sin(\gamma_m) \end{bmatrix}^T \quad (\text{E.11})$$

Note that, the last relation in (E.10) is due to the fact that the maximum value of the dot product of two unit vector is equal to one.

Due to the definition in (E.1), the term in the numerator in (E.9) is greater than or equal to zero and it can be rewritten using (3.8) as,

$$\min_{\mathbf{k}_m} \left( \|\hat{\mathbf{p}}_m(\mathbf{k}_m)\|^2 - \|\hat{\mathbf{p}}_m(\hat{\mathbf{k}}_m^0)\|^2 \right) = \min_{\mathbf{k}_m} \left( \|\hat{\mathbf{p}}_m(\mathbf{k}_m) - \mathbf{p}_m^0\|^2 - \|\hat{\mathbf{p}}_m(\hat{\mathbf{k}}_m^0) - \mathbf{p}_m^0\|^2 \right) \quad (\text{E.12})$$

where  $\hat{\mathbf{p}}_m(\mathbf{k}_m) = \left( \frac{\lambda}{2\pi} \hat{\mathbf{E}}_m + \lambda \mathbf{k}_m \right) \mathbf{U}^\dagger(\hat{\mathbf{\Theta}})$ . Let  $\varphi_m$  be the angle between the direction vectors of  $\left( \hat{\mathbf{p}}_m(\mathbf{k}_m) - \hat{\mathbf{p}}_m(\hat{\mathbf{k}}_m^0) \right)$  and  $\left( \mathbf{p}_m^0 - \hat{\mathbf{p}}_m(\hat{\mathbf{k}}_m^0) \right)$ . Then, the distance between  $\hat{\mathbf{p}}_m(\mathbf{k}_m)$  and  $\mathbf{p}_m^0$  can be expressed as

$$\|\hat{\mathbf{p}}_m(\mathbf{k}_m) - \mathbf{p}_m^0\| = \sqrt{d_{12}^2(\mathbf{k}_m) + d_{13}^2(\mathbf{k}_m) - 2d_{12}(\mathbf{k}_m)d_{13}(\mathbf{k}_m)\cos(\varphi_m)} \quad (\text{E.13})$$

where

$$\begin{aligned}
d_{12}(\mathbf{k}_m) &= \|\hat{\mathbf{p}}_m(\mathbf{k}_m) - \hat{\mathbf{p}}_m(\mathbf{k}_m^0)\| \\
&= \left\| \left( \hat{\mathbf{p}}_m(\mathbf{k}_m) + \mathbf{p}_m^0 \right) - \left( \hat{\mathbf{p}}_m(\mathbf{k}_m^0) + \mathbf{p}_m^0 \right) \right\| \\
&= \|\hat{\mathbf{p}}_m(\mathbf{k}_m) - \hat{\mathbf{p}}_m(\mathbf{k}_m^0)\| \tag{E.14}
\end{aligned}$$

$$\begin{aligned}
d_{13}(\mathbf{k}_m) &= \|\hat{\mathbf{p}}_m(\mathbf{k}_m^0) - \mathbf{p}_m^0\| \\
&= \left\| \left( \hat{\mathbf{p}}_m(\mathbf{k}_m^0) + \mathbf{p}_m^0 \right) - \mathbf{p}_m^0 \right\| \\
&= \|\hat{\mathbf{p}}_m(\mathbf{k}_m^0)\| \\
&= e_m \tag{E.15}
\end{aligned}$$

Substituting (E.13), (E.14) and (E.15) into (E.12) simplifies the expression as

$$\min_{\mathbf{k}_m} \left( \|\hat{\mathbf{p}}_m(\mathbf{k}_m)\|^2 - \|\hat{\mathbf{p}}_m(\hat{\mathbf{k}}_m^0)\|^2 \right) = \min_{\mathbf{k}_m, \varphi_m} (d_{12}(\mathbf{k}_m) (d_{12}(\mathbf{k}_m) - 2d_{13}(\mathbf{k}_m) \cos(\varphi_m))) \tag{E.16}$$

Since  $d_{12}(\mathbf{k}_m)$  and  $d_{13}(\mathbf{k}_m)$  are positive quantities, (E.16) can be simplified as

$$\min_{\mathbf{k}_m} \left( \|\hat{\mathbf{p}}_m(\mathbf{k}_m)\|^2 - \|\hat{\mathbf{p}}_m(\hat{\mathbf{k}}_m^0)\|^2 \right) = \min_{\mathbf{k}_m} (d_{12}(\mathbf{k}_m) (d_{12}(\mathbf{k}_m) - 2d_{13}(\mathbf{k}_m))) \tag{E.17}$$

Substituting (E.14), (E.15), (E.17) and (E.10) into (E.9) simplifies the relation, i.e.,

$$\|\tilde{\mathbf{p}}_m\| < \frac{1}{2} \min_{\mathbf{k}_m \neq \hat{\mathbf{k}}_m^0} \|\hat{\mathbf{p}}_m(\mathbf{k}_m) - \hat{\mathbf{p}}_m(\mathbf{k}_m^0)\| - e_m \tag{E.18}$$

Substituting (3.8) into (E.18) results the condition of Lemma-2 in (3.12)

## APPENDIX F

### Derivation of Hessian Matrix and Gradient Vector in (4.50)

The  $L \times 1$  gradient vector for the DOA angles at iteration  $j$  is  $\mathbf{g}_j(k) = \frac{\partial Q}{\partial \boldsymbol{\Theta}_j(k)}$  and the  $L \times L$  Hessian matrix is  $\mathbf{H}_j(k, m) = \frac{\partial^2 Q}{\partial \boldsymbol{\Theta}_j(k) \partial \boldsymbol{\Theta}_j(m)}$ , where  $Q$  is the overall cost function in (4.52) and  $\boldsymbol{\Theta}_j$  is the  $L \times 1$  vector composed of DOA angles at iteration  $j$ .

Then from (4.52), the  $k^{\text{th}}$  element of gradient vector is found as

$$\begin{aligned} \mathbf{g}_j(k) &= \sum_{l=1}^L -\mathbf{e}_l^H \mathbf{M} \mathbf{T} \dot{\mathbf{A}}_k \mathbf{s}_l - \mathbf{s}_l^H \dot{\mathbf{A}}_k^H \mathbf{T}^H \mathbf{M}^H \mathbf{e}_l + \mathbf{s}_l^H \dot{\mathbf{A}}_k^H \mathbf{T}^H \mathbf{M}^H \mathbf{M} \mathbf{T} \mathbf{A} \mathbf{s}_l + \mathbf{s}_l^H \mathbf{A}^H \mathbf{T}^H \mathbf{M}^H \mathbf{M} \mathbf{T} \dot{\mathbf{A}}_k \mathbf{s}_l \\ &= 2\Re \left\{ \sum_{l=1}^L \left( -\mathbf{e}_l^H + \mathbf{s}_l^H \mathbf{A}^H \mathbf{T}^H \mathbf{M}^H \right) \mathbf{M} \mathbf{T} \dot{\mathbf{A}}_k \mathbf{s}_l \right\} \end{aligned} \quad (\text{F.1})$$

where

$$\dot{\mathbf{A}}_k = \frac{\partial \mathbf{A}}{\partial \boldsymbol{\Theta}_j(k)} = \mathbf{D}_k \mathbf{A} \mathbf{n}_k \mathbf{n}_k^T \quad (\text{F.2})$$

$\mathbf{n}_k$  is the  $L \times 1$  vector with all zero but the  $k^{\text{th}}$  element one and

$$\mathbf{D}_k = j \frac{2\pi}{\lambda} \text{diag} \left( -\mathbf{x} \sin(\boldsymbol{\Theta}_j(k)) + \mathbf{y} \cos(\boldsymbol{\Theta}_j(k)) \right) \quad (\text{F.3})$$

$$\mathbf{x} = [p_{1,x}, p_{2,x}, \dots, p_{K,x}]^T \quad (\text{F.4})$$

$$\mathbf{y} = [p_{1,y}, p_{2,y}, \dots, p_{K,y}]^T \quad (\text{F.5})$$

From (F.1)  $k^{\text{th}}$  row and  $m^{\text{th}}$  column of Hessian matrix is found as

$$\begin{aligned} \mathbf{H}_j(k, m) &= \frac{\partial \mathbf{g}_j(k)}{\partial \boldsymbol{\Theta}_j(m)} \\ &= 2\Re \left\{ \sum_{l=1}^L \mathbf{s}_l^H \dot{\mathbf{A}}_m^H \mathbf{T}^H \mathbf{M}^H \mathbf{M} \mathbf{T} \dot{\mathbf{A}}_k \mathbf{s}_l - \mathbf{e}_l^H \mathbf{M} \mathbf{T} \ddot{\mathbf{A}}_{k,m} \mathbf{s}_l + \mathbf{s}_l^H \mathbf{A}^H \mathbf{T}^H \mathbf{M}^H \mathbf{M} \mathbf{T} \ddot{\mathbf{A}}_{k,m} \mathbf{s}_l \right\} \\ &= 2\Re \left\{ \sum_{l=1}^L \mathbf{s}_l^H \dot{\mathbf{A}}_m^H \mathbf{T}^H \mathbf{M}^H \mathbf{M} \mathbf{T} \dot{\mathbf{A}}_k \mathbf{s}_l + \left( -\mathbf{e}_l^H + \mathbf{s}_l^H \mathbf{A}^H \mathbf{T}^H \mathbf{M}^H \right) \mathbf{M} \mathbf{T} \ddot{\mathbf{A}}_{k,m} \mathbf{s}_l \right\} \end{aligned} \quad (\text{F.6})$$

where

$$\ddot{\mathbf{A}}_{k,m} = \frac{\partial \dot{\mathbf{A}}_k}{\partial \boldsymbol{\Theta}_j(m)} = \begin{cases} (\bar{\mathbf{D}}_k + \mathbf{D}_k \mathbf{D}_k) \mathbf{A} \mathbf{n}_k \mathbf{n}_k^T & , k = m \\ \mathbf{0}_{K \times K} & , k \neq m \end{cases} \quad (\text{F.7})$$

$\bar{\mathbf{D}}_k = -j \frac{2\pi}{\lambda} \text{diag}(\mathbf{x} \cos(\boldsymbol{\Theta}_j(k)) + \mathbf{y} \sin(\boldsymbol{\Theta}_j(k)))$  and  $\mathbf{0}_{K \times K}$  is  $K \times K$  zero matrix.

## APPENDIX G

### Proof of Lemma-3

The left hand side of equation in (4.14) can be rewritten as

$$\|\mathbf{Z} - \mathbf{XY}\|_F^2 = \left\| \begin{bmatrix} \mathbf{z}_{c1} & \mathbf{z}_{c2} & \dots & \mathbf{z}_{cM} \end{bmatrix} - \begin{bmatrix} \mathbf{Xy}_{c1} & \mathbf{Xy}_{c2} & \dots & \mathbf{Xy}_{cM} \end{bmatrix} \right\|_F^2 \quad (\text{G.1})$$

where  $\mathbf{y}_{ci}$  and  $\mathbf{z}_{ci}$  are the column vectors composed of the  $i^{\text{th}}$  column of matrices  $\mathbf{Y}$  and  $\mathbf{Z}$ , respectively. Since Frobenious norm can be written as vector norm, the right hand side of (G.1) can be rewritten as

$$\begin{aligned} \|\mathbf{Z} - \mathbf{XY}\|_F^2 &= \left\| \begin{bmatrix} \mathbf{z}_{c1} \\ \mathbf{z}_{c2} \\ \vdots \\ \mathbf{z}_{cM} \end{bmatrix} - \begin{bmatrix} \mathbf{Xy}_{c1} \\ \mathbf{Xy}_{c2} \\ \vdots \\ \mathbf{Xy}_{cM} \end{bmatrix} \right\|^2 \\ &= \left\| \begin{bmatrix} \mathbf{z}_{c1} \\ \mathbf{z}_{c2} \\ \vdots \\ \mathbf{z}_{cM} \end{bmatrix} - \begin{bmatrix} \mathbf{X} & \mathbf{0}_{K \times L} & \dots & \mathbf{0}_{K \times L} \\ \mathbf{0}_{K \times L} & \mathbf{X} & \dots & \mathbf{0}_{K \times L} \\ \vdots & \vdots & \ddots & \vdots \\ \mathbf{0}_{K \times L} & \mathbf{0}_{K \times L} & \dots & \mathbf{X} \end{bmatrix} \begin{bmatrix} \mathbf{y}_{c1} \\ \mathbf{y}_{c2} \\ \vdots \\ \mathbf{y}_{cM} \end{bmatrix} \right\|^2 \\ &= \|\text{vect}(\mathbf{Z}) - (\mathbf{I}_M \otimes \mathbf{X}) \text{vect}(\mathbf{Y})\|^2 \end{aligned} \quad (\text{G.2})$$

## APPENDIX H

### Permutation Ambiguity in CIHOSS

As stated in Section 4.3.1.2, each row of the actual array steering matrix is estimated separately from the eigenvalue decomposition of cumulant matrix for different sensor pair as in (4.15) - (4.21). The eigenvalue decomposition gives us the ratios of the elements in the two rows of the actual array steering matrix estimate as in (4.21). The two rows are determined by the selected sensor pair and the ratios corresponding to the different sensor pair are arbitrarily ordered. This problem is defined as the permutation ambiguity and for the solution, a cost function in (4.25) is proposed. To explain the proposed cost function in a better way, we illustrate the aligning process in the following figures. We illustrate the actual array steering matrix in Fig. H.1 for four sensors and three sources. In Fig. H.1, the red, green and blue colors are used to represent the first, second and third sources, respectively.

$\mathbf{a}_1$	$\mathbf{b}_1$	$\mathbf{c}_1$
$\mathbf{a}_2$	$\mathbf{b}_2$	$\mathbf{c}_2$
$\mathbf{a}_3$	$\mathbf{b}_3$	$\mathbf{c}_3$
$\mathbf{a}_4$	$\mathbf{b}_4$	$\mathbf{c}_4$

Figure H.1: The actual array steering matrix.

When the eigenvalue decomposition of the cumulant matrices for the sensor pairs  $(1, j)$  and  $(2, j)$ ,  $1 \leq j \leq 4$ , is performed, we can obtain the actual array steering matrix in the form such as in Fig. H.2. As it can be seen, while the first two rows are in the same order, the remaining

rows are arbitrarily ordered. Note that, the first and second rows of the actual array steering matrix are found by using the DOA angles as explained in Section 4.3.1.2. On the other hand, the elements in the remaining rows are the ratios of the elements corresponding to the selected sensor pair. For example, the third row is composed of the ratios of the third and first rows of the actual array steering matrix.

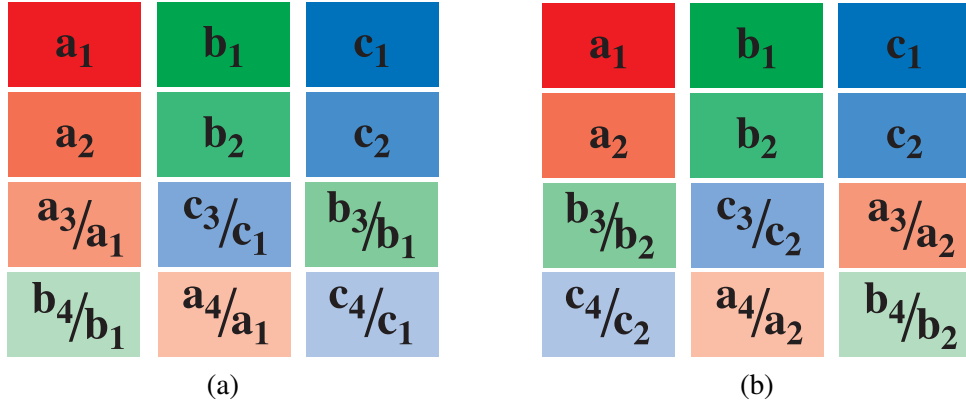


Figure H.2: The results of the eigenvalue decomposition of the cumulant matrix for sensor pairs (a) (1,j) and (b) (2,j),  $1 \leq j \leq 4$ .

Since the numerators and denominators are the elements of the first and second rows of the actual array steering matrix, the scale factor on the other rows can be eliminated by multiplying them with the elements in the first or second row of the matrix in Fig. H.2. Since the elements in each row are ordered arbitrarily, we should align the rows before the multiplication. To decide that the alignment is correct or not we use a cost function in (4.25), which measures the difference between the two vectors. When the elements of the rows are not aligned correctly, the two vectors are completely different as shown in Fig. H.3 and the cost function results a large value. On the other hand when the alignment is correct, the two vectors are almost the same as shown in Fig. H.4 and a smaller cost value is obtained.

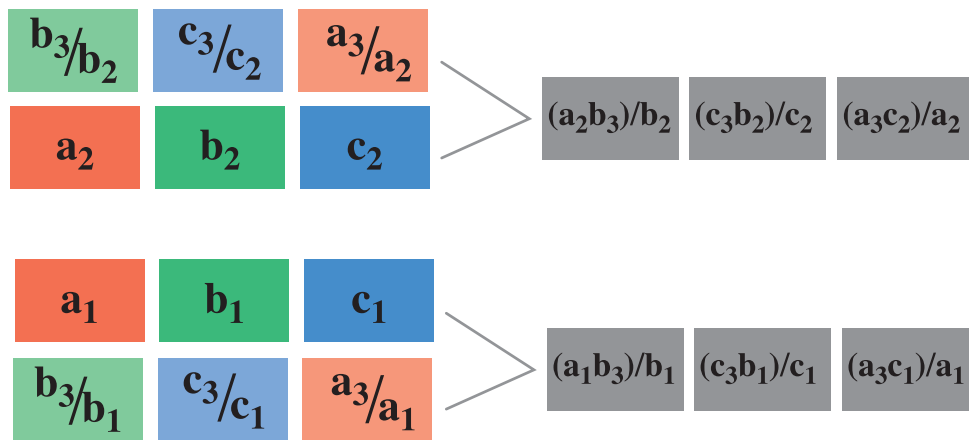


Figure H.3: The cost function evaluation for the aligning process when the alignment is not correct.

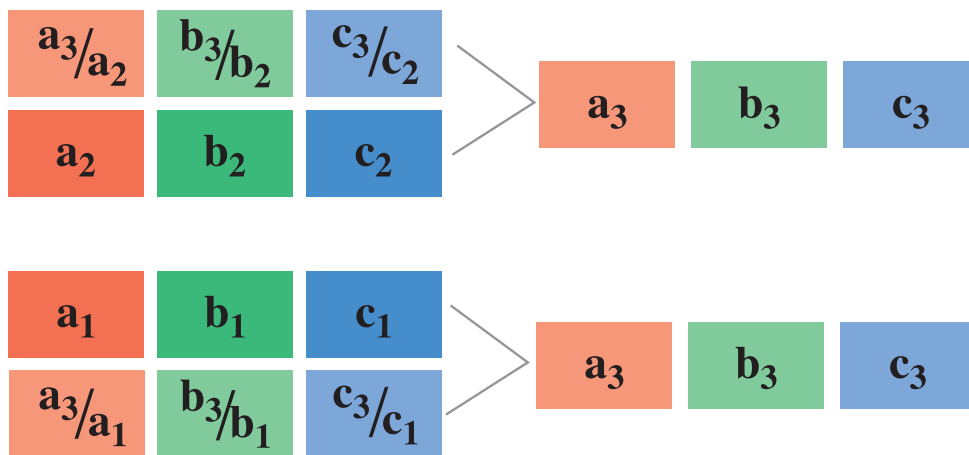


Figure H.4: The cost function evaluation for the aligning process when the alignment is correct.

# CURRICULUM VITAE

## PERSONAL INFORMATION

Surname, Name : Aktaş, Metin  
Nationality : Turkish (TC)  
Date and Place of Birth : 12 March 1979 , Afyon, TURKEY  
email : maktas@eee.metu.edu.tr, maktas@aselsan.com.tr

## EDUCATION

Degree	Institution	Year of Graduation
PhD	: METU, Electrical and Electronics Engineering,	2012
M.Sc.	: METU, Electrical and Electronics Engineering,	2004
BS	: Dokuz Eylül Univ., Electrical and Electronics Engineering,	2002

## WORK EXPERIENCE

Year	Place	Enrollment
2005–Present	ASELSAN, Mgeo Division	Senior Engineer
2004–2005	ODTU Parlar Vakfi	Research Engineer
2004–2004	SYS Inc.	Engineer

## FOREIGN LANGUAGES

English

## PUBLICATIONS

1. M. Aktaş and T. E. Tuncer, *HOS Based Online Calibration*, European Signal Processing Conference (EUSIPCO-2011), Barcelona, Aug. 31, 2011.
2. M. Aktaş and T. E. Tuncer, *Array Calibration with Modified Iterative HOS-SOS (MI-*

- HOSS) Algorithm*, European Signal Processing Conference (EUSIPCO-2011), pp. 614–618, Barcelona, Aug. 31, 2011.
3. M. Aktaş and T. E. Tuncer, *Iterative HOS-SOS (IHOSS) Algorithm for Direction-of-Arrival Estimation and Sensor Localization*, IEEE Trans. on Signal Proc., Vol. 58, pp. 6181–6194, Dec. 2010.
  4. M. Aktaş and T. E. Tuncer, *Iterative HOS-SOS (IHOSS) Based Sensor Localization and Direction-Of-Arrival Estimation*, IEEE International Conference on Acoustics, Speech, and Signal Processing, ICASSP-2010, March 2010.
  5. T. E. Tuncer and M. Aktaş, *LSE and MSE optimum partition-based FIR-IIR deconvolution filters with best delay*, IEEE Trans. on Signal Proc., Vol. 53, pp. 3780–3790, October 2005.
  6. M. Aktaş and T. E. Tuncer, *MSE Optimum Zone and Multi-Zone Filtering*, EUSIPCO2005, Antalya, Turkey, Sept. 4–8, 2005.
  7. M. Aktaş and T. E. Tuncer, *Ring based FIR-IIR best delay LS inverse filters*, IEEE International Conference on Acoustics, Speech, and Signal Processing, ICASSP'04, May 2004.